

The Texas Medical Center Library

DigitalCommons@TMC

---

The University of Texas MD Anderson Cancer  
Center UTHealth Graduate School of  
Biomedical Sciences Dissertations and Theses  
(Open Access)

The University of Texas MD Anderson Cancer  
Center UTHealth Graduate School of  
Biomedical Sciences

---

5-2010

## THE ROLE OF PLATELETS IN OVARIAN CARCINOMA

Rebecca L. Stone

Follow this and additional works at: [https://digitalcommons.library.tmc.edu/utgsbs\\_dissertations](https://digitalcommons.library.tmc.edu/utgsbs_dissertations)



Part of the [Medicine and Health Sciences Commons](#)

---

### Recommended Citation

Stone, Rebecca L., "THE ROLE OF PLATELETS IN OVARIAN CARCINOMA" (2010). *The University of Texas MD Anderson Cancer Center UTHealth Graduate School of Biomedical Sciences Dissertations and Theses (Open Access)*. 46.

[https://digitalcommons.library.tmc.edu/utgsbs\\_dissertations/46](https://digitalcommons.library.tmc.edu/utgsbs_dissertations/46)

This Thesis (MS) is brought to you for free and open access by the The University of Texas MD Anderson Cancer Center UTHealth Graduate School of Biomedical Sciences at DigitalCommons@TMC. It has been accepted for inclusion in The University of Texas MD Anderson Cancer Center UTHealth Graduate School of Biomedical Sciences Dissertations and Theses (Open Access) by an authorized administrator of DigitalCommons@TMC. For more information, please contact [digitalcommons@library.tmc.edu](mailto:digitalcommons@library.tmc.edu).



## **The Role of Platelets in Ovarian Carcinoma**

Rebecca L. Stone, M.D.

APPROVED:

---

Anil K. Sood, M.D.

---

Vahid Afshar-Kharghan, M.D.

---

Gary Gallick, Ph.D.

---

Gabriel Lopez-Berestein, M.D.

---

Ana Tari, Ph.D.

APPROVED:

---

Dean, the University of Texas  
Health Science Center at Houston  
Graduate School of Biomedical Sciences

# **THE ROLE OF PLATELETS IN OVARIAN CARCINOMA**

A

THESIS

Presented to the Faculty of  
The University of Texas  
Health Science Center at Houston  
and  
The University of Texas  
M.D. Anderson Cancer Center  
Graduate School of Biomedical Sciences  
In Partial Fulfillment

of the Requirements

for the Degree of

MASTER OF SCIENCE

by

Rebecca L. Stone, M.D.  
Houston, Texas

May, 2010

## **Acknowledgements**

I would like to take this opportunity to express great gratitude to my Committee Chairman and research mentor, Dr. Anil Sood. He first inspired me to train to become a gynecologic oncologist at M.D. Anderson Cancer Center. Since, he has profoundly influenced my professional development in academic medicine. His rigorous and dedicated mentoring has been instrumental to me in learning the practice of translational research as a clinician scientist. Working with him has been one of the most positive experiences of my career. I would also like to thank the other individuals who kindly served on my committee: Drs. Afshar-Kharghan, Gary Gallick, Gabe Lopez-Berestein, and Ana Tari. Their support and guidance helped me to succeed in bringing this project to fruition. In addition, this valuable experience would not have been possible without generous provisions made by the Department of Gynecologic Oncology at M.D. Anderson Cancer Center. I would especially like to thank my Chairman, Dr. David Gershenson and program director, Dr. Diane Bodurka for providing me with protected research time and the resources to pursue a Master of Science degree in Cancer Biology. Lastly, I could not have endured the past two years without the friendships I now share with my co-fellows and SRB colleagues. I am indebted to Chip Landen and Alpa Nick for coaching me in the techniques of basic science research and for their willingness to engage in frank intellectual discussion. Of course, my life will never be the same since growing to know Guillermo Armaiz Pena. He is a most dependable voice of reason, cherished confidant, and genuinely good person. I probably owe the equivalent of a first born child to every member of the BarEli lab. Gabe Villares, Andrey Dobroff, Maya Zigler, and Russel Braeuer have come to my rescue on an infinite number of



occasions. They are loyal friends and a tremendous source of good humor. I should be so lucky if I ever have the opportunity to work with these phenomenal individuals again. I would also like to sincerely thank Jennifer Burzawa and Matt Schlumbrecht for helping me maintain perspective and for routinely resurrecting my personal life. Lastly, I dare contemplate where I would be without the unconditional support of my loving family. They have faithfully been beside me through a life of exploration and discovery.

# THE ROLE OF PLATELETS IN OVARIAN CARCINOMA

Publication No. \_\_\_\_\_

Rebecca Lynn Stone, M.D.

Supervisory Professor: Anil K. Sood, M.D.

Background: Platelets represent one of the largest storage pools of angiogenic and oncogenic growth factors in the human body. The observation that thrombocytosis (platelet count  $>450,000/\mu\text{L}$ ) occurs in patients with solid malignancies was made over 100 years ago. However, the clinical and biological implications as well as the underlying mechanism of paraneoplastic thrombocytosis associated with ovarian carcinoma remains unknown and were the focus of the current study.

Materials and Methods: Following IRB approval, patient data were collected on 619 patients from 4 U.S. centers and used to test associations between platelet count at initial diagnosis, clinicopathologic factors, and outcome. *In vitro* effects of plasma-purified platelets on ovarian cancer cell proliferation, docetaxel-induced apoptosis, and migration were evaluated using BrdU-PI flow cytometric and two-chamber chemotaxis assays. *In vivo* effects of platelet depletion on tumor growth, proliferation, apoptosis, and angiogenesis were examined using an anti-platelet antibody (anti-mouse glycoprotein  $1b\alpha$ , Emfret) to reduce platelets by 50%. Complete blood counts and number of mature megakaryocytes in the spleen and bone marrow were compared between control mice and ovarian cancer-bearing mice. Plasma levels of key megakaryo- and thrombopoietic factors including thrombopoietin (TPO),  $\text{IL-1}\alpha$ ,  $\text{IL-3}$ ,  $\text{IL-4}$ ,  $\text{IL-6}$ ,  $\text{IL-11}$ , G-CSF, GM-CSF, stem cell factor, and FLT-3 ligand were assayed in a subset of 150 patients at the time of initial diagnosis with advanced stage, high grade epithelial ovarian cancer using

immunobead-based cytokine profiling coupled with the Luminex® xMAP platform. Plasma cytokines significantly associated with thrombocytosis in ovarian cancer patients were subsequently evaluated in mouse models of ovarian cancer using ELISA immunoassays. The results of human and mouse plasma cytokine profiling were used to inform subsequent *in vivo* studies evaluating the effect of siRNA-induced silencing of select megakaryo- and thrombopoietic cytokines on paraneoplastic thrombocytosis.

Results: Thirty-one percent of patients had thrombocytosis at initial diagnosis. Compared to patients with normal platelet counts, women with thrombocytosis were significantly more likely to have advanced stage disease ( $p<0.001$ ) and poor median progression-free (0.94 vs 1.35 years,  $p<0.001$ ) and overall survival (2.62 vs 4.65 years,  $p<0.001$ ). On multivariate analysis, thrombocytosis remained an independent predictor of decreased overall survival. Our analysis revealed that thrombocytosis significantly increases the risk of VTE in ovarian cancer patients and that thrombocytosis is an independent predictor of increased mortality in women who do develop a blood clot. Platelets increased ovarian cancer cell proliferation and migration by 4.1- and 2.8-fold ( $p<0.01$ ), respectively. Platelets reduced docetaxel-induced apoptosis in ovarian cancer cells by 2-fold ( $p<0.001$ ). *In vivo*, platelet depletion reduced tumor growth by 50%. Staining of *in vivo* specimens revealed decreased tumor cell proliferation ( $p<0.001$ ) and increased tumor and endothelial cell apoptosis ( $p<0.01$ ). Platelet depletion also significantly decreased microvessel density and pericyte coverage ( $p<0.001$ ). Platelet counts increase by 31-130% in mice with invasive ovarian cancer compared to controls ( $p<0.01$ ) and strongly correlate with mean megakaryocyte counts in the spleen and bone marrow

( $r=0.95$ ,  $p<0.05$ ). Plasma levels of TPO, IL-6, and G-CSF were significantly increased in ovarian cancer patients with thrombocytosis. Plasma levels of the same cytokines were found to be significantly elevated in orthotopic mouse models of ovarian cancer, which consistently develop paraneoplastic thrombocytosis. Silencing TPO, IL-6, and G-CSF significantly abrogated paraneoplastic thrombocytosis *in vivo*.

Conclusions: This study provides new understanding of the clinical and biological significance of paraneoplastic thrombocytosis in ovarian cancer and uncovers key humoral factors driving this process. Blocking the development of paraneoplastic thrombocytosis and interfering with platelet-cancer cell interactions could represent novel therapeutic strategies.

## Table of Contents

Approvals.....	i
Title.....	ii
Acknowledgements.....	iii
Abstract.....	v
Table of Contents.....	viii
List of Figures.....	ix
List of Tables.....	xi
Background and Introduction.....	1
Hypotheses and Specific Aims.....	14
Methods.....	17
Results.....	47
Summary.....	82
Discussion.....	83
Bibliography.....	95
Vita.....	115

## List of Figures

Figure 1. Markers of megakaryocyte differentiation and factors influencing discrete stages of megakaryocyte maturation.....	9
Figure 2. Central hypothesis.....	16
Figure 3. Dose-time kinetics of platelet depletion in mice using anti-platelet antibody.....	25
Figure 4. Confirmation of the specificity of anti-platelet antibody (APA) for mouse platelets.....	26
Figure 5a & b. Selection of effective siRNA sequences for targeting thombopoietin.....	39
Figure 6. Validation of human thrombopoietin silencing at the protein level.....	40
Figure 7a & b. Selection of effective siRNA sequences for targeting IL-6.....	42
Figure 8. Selection of effective siRNA sequences for targeting murine G-CSF.....	43
Figure 9. Changes in other CBC parameters according to platelet count.....	49
Figure 10a & b. Thrombocytosis and survival.....	51
Figure 11a & b. Platelet counts and correlation with tumor burden in orthotopic mouse models of ovarian cancer.....	54
Figure 12a & b. Changes in other CBC parameters in orthotopic mouse models of ovarian cancer.....	55
Figure 13a & b. Platelet counts in syngeneic mouse models of ovarian cancer and mouse models of other solid malignancies.....	56
Figure 14. Time course delineating the onset and progression of thrombocytosis in ovarian cancer-bearing mice.....	57
Figure 15a-c. Platelet extravasation into solid tumor and ascites.....	58
Figure 16. Macroscopic appearance of A2780ip2 tumors resected from mice treated with control IgG and anti-platelet antibody.....	60
Figure 17a-e. <i>In vivo</i> effects of platelet depletion on tumor growth, cell proliferation, microvessel density, pericyte coverage, and apoptosis.....	61

Figure 18. Effect of platelets on ovarian cancer cell migration <i>in vitro</i> .....	64
Figure 19. Effect of platelets on ovarian cancer cell proliferation and apoptosis <i>in vitro</i> .....	65
Figure 20a & b. Platelet derived growth factor alpha (PDGFR $\alpha$ ) expression in ovarian cancer cell lines.....	66
Figure 21. Effect of fully humanized anti-PDGFR $\alpha$ antibody, IMC-3G3, on platelet induced taxane resistance.....	67
Figure 22. Medullary and splenic megakaryocyte counts.....	69
Figure 23. <i>In vitro</i> and <i>in vivo</i> ovarian cancer cell thrombopoietin expression.....	70
Figure 24. Hepatic thrombopoietin transcript levels.....	71
Figure 25. Bone marrow aspirates from patients with epithelial ovarian cancer.....	72
Figure 26. Examination of ovarian cancer patient spleens for megakaryocytes.....	73
Figure 27. Thrombopoietin protein expression in patient specimens of serous papillary ovarian carcinoma.....	74
Figure 28a & b. Spearman's correlation of plasma IL-6 (a) and TPO (b) levels with platelet counts in 150 ovarian cancer patients.....	76
Figure 29. IL-6, thrombopoietin, and G-CSF plasma levels in ovarian cancer patients.....	77
Figure 30. IL-6, thrombopoietin, and G-CSF plasma levels in non-tumor bearing mice and mouse models of ovarian cancer.....	79
Figure 31. Revised hypothesis.....	93

## List of Tables

Table 1. Incidence, timing, predictors, and prognostic implications of VTE in ovarian cancer patients.....	3
Table 2. Platelet secretory granule content.....	7
Table 3. Megakaryopoietic & thrombopoietic cytokines.....	11
Table 4. siRNA sequences screened for targeting TPO, IL-6, and G-CSF.....	38
Table 5. Platelet counts in patients with invasive ovarian cancer.....	47
Table 6. Associations between thrombocytosis and clinicopathological variables.....	48
Table 7. Prevalence of thrombocytosis in solid malignancies.....	49
Table 8a & b. Multivariate Cox proportional hazards analysis of prognostic factors on progression free and overall survival.....	52
Table 9a & b. Multivariate Cox proportional hazard analysis of prognostic factors including VTE on progression free and overall survival.....	53
Table 10. Spearman's correlation of platelet counts with plasma cytokine levels in 150 ovarian cancer patients.....	75
Table 11. Wilcoxon rank sum test testing differences in plasma cytokine levels (pg/mL) between patients with normal platelet counts and thrombocytosis.....	77
Table 12. Impact of targeting IL-6, TPO, and G-CSF alone and in combination on thrombocytosis in A2780ip2 orthotopic mouse model of ovarian cancer.....	80
Table 13. Impact of targeting IL-6, TPO, and G-CSF alone and in combination on thrombocytosis in 2774 orthotopic mouse model of ovarian cancer.....	80



## **Background and Introduction**

### Human epithelial ovarian cancer

Epithelial ovarian cancer is the fifth leading cause of cancer death among women and is the most lethal gynecological malignancy. An estimated 21,000 women are diagnosed with and 15,000 women die from this disease annually (1). While disease-specific mortality has changed minimally, median survival time for women with advanced ovarian cancer has consistently improved, corresponding to a 1.6 year gain in life expectancy between 1973 and 2000 (2). The negligible increase in cure rates over the past 30 years is multi-factorial. Principally, disease onset is insidious with most women experiencing vague symptoms that often evade early clinical detection. Further, no sufficiently accurate screening test is currently available even for women at increased genetic risk for ovarian cancer. These two factors largely contribute to advanced disease at the time of diagnosis (3). The standard of care for ovarian cancer involves tumor reductive surgery followed by 6 cycles of platinum/taxane based chemotherapy (4). Fortunately, epithelial ovarian cancer is among the most chemosensitive malignancies, with an initial 70-80% response rate to combination platinum/taxane chemotherapy (5). Unfortunately, the vast majority of patients develop recurrent ovarian cancer and eventually succumb to their disease. First-line chemotherapy fails in more than 20 percent of patients with epithelial ovarian cancer and approximately 40 to 50 percent of women who respond to initial treatment relapse within 2 years. In the setting of recurrent, platinum resistant ovarian cancer, second line cytotoxic agents have a 15 to 20 percent response rate with virtually no cures (6-8). Clinical studies published over the past 15 years, including Gynecologic Oncology Group (GOG) 111, GOG 132,

and International Collaborative Ovarian Neoplasm (ICON) 3 trials, report an 11 to 18 month median progression-free survival and a 24 to 40 month median overall survival for women with epithelial ovarian cancer depending on the stage and extent of surgical cytoreduction (9-11). This poor prognosis implores development of more efficacious therapeutic options for women with epithelial ovarian cancer, both in first-line and relapsed disease settings. While new developments in surgery and chemotherapy have advanced the field, recent studies suggest that the addition of more cytotoxic drugs to the current standard of platinum/paclitaxel is unlikely to result in substantial improvements in clinical outcome. Recently, GOG 182/ICON5 trial demonstrated that the addition of gemcitabine, liposomal doxorubicin, or topotecan to paclitaxel and carboplatin provides no additional benefit (12). Fortunately, clinical investigations currently evaluating the efficacy of therapies that specifically target biological processes driving the growth and progression of ovarian cancer are showing promising results. Anti-VEGF agents that inhibit tumor angiogenesis, such as bevacizumab, illustrate the potential advantage of this approach. Response rates to single agent bevacizumab as second-line therapy for ovarian cancer range from 16-21%, which approximates the clinical benefit derived from other approved second-line cytotoxic agents such as topotecan (13.7-20.5%) and gemcitabine (15-20%) (13-15). This sets new precedent for exploring the role of host factors in promoting malignancy and for developing therapeutic strategies based on undermining fundamental host-tumor interactions.

#### Vascular thromboembolism in ovarian cancer

Most women with ovarian cancer present with advanced disease and suffer a variety of complications, including vascular thromboembolism (VTE), during extended

treatment courses entailing one or more surgeries and several lines of chemotherapy. VTE is often the sentinel event that leads to a new diagnosis of occult ovarian cancer in many of these patients. A recently published, large population-based study found that the incidence of VTE was nearly three times higher in the year preceding ovarian cancer diagnosis (16). Vascular thromboembolism complicates the treatment course of up to 25% of ovarian cancer patients and is a poor prognostic factor (Table 1) (17, 18).

**Table 1.** Incidence, timing, predictors, and prognostic implications of VTE in ovarian cancer patients

events/total # (%)	Timing	associated factors*	impact on survival	Reference
18/72 (25%)	all cases at time of dx	clear cell histology* massive ascites*	not examined	(19)
19/86 (22%)	at diagnosis: 6 (31%) perioperative: 6 (32%) during long-term f/u: 7 (37%)	stage	not examined	(20)
42/253 (16.6%)	at diagnosis: 8 (19%) perioperative: 6 (14.3%) during initial treatment: 16 (38.1%) during long-term f/u: 12 (28.6%)	prior event age stage suboptimal TRS* BMI*	not examined	(21)
57/559 (10%)	all cases perioperative	stage ascites suboptimal TRS	no impact	(22)
672/13,031 (5.2%)	perioperative: 257 (38.2%)	age* stage*	reduced	(23)
76/2,743 (2.8%)	preoperative & during initial rx: 38 (50%)	age* BMI > 30 kg/m <sup>2</sup> *	reduced	(24)
128/12,835 (1%)	all cases predated diagnosis of ovarian cancer	stage	reduced	(25)

\* in multivariate analysis

Taking prevalence into account, cancers of the pancreas, ovary, and brain are the most strongly associated with thrombotic complications (26). The association between VTE and underlying cancer is well established. The connection was first

made in the early 19<sup>th</sup> century by the French clinician Armand Trousseau, who observed that patients presenting with idiopathic VTE frequently have an underlying visceral malignancy (27). In 1845, the functional triad mediating the pathogenesis of thrombosis was described by pathologist Rudolf Virchow and subsequently became known as “Virchow’s triad,” which includes vascular endothelial injury/dysfunction, stasis, and hypercoagulability. Direct injury to the vessel wall can be inflicted by extrinsic factors such as chemotherapy (28). The specific mechanism of chemotherapy-induced thrombosis may be related to decreased protein C, increased fibrinopeptide A production, increased endothelial cell reactivity, release of tissue factor from monocytes and endothelial cells, down regulation of thrombomodulin, and decreased fibrinolytic response (21). Large tumor burden and/or massive ascites characteristic of ovarian cancer may predispose to VTE by compressing intrapelvic veins and inducing venous stasis. Large volume ascites may also be indicative of increased blood viscosity because the accumulation of ascites represents a profound redistribution of body fluid from the intravascular to the interstitial compartment. Additionally, venous stasis is an inevitable risk in ovarian cancer patients undergoing surgery secondary to prolonged operative time and a protracted postoperative course. Further, there is accumulating evidence that cancer in general, and ovarian cancer in particular, are exceptionally hypercoagulable states. A multitude of coagulation pathway proteins are increased in ovarian cancer including factor II (thrombin), thrombin receptor (protease-activated receptors), factor I (fibrinogen), factor III (tissue factor), fibrin, and factors VII, VIII and X (29). Increased numbers and reactivity of circulating platelets also significantly contributes to heightened systemic coagulation activation

in ovarian cancer patients. While there have been numerous investigations evaluating the contribution of the aforementioned risk factors for VTE in ovarian cancer patients, no studies have defined the role of thrombocytosis.

#### Platelets and malignancy

Platelets are small anucleate cell fragments derived from megakaryocytes in the bone marrow and are highly reactive cellular effectors of hemostasis, inflammation, and immunity. As such, they represent one of the largest reservoirs of angiogenic and oncogenic growth factors in the human body. The concept that platelets might play key roles in invasive tumor growth and metastasis is longstanding. In fact, the clinical observation that thrombocytosis (platelet count  $>450,000/\mu\text{L}$  according to the National Heart, Lung, and Blood Institute, NHLBI) occurs in patients with solid malignancies was made over 100 years ago (27). Nearly 40% of individuals incidentally found to have platelet counts exceeding  $400,000/\mu\text{L}$  have an occult malignancy; most commonly a gastrointestinal, lung, breast, or ovarian primary (30). There is also existing evidence that experimentally induced thrombocytopenia and anti-platelet treatment decreases metastasis in various tumor models. For example, platelet-deficient mice due to knockout of NF-E2, a transcription factor required for the production of platelets from megakaryocytes, are protected against hematogenous metastasis (31, 32). Additionally, platelet depletion using anti-platelet serum reduces colon cancer lung metastases, which can be restored by re-infusing human or mouse platelets (33). Several possible mechanisms could account for platelet induced growth and dissemination of malignancy. Platelet adherence to tumor cells may help tumor cells lodge in the microvasculature where they may form intravascular colonies or extravasate into target organs. Platelet

adherence may also shield tumor cells from immune surveillance. Factors released by platelets may support tumor cell survival, proliferation, and invasion. Additionally, platelets may release pro-angiogenic factors that stabilize the tumor vasculature. The platelet membrane contains a dense layer of glycoproteins, integrins, and selectins which mediate platelet adhesion and aggregation. Platelet adherence to tumor cells is mediated by these receptors and blocking them decreases *in vivo* experimental pulmonary metastasis, increases tumor cell interaction with monocytes, and increases tumor cell lysis by natural killer cells (34, 35). Activated platelets release numerous bioactive molecules including chemokines, cytokines, growth factors, coagulation factors, and metalloproteinases from 3 types of secretory vesicles: alpha granules, dense granules and lysosomes. In particular, platelet alpha granules are a rich source of both pro- and anti-angiogenic factors (Table 2). Recent evidence suggests that pro- and anti-angiogenic factors are differentially packaged into distinct subpopulations of alpha granules that can be selectively deployed by platelets upon engagement of specific surface receptors, such as protease-activated receptors (36).

<b>Table 2. Platelet secretory granule content</b>	
<b><math>\alpha</math>-granules pro-angiogenic</b>	<b><math>\alpha</math>-granules anti-angiogenic</b>
vascular endothelial growth factor	thrombospondin 1
platelet-derived growth factor	platelet factor 4
basic fibroblast growth factor	plasminogen activator inhibitor 1
epidermal growth factor	endostatin
transforming growth factor	angiostatin
insulin-like growth factor	<b>Dense granules</b>
angiopoietin-1	serotonin
sphingosine-1-phosphate	catecholamines
matrix metalloproteinases	adenosine
glycoproteins	calcium ADP/ATP
p-selectin	histamine
fibrinogen	<b>Lysosomes</b>
von willibrand factor	proteinases glycosidases

In addition to the paracrine effects of platelet growth factors, there is evidence for a direct role for platelets in stimulating angiogenesis. Platelet remnants and microparticles are found at sites of angiogenic sprouts and *in vitro* data demonstrate a clear dose-response relationship between platelet count and the extent of sprouting angiogenesis (37). Platelets promote the migration and adherence of bone-marrow derived cells to sites of angiogenesis and induce differentiation of endothelial-cell progenitors into mature endothelial cells (38). Moreover, activated platelets are critical regulators of tumor vascular homeostasis by preventing tumor hemorrhage through selective unloading of their granule content (39). This is a

particularly important contribution to the tumor microenvironment given that cancer angiogenesis is characterized by morphologically abnormal, immature, dilated and leaky blood vessels (40).

#### Physiologic mechanisms of megakaryopoiesis and thrombopoiesis

Given that the average lifespan of a circulating platelet is only 10 days, the adult human must produce approximately one hundred billion platelets daily in order to maintain a normal platelet count under steady-state conditions (41, 42). This tremendous baseline level of production has the potential to markedly increase (by  $\geq 20$ -fold) in response to contextual cues, including humoral factors resulting from malignancies. Megakaryopoiesis is a highly complex process and is conserved across mammalian species. Nearly one billion megakaryocytes turn over in the bone marrow every day (43). Common myeloid progenitor cells give rise to megakaryocyte/erythroid progenitor cells which beget a cellular continuum of lineage-committed megakaryocyte progenitor cells with distinct phenotypic differences and cytokine requirements. The most primitive progenitor cell committed to megakaryocyte differentiation, the burst-forming megakaryocyte (BFU-MK), generates colony-forming megakaryocytes (CFU-MK) capable of producing several megakaryoblasts. Megakaryoblasts characteristically have a high nuclear/cytoplasmic ratio, round compact nucleus, and basophilic cytoplasm. While megakaryoblasts morphologically resemble lymphocytes, they are readily distinguished by their emergent expression of platelet glycoproteins such as  $\beta_3$  integrin CD61 (GPIIIa) (Figure 1) (44).



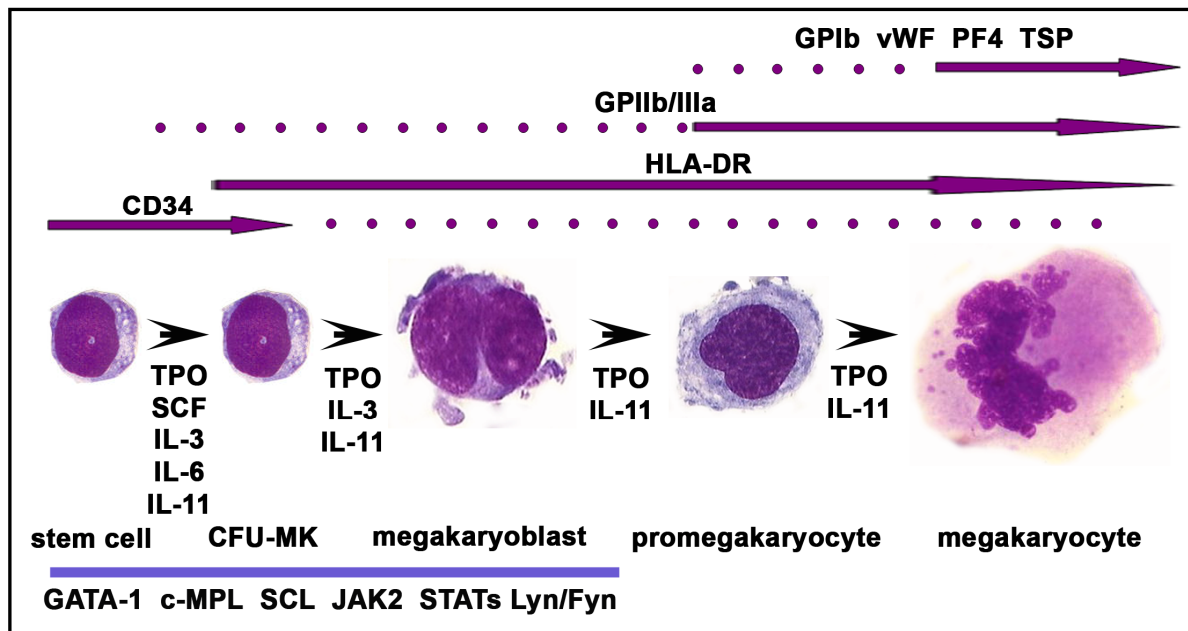


**Figure 1. Markers of megakaryocyte differentiation and factors influencing discrete stages of megakaryocyte maturation.** Changes in cell surface markers with megakaryocyte differentiation appear above the purple arrows. Known humoral and signaling factors regulating this process appear under the black arrows and purple bar, respectively. Abbreviations: glycoprotein (GP), von Willibrand Factor (vWF), platelet factor 4 (PF4), thrombospondin (TSP), thrombopoietin (TPO), stem cell factor (SCF), c-MPL (TPO receptor).

As maturation progresses, the megakaryocyte cytoplasm becomes highly specialized with the elaboration of a complex system of membranes, called the demarcation membrane system, and the aforementioned discrete types of secretory granules: alpha granules, dense granules, and lysosomes. Proteins packaged into alpha granules can either be synthesized (eg. platelet factor 4 and von Willibrand Factor) or endocytosed (eg. fibrin and growth factors) (45). Battinelli and colleagues postulate that the megakaryocyte uses some type of counting

mechanism to ensure that each platelet is correctly allocated alpha granules, dense granules, and essential organelles (46).

Once synthesis of platelet proteins has commenced, the promegakaryoblast begins to increase its ploidy by DNA replication without concomitant cell division by a unique biological event termed endomitosis (47). The process of megakaryocyte maturation terminates in massive rearrangement of the megakaryocyte cytoskeleton into multiple long and branching cytoplasmic extensions known as proplatelets. The demarcation membrane system ultimately serves as the reservoir for proplatelet membranes (48). Beta-1 tubulin largely comprises the internal scaffolding of the proplatelet and which forms the “highway” on which cargo from mitochondria and granules traffic to the end termini, dispersing into approximately 100-200 platelets per terminus. Proplatelet formation represents a suicidal process for the megakaryocyte since it entirely consumes the cytoplasm, leaving behind an isolated, apoptotic nucleus (49).

Numerous cytokines, such as thrombopoietin (leukemia virus oncogene ligand, TPO) and various interleukins, have been implicated in megakaryopoiesis and platelet production, many having additive or synergistic effects at various stages in the process. While the cytokines listed in Table 3 are predominantly thought to have a stimulatory effect on megakaryo- and thrombopoiesis, there is some evidence that transforming growth factor  $\beta$ 1, platelet factor-4, and IL-4 may have inhibitory functions (46).

**Table 3.** Megakaryo- & thrombopoietic cytokines

Thrombopoietin
IL-1 $\alpha$
IL-3
IL-4
IL-6
IL-11
Stem Cell Factor
GM-CSF
G-CSF
FLT3 Ligand

Thrombopoietin is a heavily glycosylated, 332-amino-acid protein and is the key humoral factor that drives thrombopoiesis. It is estimated that TPO stimulates the growth of 75% of all CFU-MK (50). Genetic elimination of TPO or the TPO receptor, c-Mpl, in mice reduces platelet counts by approximately 85% of normal (51). The liver is the dominant source of TPO production. Reciprocal liver transplant experiments between normal and TPO-null mice demonstrated that the liver synthesizes at least half of all TPO (52). Under normal physiological conditions, blood and marrow levels of TPO are inversely proportional to platelet and megakaryocyte numbers. Since the liver produces TPO at a constitutive rate, TPO levels are largely determined by receptor-mediated uptake and degradation by high affinity c-Mpl receptors on platelets and megakaryocytes. Thus, properly regulated expression of c-Mpl is critical for controlling thrombopoiesis. Multiple active and inactive splice forms of the c-Mpl receptor exist. Alternative gene splicing can result in the production of truncated receptor proteins inapt for cell surface expression, thus resulting in a functional down-regulation of c-Mpl receptors (53). Substitution of a truncated c-Mpl promoter has been shown to result in diminished platelet c-Mpl

expression and thrombocytosis (54). Additionally, platelet c-Mpl receptor expression is decreased in patients with essential thrombocythemia, providing further evidence that impaired platelet c-Mpl protein expression likely contributes to elevated platelet counts (55). The 8<sup>th</sup> ATG codon in the 5' untranslated region of TPO mRNA serves as the initiation codon for TPO translation and is embedded in a short open reading frame initiated by the 7<sup>th</sup> ATG. This juxtaposition of start codons results in inefficient TPO translation. Interestingly, numerous mutations that greatly improve the efficiency of TPO translation have been identified in this region and linked to familial thrombocytosis (56).

There is also evidence to suggest that cytokine-independent mechanisms of megakaryopoiesis exist involving chemokine-driven cell interactions mediated by fibroblast growth factor (FGF)-4 and stromal-derived factor (SDF)-1 chemokine. Recent studies reveal that FGF-4 and SDF-1 guide megakaryocyte progenitors to the marrow microvascular niche and that this ligand pair can restore normal platelet counts in TPO- and c-Mpl-deficient mice as well as following myelosuppressive insults (57).

Two transcription factors, GATA-1 and nuclear factor erythroid-2 (NF-E2) are also absolutely necessary for terminal megakaryocyte differentiation and release of blood platelets (49). GATA-1 directs platelet-specific gene transcription and is a prominent regulator of megakaryocyte endomitosis (31). NF-E2 regulates the expression of many genes important for thrombopoiesis. Recently, McCormack and colleagues demonstrated that the basic helix-loop-helix (bHLH) transcription factor SCL acts upstream of NF-E2 to control megakaryocyte differentiation and platelet release in instances of thrombopoietic stress, such as following chemotherapy (58).

Any number of aberrations in this intricate process of megakaryo- and/or thrombopoiesis could give rise to paraneoplastic thrombocytosis. While there have been some studies examining the link between perturbations in the regulation of megakaryo- and/or thrombopoiesis and thrombocytopenia, there has not been a concerted effort to identify the determinants of thrombocytosis associated with malignancy. Furthermore, while the supporting function of platelets in metastasis has been demonstrated in a variety of experimental models, the contribution of platelets to tumor growth and angiogenesis is less well known. It is also unclear when platelet numbers begin to rise during the course of malignant progression and if extravascular contact between platelets and tumor cells occurs. Thus, in order to further define the clinical implications, biological role, and underlying mechanism of paraneoplastic thrombocytosis in ovarian carcinoma, we undertook the current investigation.

## **Hypotheses and Specific Aims**

The overall hypotheses of this project are:

- 1) Thrombocytosis develops in a substantial proportion of patients with advanced epithelial ovarian cancer and compromises disease specific survival.
- 2) Platelets promote ovarian cancer growth and angiogenesis by increasing tumor cell proliferation and migration, supporting microvessel pericyte coverage, and sustaining tumor and endothelial cell survival.
- 3) Increased megakaryo- and thrombopoiesis in response to humoral factors resulting from ovarian cancer accounts for paraneoplastic thrombocytosis.

These individual hypotheses can be synthesized into one unified hypothesis. Figure 2 illustrates the conceptual framework of the central hypothesis that tumor cells, constituents of the tumor microenvironment such as tumor-associated endothelial cells, and tumor-bearing host tissues produce megakaryopoietic and thombopoietic cytokines, which stimulate megakaryopoiesis and the enumeration of platelets, which in turn promote tumor growth and angiogenesis, creating a continuous feed-forward loop. The following specific aims will test this hypothesis.

Specific Aim 1: Ascertain the prevalence and clinical implications of thrombocytosis in human epithelial ovarian cancer.

Specific Aim 2: Examine the biological effects of platelets on ovarian cancer cell proliferation and migration, microvessel pericyte coverage, and tumor and endothelial cell survival using *in vitro* and *in vivo* assays.

Specific Aim 3: Characterize an underlying mechanism of paraneoplastic thrombocytosis in ovarian cancer by identifying megakaryo- and thrombopoietic cytokines associated with thrombocytosis in both ovarian cancer patients and mouse models of ovarian cancer and by subsequently determining the impact of silencing these cytokines on paraneoplastic thrombocytosis *in vivo*.

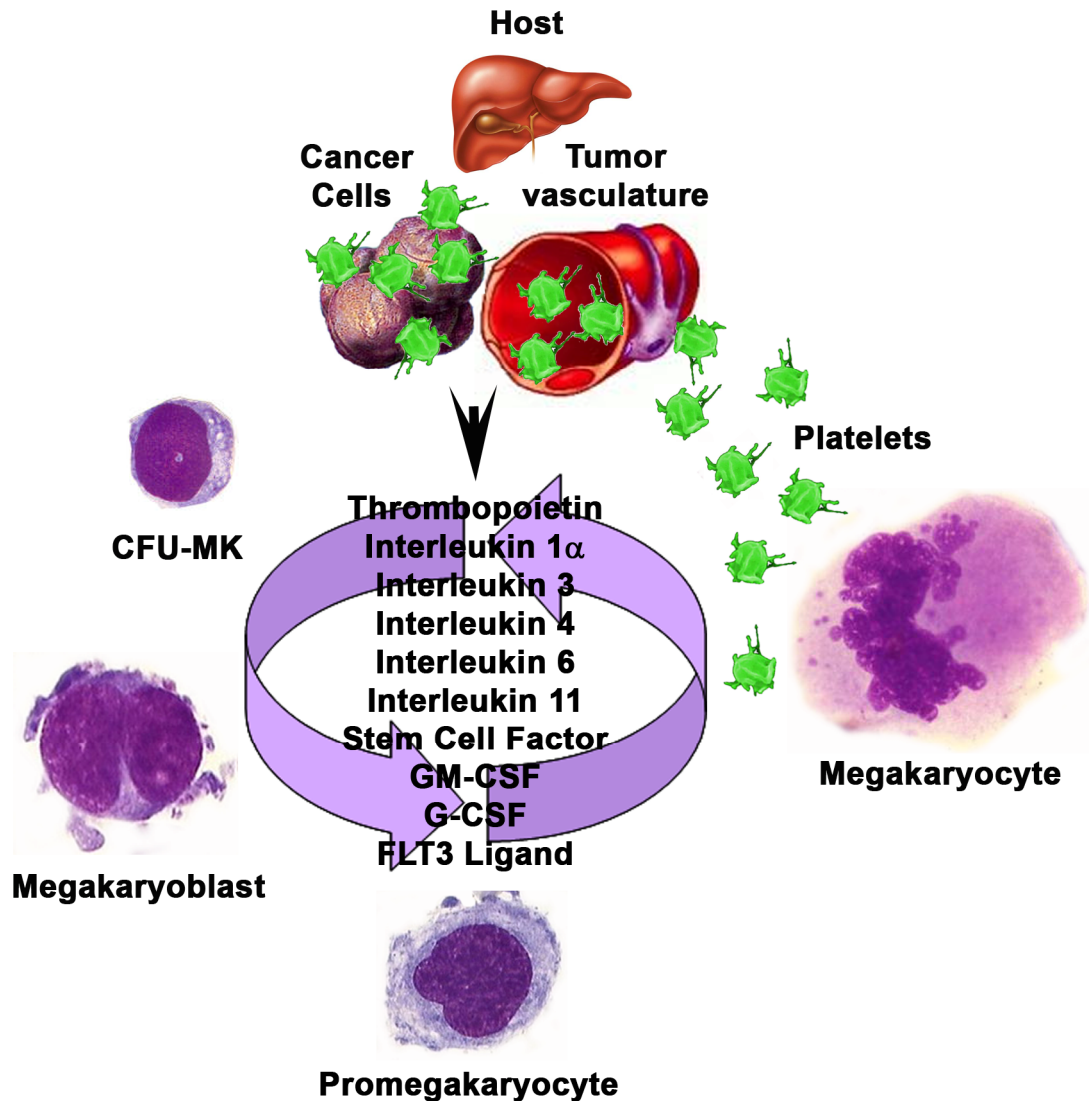


**Figure 2. Central hypothesis.** The central hypothesis of the present study is that tumor cells, constituents of the tumor microenvironment such as tumor-associated endothelial cells, and the tumor-bearing host tissues such as the liver parenchyma produce megakaryopoietic and thrombopoietic cytokines, which stimulate megakaryopoiesis and the enumeration of platelets, which in turn promote tumor growth and angiogenesis, creating a continuous feed-forward loop.



## **Methods**

### Patient clinicopathologic data analysis

Following Institutional Review Board approval, clinicopathologic data were collected on 619 women with primary epithelial ovarian, primary peritoneal, or fallopian tube carcinoma treated at one of 4 U.S. centers including University of Texas M.D. Anderson Cancer Center (MDACC) (n=150), University of Virginia (n=115), University of Iowa (n=131), and University of Maryland (n=223) between 1995 and 2007. Patients with prior histories of cancer, myeloproliferative disorders, acute inflammatory diseases or splenectomies were excluded. All patients underwent initial surgical cytoreduction by a gynecological oncologist followed by 6-8 cycles of taxane/platinum based chemotherapy. A gynecological pathologist reviewed all specimens. Staging was performed according to the International Federation of Gynecology and Obstetrics surgical staging system. Clinicopathologic data collected on all patients included age, stage, grade, histology, extent of surgical cytoreduction, progression-free interval, disease status, and overall survival. Optimal cytoreduction was defined as residual disease less than 1 cm. Platelet and leukocyte counts as well as hemoglobin (Hgb) and CA-125 at the time of initial diagnosis were also recorded for all patients. Thrombocytosis was defined as a platelet count greater than 450,000/ $\mu$ L according to the NHLBI (59). The incidence and timing of vascular thromboembolic (VTE) events were documented for patients receiving therapy at the Universities of Virginia and Iowa (n=246). The Fisher's exact test was used to test the associations between platelet count at the time of initial diagnosis and clinicopathologic variables with SAS (SAS Inc., Cary, NC). Kaplan-Meier survival curves were generated and compared using

a 2-sided log-rank statistic. Patients who were alive at the time of last follow-up were censored. The Cox proportional hazards model was used for multivariate analysis. A pre-specified subset analysis was performed in the patients for whom VTE events were known to determine the prognostic significance of VTE in patients with and without thrombocytosis. A p value < 0.05 was considered statistically significant.

#### Cell lines and culture conditions

The derivation and source of the human epithelial ovarian cancer cell lines A2780ip2, HeyA8, SKOV3ip1, OVCA433, ES2, and 2774 have been described previously (60-64). A2780ip2, HeyA8, SKOV3ip1, and ES2 cells were maintained and propagated in RPMI-1640 medium supplemented with 15% fetal bovine serum (FBS) and 0.1% gentamicin sulfate (Mediatech Inc. Manassas, VA). OVCA433 cells were maintained in MEM supplemented with 10% FBS, 1x L-glutamine (200mM stock), 1x MEM vitamins (Invitrogen, Carlsbad, CA), 1x non-essential amino acids (NEAA, Mediatech Inc. Manassas, VA), and 0.1% gentamicin sulfate. 2774 cells were maintained in MEM supplemented with 5% FBS, 1x L-glutamine, 1x sodium pyruvate (100mM stock, Invitrogen, Carlsbad, CA), 1x NEAA, and 0.1% gentamicin sulfate. HeyA8-MDR and SKOV3-TR are taxane-resistant variants of HeyA8 and SKOV3ip1, respectively (gift from Dr. Isaiah J. Fidler, MDACC, Houston, TX). The phenotype of these cell lines is maintained by adding 300 ng/mL (HeyA8-MDR) and 100 ng/mL (SKOV3-TR) of paclitaxel to complete media. ID8 and IG10 represent cell lines derived from spontaneous malignant transformation of C57BL/6 mouse ovarian surface epithelium (MOSE) cells *in vitro* (65, 66). In this instance, we used a more tumorigenic variant VEGF-mutated ID8 strain (ID8<sup>VEGF164</sup>)

generated by transfection with a retroviral vector containing VEGF-164 (gift from Dr. George Coukos, University of Pennsylvania Medical Center, Philadelphia, PA) (67). For this investigation, we also used the more tumorigenic IG10ip1 line which was developed by passaging tumors grown in the mouse intraperitoneal cavity following injection of parental IG10 cells (gift from Dr. Isaiah J. Fidler, MDACC, Houston, TX). ID8<sup>VEGF164</sup> and IG10ip1 cells were maintained in DMEM-F12 supplemented with 5% FBS, 1x insulin-transferrin-sodium selenite supplement, (Roche Diagnostics, Mannheim, Germany), and 0.1% gentamicin sulfate. The GILM2 metastatic human breast cancer cell line was established from lung metastases of GI101A cells in nude mice and has been previously characterized (gift from Dr. Janet Price, MDACC, Houston, TX) (68). GILM2 cells were maintained in DMEM-F12 supplemented with 10% FBS, 1x L-glutamine, 5% v/v insulin-transferrin-sodium selenite supplement, and 0.1% gentamicin sulfate. The Ishikawa human endometrial cancer cell line was maintained in MEM supplemented with 10% FBS and 0.1% gentamicin sulfate (gift from Dr. Russell Broaddus, MDACC, Houston, TX) (69). NOD/SCID mice bearing heterotopic pancreatic tumors derived from patient samples were a gift from Dr. Gary Gallick (MDACC, Houston, TX). The derivation and characterization of murine ovarian endothelial cells (MOECs, gift of Dr. Robert Langley, MDACC, Houston, TX) and of pericyte-like murine vascular smooth muscle cells (C3H/10T1/2, ATCC) have been described previously (70, 71). MOECs were maintained in DMEM supplemented with 5% FBS and 0.1% gentamicin sulfate. Pericyte 10T1/2 cells were maintained in BME supplemented with 10% FBS, recombinant bFGF (10 ng/mL), and 0.1% gentamicin sulfate. All experiments were

performed using cells grown to 60-80% confluence. All cell lines were routinely genotyped and tested to confirm absence of Mycoplasma.

Determination of platelet counts in mouse models of ovarian, breast, uterine, and pancreatic cancer

Female athymic nude (NCr-*nu*) and C57BL/6 mice were purchased from Taconic Farms Inc. (Rockville, MD) or Experimental Radiation Oncology (MDACC, Houston, TX), respectively. All experiments were approved and supervised by the MDACC Institutional Animal Care and Use Committee. The development and characterization of the orthotopic mouse model of advanced ovarian cancer used in this investigation has been previously described by our laboratory (72-74). Briefly, A2780ip2 ( $1 \times 10^6$ ), HeyA8 ( $0.25 \times 10^6$ ), or 2774 ( $2 \times 10^6$ ) human ovarian cancer cells resuspended in 200  $\mu$ L of Hank's balanced salt solution (HBSS, Mediatech Inc. Manassas, VA) were injected into the peritoneal cavity of female nude mice. A2780ip2 and HeyA8 reliably form macroscopic tumor implants in the adnexa, peritoneum, small bowel mesentery, omentum, and porta hepatis (tumor-bearing mice, n=9) while 2774 also produces large volume ascites (tumor- and ascites-bearing mice, n=7). Immunocompetent *in vivo* models based on syngeneic mouse ovarian epithelial cancer cells physiologically and biologically closely resemble human epithelial ovarian cancer. These models were generated by injecting ID8<sup>VEGF164</sup> or IG10ip1 ( $1 \times 10^6$ ) cells resuspended in 200  $\mu$ L HBSS into the peritoneal cavity of female C57BL/6 mice (n=6). Once tumors and/or ascites were detectable on physical exam, whole blood was collected from anesthetized mice by intra-cardiac stick and processed for complete blood counts (CBCs) by the MDACC veterinary laboratory. Blood was similarly collected and processed for CBCs from

healthy female nude and C57BL/6 mice (n=8) for comparison. Additionally, tumor weight and number of intraperitoneal metastases were quantified in the tumor- and ascites-bearing orthotopic model. The orthotopic nude mouse model of human metastatic breast cancer used in this investigation was generated by injecting  $1 \times 10^6$  GILM2 cells under direct visualization into the second mammary fat pad through a posterior incision. By 6 weeks all mice had developed  $\geq 1$  cm tumors and blood was collected for CBCs (n=7). The development and characterization of the orthotopic mouse model of uterine cancer used in this investigation has been previously described by our laboratory (75). Briefly, mice were anesthetized and a 0.5 cm incision was made in the left lower flank to expose the left uterine horn. The distal portion of the horn was brought up to the incision and a single-cell suspension of  $4 \times 10^6$  Ishikawa cells in 50  $\mu$ L was injected into the lumen. By 6 weeks, all mice had developed palpable tumors and blood was collected for CBCs (n=6). NOD/SCID mice bearing heterotopic human pancreatic cancer xenografts were obtained from Dr. Gary Gallick. Methodology for heterotopic implantation of tumor fragments from patient specimens, processing of direct xenograft tumors into single-cell suspensions, and heterotopic reimplantation of pancreatic cancer cells into NOD/SCID mice has been recently published (76). When xenografts reached approximately 1 cm in diameter, blood was collected for CBCs. All measurements are represented as the average  $\pm$  S.E. of the mean. Two-tailed Student's t-test was used to compare blood counts between tumor-bearing mice  $\pm$  ascites and healthy controls. Pearson's correlation coefficient was used to test associations between platelet counts, tumor weight, and number of intraperitoneal metastases in tumor- and ascites-bearing mice.

Characterization of the onset and longitudinal progression of thrombocytosis in an orthotopic mouse model of ovarian cancer

For this time course experiment, we utilized a HeyA8-luciferase-transfected cell line (HeyA8-Luc) that had been previously established in our laboratory with a lentivirus system (77). On day 1, 50 mice received i.p. injections of HeyA8-Luc cells and were subsequently divided into 5 groups (n=10 per group) for weekly quantification of tumor burden and platelet counts. Due to the detection limits of physical exam, bioluminescence imaging was used to detect disease in groups 1 and 2 on days 8 and 15, respectively. Bioluminescence imaging was conducted on a cryogenically cooled IVIS 100 imaging system coupled to a data acquisition computer running Living Image software (Xenogen). Before imaging, animals were anesthetized in an acrylic chamber with 1.5% isoflurane/air mixture and injected i.p. with 15 mg/mL of D-luciferin firefly potassium salt (Caliper Life Sciences, Hopkinton, MA) in PBS at a dose of 150 mg/kg body weight. A digital gray-scale animal image was acquired followed by acquisition and overlay of a pseudocolor image representing the spatial distribution of detected photon emerging from active luciferase within the animal. In our experience, the lower limit of detection for bioluminescence imaging using the IVIS system is  $0.5-1 \times 10^4$  and  $0.5-1 \times 10^6$  cells injected subcutaneously and i.p., respectively (unpublished data). The presence of macroscopic disease could be reliably detected on physical exam starting on day 22. Blood was collected for platelet counts following imaging of groups 1 and 2 on days 8 and 15 and prior to sacrificing groups 3, 4, and 5 for necropsy and measurement of tumor weight on days 22, 29, and 36, respectively.

## YFP-labeled platelet isolation, transfusion, and localization in ovarian tumors and ascites

YFP-labeled platelets were isolated from whole blood obtained from female transgenic C57BL/6 mice expressing yellow fluorescent protein (YFP) under the control of the PF4 platelet specific promoter (gift from Dr. Francisca Gushiken, Thrombosis Research Section in Baylor College of Medicine, Houston TX). In this mouse strain, YFP protein is exclusively present in megakaryocytes and platelets. We used standard techniques to collect blood and prepare platelet rich plasma (PRP) from these mice (78). Briefly, 1 mL of whole blood was withdrawn into a syringe preloaded with 1.9 v/v acid-citrate dextrose solution (ACD, 75 mM trisodium citrate, 124 mM dextrose, and 38 mM citric acid) from anesthetized mice by intracardiac stick. PRP was separated from red blood cells and leukocytes by room temperature centrifugation of citrated whole blood at 540 rpm for 10 minutes. This yielded approximately 500  $\mu$ L of PRP containing  $300 \times 10^6$  YFP-labeled platelets, which was then transfused into ID8<sup>VEGF164</sup> tumor-bearing mice by tail vein injection. After 1 hour had elapsed, recipient mice were anesthetized and perfused with 4% paraformaldehyde through the ascending aorta for 2 minutes for intravital fixation of tumor tissue. Intravital fixation was necessary in order to circumvent spillage of YFP-labeled platelets into the tumor bed that can occur as an artifact of dissecting fresh tissue. Following intravital fixation, tumors were resected, immersed in 30% sucrose overnight, and then embedded in OCT. Immunofluorescent (IF) staining of frozen sections for CD31 antigen to label the tumor vasculature was then performed. Sections were washed in PBS, blocked with 4% fish gel for 20 minutes, and probed with rat anti-mouse CD31 diluted in protein block (1:800, BD

Pharmingen, San Diego, CA) at 4°C overnight. Sections were again washed in PBS, blocked with 4% fish gel for 10 minutes, and incubated with goat anti-rat Alexa 594 diluted in protein block for 1 hour at room temperature (1:800, Invitrogen, Eugene, OR). After extensive washing in PBS, nuclei were counterstained with Hoechst (1:10,000 diluted in PBS, Invitrogen, Carlsbad, CA) for 10 minutes. Images were captured at x200 magnification. Whole mounts of ascites were immediately prepared and examined by fluorescent and confocal microscopy upon removal of ascites by paracentesis 1 hour following YFP-platelet transfusion, but prior to intravital fixation. Microscopy was performed using a band pass emission filter for peak wavelength of 519 nm given that the emission peak of YFP is 527 nm.

#### Evaluation of the effect of platelet depletion on tumor growth and biology

To deplete platelets in mice, we used an antibody preparation of purified rat monoclonal antibodies directed against mouse glycoprotein (GP) Ib $\alpha$  (CD42b, Emfret Analytics, Eibelstadt, Germany). Originally developed to study the pathogenic effects of anti-platelet antibodies in autoimmune thrombocytopenic purpura, this antibody causes irreversible Fc-independent platelet depletion in mice within 60 minutes of administration without inducing platelet activation. To identify the optimal dose and treatment schedule of antibody for subsequent therapy experiments, we first determined the dose-time kinetics of antibody mediated platelet depletion. Platelets were quantified on days 2 and 7 following a single tail vein injection of 0.5 to 4  $\mu$ g/g body weight of antibody. Given that the 0.5  $\mu$ g/g dose of antibody decreased platelet counts by 50% with return to baseline on day 4, we administered this dose of antibody every 4 days for *in vivo* studies (Figure 3).



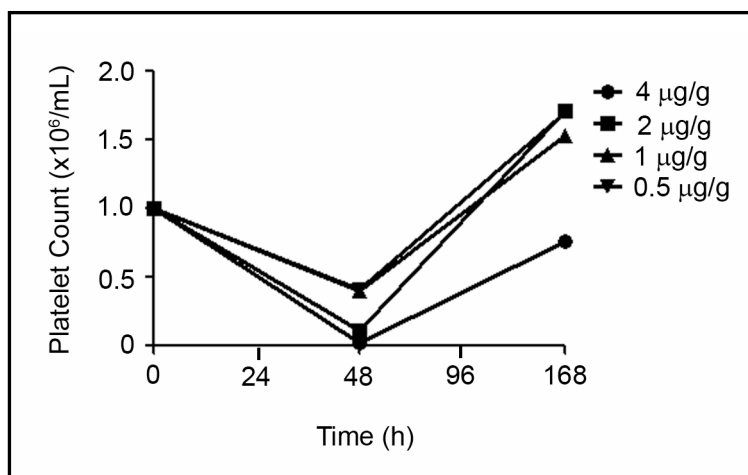


**Figure 3. Dose-time kinetics of platelet depletion in mice using anti-platelet antibody (APA, anti-mouse glycoprotein 1b $\alpha$  antibody).**

Prior to initiating *in vivo* therapy experiments, we also used flow cytometric analysis to confirm the specificity of this antibody for platelets in order to exclude the possibility that antibody recognition of cells other than platelets such as pericytes, tumor and endothelial cells might account for observed anti-tumor and/or anti-angiogenic effects. Nude mouse platelets, A2780ip2 ovarian cancer cells, MOECs, and 10T1/2 cells were incubated with the GP 1b $\alpha$  antibody for 1 hour. Antibody binding was assessed by flow cytometry following a 1 hour incubation with an anti-rat secondary antibody conjugated to APC. Only mouse platelets labeled positively. In all other instances, the APC signal did not differ from the negative control (APC secondary antibody alone) (Figure 4).

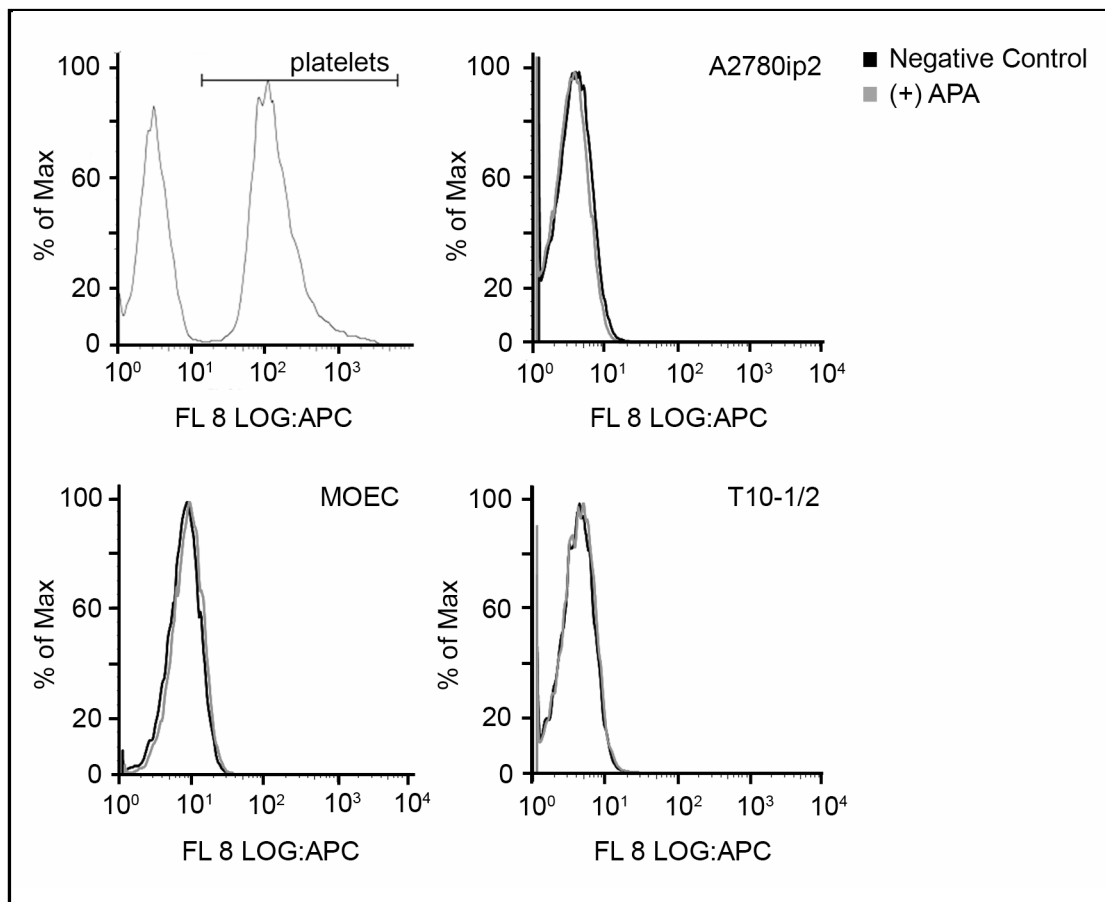


**Figure 4. Confirmation of the specificity of anti-platelet antibody (APA) for mouse platelets.** Mouse platelets, A2780ip2 human ovarian cancer cells, murine ovarian endothelial cells (MOEC), and pericyte-like murine vascular smooth muscle cells (T101/2) were incubated with APA for 1 hour. Binding of secondary antibody conjugated to APC was detected using flow cytometry.

After characterizing the activity and specificity of the antibody, we evaluated the effect of platelet depletion on tumor growth in an orthotopic mouse model of ovarian cancer. Treatment was initiated 8 days after the introduction of A2780ip2 ovarian cancer cells i.p. Mice were treated with either 0.5  $\mu$ g/g anti-GP1b $\alpha$  antibody or control IgG by tail vein injection every 4 days until they became moribund (n=10/group). Tumor weight was recorded at the time of necropsy and tumor tissue

was harvested for histopathological analysis. Proliferation index and microvessel density were evaluated in tumor sections with immunohistochemical staining for Ki67 and CD31 antigens, respectively. Frozen sections were fixed in acetone + chloroform 1:1 for 5 minutes between two 5 minute incubations in cold acetone alone. Endogenous peroxidases and non-specific epitopes were blocked with 3% H<sub>2</sub>O<sub>2</sub> in PBS and 5% normal horse serum + 1% normal goat serum in PBS, respectively. Sections were then incubated with primary antibody directed against either Ki-67 (1:200, Neomarker, Fremont, CA) or CD31 (1:800, PharMingen, San Diego, CA) at 4°C overnight. After washing with PBS, the appropriate HRP-conjugated secondary antibody in blocking solution was added for 1 hour at room temperature. Slides were developed with 3, 3'-diaminobenzidine (DAB) chromogen (Invitrogen, Carlsbad, CA) and counterstained with Gil No.3 hematoxylin (Sigma-Aldrich, St. Louis, MO). Proliferative index was calculated by dividing the number of Ki67 positive nuclei (brown) by the total number of cells for each of 5 randomly selected x200 high power fields per tumor specimen for each treatment group. MVD was calculated by viewing 5 representative x100 fields per slide in each treatment group and counting the number of microvessels per field. A microvessel was defined as an open lumen with at least one CD31-positive cell immediately adjacent to it (79, 80).

Dual immunofluorescent staining for CD31 and desmin was used to assess pericyte coverage. Fixed frozen sections were first probed with CD31 antibody as described above. After washing with PBS, the sections were incubated with Alexa 594-conjugated anti-rat antibody (1:1000, Invitrogen, Eugene, OR) for 1 hour at room temperature. After extensive washing with PBS, sections were next probed

with anti-desmin antibody (1:400, DakoCytomation, Denmark) for 2 hours, followed by washing with PBS and incubation with Alexa 488-conjugated anti-rabbit antibody (1:1000, Invitrogen) for 1 hour at room temperature. Nuclei were counterstained with Hoechst. To quantify pericyte coverage, we calculated the endothelial cell (red staining) to pericyte ratio (green staining) for 5 random high power fields at x200 magnification by dividing the number of pericytes by the number of endothelial cells.

Tumor and endothelial cell apoptosis was examined with dual immunofluorescent staining for CD31 and terminal deoxynucleotidyl transferase dUTP nick end labeling (TUNEL). Fixed frozen sections were first probed with CD31 antibody, as described above. Slides were washed in PBS, fixed again in 4% paraformaldehyde in PBS, washed twice in PBS, and incubated with 0.2% Triton X-100 in PBS for 15 minutes. After two more washes in PBS, slides were incubated for 10 minutes with the equilibration buffer in the TUNEL detection kit (Promega, Madison, WI). Equilibration buffer was removed, and reaction buffer (consisting of equilibration buffer in the kit, fluorescein-12-dUTP [where dUTP is deoxyribouridine triphosphate], and terminal deoxynucleotidyltransferase) was then added. After 1-hour incubation at 37°C in the dark, the reaction was stopped by addition of the provided 2x standard saline-buffered citrate (8.77 g of NaCl, 4.41 g of sodium citrate, and 400 mL of deionized water) for 15 minutes. Excess dUTP was removed by washing, and nuclei were stained with Hoechst (Molecular Probes, in PBS; 1.0 µg/mL) for 10 minutes. The total number of apoptotic tumor cells (green nuclei alone) and CD31-positive cells (red cells plus green nuclei) were counted. Controls included exposure to only secondary antibodies, exposure to reaction buffer that did not contain terminal deoxynucleotidyltransferase, and exposure to DNase to

fragment the DNA (positive control). Apoptotic cells were counted in 5 random microscopic fields from each tumor at x200 magnification. Microscopy was performed with a Zeiss AxioPlan 2 microscope, Hamamatsu ORCA-ER digital camera, and ImagePro software. All measurements are represented as the average  $\pm$  S.E. of the mean. Two-tailed Student's t test was used to make comparisons between the two treatment groups. A p-value of  $< 0.05$  was considered statistically significant.

*In vitro* assays evaluating the effect of platelets on ovarian cancer cell migration, proliferation, and survival

Citrated plasma is not an ideal medium for evaluating platelet function due to factors such as plasma protein content, calcium chelation, and platelet agglutination by the action of thrombin. Therefore, we used plasma-free platelets prepared with sterile technique for *in vitro* assays. Whole blood withdrawn into a syringe preloaded with 1.9 v/v acid-citrate dextrose solution from anesthetized mice by intracardiac stick was gently mixed with 1:1 v/v tyrodes buffer (140 mM NaCl, 2.7 mM KCl, 12 mM NaHCO<sub>3</sub>, 6.45 mM NaH<sub>2</sub>PO<sub>4</sub>, 5.5 mM glucose in diH<sub>2</sub>O) lacking Mg<sup>2+</sup> and Ca<sup>2+</sup>. PRP was separated from red blood cells and leukocytes by room temperature centrifugation of blood at 540 rpm for 10 minutes. A plasma-free platelet suspension was then prepared by passing PRP through a gel filtration column of Sepharose 2B (Sigma Aldrich, St Louis, MO). Specifically, a siliconized glass column containing a 10  $\mu$ m nylon net filter was assembled (Millipore, Billerica, MA). Sepharose 2B beads were equilibrated by washing in acetone (3-4 vol.), followed by 0.9% NaCl (5-6 vol.), and buffer 1 (5-6 vol. 134 mM NaCl, 12 mM NaHCO<sub>3</sub>, 2.9 mM KCl, 0.34 mM Na<sub>2</sub>HPO<sub>4</sub>, 1 mM MgCl<sub>2</sub>, 10 mM Hepes, 5 mM

glucose, 0.3g/100 mL BSA, pH 7.4). The beads were loaded onto the column and washed again with buffer 1 (2-3 vol.). PRP was then applied to the column and allowed to completely enter the gel before adding additional buffer 1 (2-3 vol.). The eluate was discarded until it began to change from clear to opaque, signifying the presence of platelets. The opaque platelet fraction was collected in a fresh polyethylene tube until the eluate again began to clear. Platelets were counted with a hemocytometer by phase microscopy at x400 magnification. Platelets present in all 25 of the small squares in the center of each chamber of the hemocytometer were counted and the mean value gives a platelet count  $\times 10^3/\mu\text{L}$ .

Migration assays were performed to determine if ovarian cancer cells have a chemotactic response to platelets. A modified Boyden chamber with upper and lower wells separated by a 0.1% gelatin coated cell-permeable membrane was used for these assays. Platelets ( $100 \times 10^6$ ) or equal volumes of buffer 1 were added to serum free cell culture media in the bottom wells. Since platelets were eluted in buffer 1, an equal volume of buffer 1 was used as the vehicle control. A2780ip2, HeyA8, or 2774 ovarian cancer cells suspended in serum free cell culture media were added to the top wells (100,000 cells per well). Chambers were incubated for 6 hours at 37°C. At completion, cells in bottom chambers were removed with 0.1% EDTA, loaded onto a 3.0 micron polycarbonate filter (Osmonics, Livermore, CA) using an S&S Minifold I Dot-Blot System (Schleicher & Schuell, Keene, NH), fixed, stained, and counted by light microscopy. Cells from 5 random fields (final magnification x100) were counted.

The effect of platelets on ovarian cancer cell proliferation and survival was evaluated in A2780ip2, HeyA8, SKOV3ip1, OVCA433, ES2, and 2774 cell lines.

Plasma-free platelets were prepared as described above. For proliferation assays, cells were plated in 6-well plates (50,000 per well) and serum starved overnight. The following day,  $20 \times 10^6$  platelets suspended buffer 1 were directly added to each well for a final concentration of  $10 \times 10^6$  platelets per mL serum free media. Cells treated with an equal volume of buffer 1 served as controls. After cells were co-cultured with platelets for 24 hours, the percentage of proliferating cells was determined using the Click-iT EdU flow cytometry assay kit (Invitrogen). Cells were incubated with 10  $\mu$ M 5-ethynyl-2'-deoxyuridine (EdU, modified BrdU nucleoside analog) for 1 hour, harvested, and washed with 1% BSA/PBS. Following overnight fixation with 4% paraformaldehyde in PBS at 4°C, cells were washed in 1% BSA/PBS and permeabilized with 1X saponin-based permeabilization reagent for 20 minutes at room temperature. S-phase cells were then detected by incubating cells with Click-iT detection cocktail containing 1x Click-iT reaction buffer,  $\text{CuSO}_4$ , Alexa Fluor 488 azide dye, and reaction buffer additive for 30 minutes at room temperature prior to flow cytometry.

For cytotoxicity assays, cells were plated in 10 cm plates (300,000 per plate). The following day  $100 \times 10^6$  platelets were directly added to each well for a final concentration of  $10 \times 10^6$  platelets per mL of serum free media  $\pm$  0.5 nM docetaxel. Cells treated with an equal volume of buffer served as controls. After co-culturing cells with platelets  $\pm$  docetaxel for 72 hours, cell viability was assessed with propidium iodide (PI) by flow cytometry. Cells were harvested, washed in PBS, and fixed with 20% EtOH in PBS at 4°C overnight. Prior to flow cytometric analysis, cells were washed in PBS and incubated with 500  $\mu$ L PI + RNase (50  $\mu$ g/mL in PBS + 20  $\mu$ g/mL RNase) for 10 minutes.

Western blot analysis was used to evaluate PDGFR $\alpha$  expression in the ovarian cancer cell lines subjected to proliferation and cytotoxicity experiments as well as in the taxane-resistant cell lines HeyA8-MDR and SKOV3-TR. Cell lysate was prepared from ovarian cancer cells in log growth phase at 70% confluency. Cells were washed with PBS, lifted by scraping, and lysed with modified radioimmunoprecipitation assay (RIPA) lysis buffer with 1x protease inhibitor (Roche, Mannheim, Germany) and 1 mM sodium orthovanadate for 20 minutes on ice. Cell lysate was centrifuged at 13,000 rpm for 20 min at 4°C. Protein concentration was determined by a bicinchoninic acid protein assay reagent kit. Forty micrograms of protein from whole-cell lysate was fractionated by 6% SDS-PAGE, transferred to nitrocellulose, blocked with 5% nonfat milk for 1 hour at room temperature and probed with primary antibody (1:500, Millipore, Temecula, CA) at 4°C overnight. Blots were then incubated with horseradish peroxidase conjugated anti-rabbit secondary antibody (1:3000, The Jackson Laboratory, Bar Harbor, ME). Blots were developed with use of an enhanced chemiluminescence detection kit (ECL, Amersham Pharmacia Biotech, Piscataway, NJ). To ensure equal protein loading, a monoclonal vinculin antibody (1:1000, Sigma-Aldrich, St. Louis, MO) was used.

To determine whether taxane resistance conferred by platelets could be mediated through PDGFR $\alpha$ , SKOV3ip1 cells were pretreated with the fully humanized anti-PDGFR $\alpha$  antibody, IMC-3G3 (100  $\mu$ g/mL in PBS, Imclone, New York, New York), for 2 hours. Treatment was then continued with either IMC-3G3, 0.5 nM docetaxel, or the combination  $\pm$  platelets ( $10 \times 10^6$ /mL) for 72 hours. Flow cytometric assay of PI staining was used to quantify cell death as described above.



All measurements are reported as mean change relative to vehicle control  $\pm$  SEM of triplicate experiments. Two-tailed Student's t test was used to make comparisons between groups. A p-value of  $< 0.05$  was considered statistically significant.

#### Megakaryocyte quantification

The lung, liver, spleen, and femur/tibia were harvested from healthy nude mice and mice with A2780ip2, HeyA8, and 2774 orthotopic human ovarian cancers (n = 5 per group), fixed in 10% buffered formalin overnight, paraffin embedded, and sectioned. Prior to paraffin embedding, bones were decalcified in 10% EDTA (pH 7.4) for 10 days. Tissue sections were hemotoxylin-eosin stained and examined by light microscopy. Mature megakaryocytes were readily identified by their large size (50-100  $\mu$ m), multilobulated nuclei, and abundant granular, eosinophilic cytoplasm (81). The number of megakaryocytes per 5 randomly selected x200 high power fields was recorded. Pearson's correlation coefficient was used to test the associations between mean platelet counts and mean megakaryocyte counts in the spleen and bone marrow across control and tumor-bearing mice  $\pm$  ascites.

#### Detection of thrombopoietin transcript by RT-PCR

Total RNA was extracted from A2780ip2 and 2774 cells growing *in vitro* and liver tissue from healthy nude mice and mice with orthotopic HeyA8 tumors using guanidinium thiocyanate-phenol-chloroform (TRIzol, Invitrogen) extraction. Cells were washed twice with cold PBS and fresh frozen liver (0.3 grams per sample) was pulverized to a fine powder in liquid nitrogen by mortar and pestle before the addition of 1 mL of TRIzol. Samples were transferred to sterile microfuge tubes, combined with 200  $\mu$ L of chloroform, and centrifuged at 12,000 g for 10 minutes at 4°C. The upper aqueous layer was then transferred to a fresh tube and RNA was

precipitated by adding 0.5 mL of isopropanol. RNA was pelleted by centrifugation, washed once with 75% ethanol, and dissolved in 25  $\mu$ L of RNase-free water. RNA was quantified by spectrophotometer and 1  $\mu$ g transcribed into complementary DNA (cDNA) using the Verso cDNA kit (Thermo Fisher Scientific) according to the manufacturer's protocol. The cDNA was then used for PCR amplification of TPO and  $\beta$ -actin according to the following conditions: 94 °C for 5 minutes for denaturing, followed by 32 cycles of melting at 94 °C for 45 seconds and annealing-extending with Taq thermostable polymerase (at the  $T_m$  specific to the primer set) for 60 seconds, followed by a final step at 72 °C for 10 minutes. The primers used for PCR amplification were human TPO sense (5'-TGTCCTTCACAGCAGACTGA-3') and antisense (5'-GTGTTGGAAGCTCAGGAAGA-3')  $T_m$  55°C, murine TPO sense (5'-CCCAATGCCCTCTTCTTGAG-3') and antisense (5'-GAGCAAGGCTTGGAGAAGGA-3')  $T_m$  66°C, and  $\beta$ -actin sense (5'-ATCTGGCACCCACACCTTCTACAATGA-3') and antisense (5'-CGTCATACTCCTGCTTGCTGATCCAG-3')  $T_m$  62°C. Amplified PCR products were analyzed by electrophoresis on 1.5% agarose gel with Tris-borate-EDTA buffer and visualized under UV light after staining with ethidium bromide.

#### Detection of thrombopoietin protein expression by immunohistochemical staining

Immunohistochemical staining was used to assess TPO expression in A2780ip2, HeyA8, and 2774 tumors and in a panel of 10 human serous papillary ovarian cancers (5 patients with normal platelet counts and 5 patients with thrombocytosis). Paraffin embedded tumor sections were deparaffinized sequentially in xylenes and declining grades of ethanol prior to rehydration. Antigen retrieval was performed by steaming slides at 100°C for 30 minutes in 0.01M

sodium citrate buffer, pH 6.0. Nonspecific epitopes were blocked with 10% fish gelatin in 1x TBS with Tween (TBST). Sections were incubated with rabbit anti-human thrombopoietin antibody (1:1000) overnight at 4°C. After washing with TBST, sections were incubated with 4plus biotinylated anti-rabbit IgG followed by 4plus streptavidin-HRP (Biocare Medical, Concord, CA) for 20 minutes at room temperature. Slides were developed with DAB chromogen (Invitrogen) and counterstained with Gil No.3 hematoxylin (Sigma-Aldrich).

#### Multiplex platform for quantification of megakaryo- and thrombopoietic cytokine levels in patient plasma samples

Quantitative multiplex detection of plasma cytokines in banked plasma collected from 150 patients at the time of primary tumor reductive surgery for advanced, high grade epithelial ovarian cancer was accomplished using Milliplex™ human cytokine/chemokine panels (Millipore) coupled with the Luminex® xMAP® platform. Platelet counts obtained at preoperative clinic visits were recorded for each patient. Banked plasma was separated from whole blood collected in EDTA blood collection tubes by centrifuging for 10 minutes at 1000 g. We customized human cytokine panel I for detection of Flt-3 Ligand, G-CSF, GM-CSF, IL-1 $\alpha$ , IL-3, IL-4, and IL-6. Human cytokine panel II was customized for TPO and SCF and panel III was customized for IL-11. Immunoassay procedure was executed according to the manufacturer's protocol. Briefly, microtiter filter plates were prewetted with assay buffer on a plate shaker for 10 minutes at room temperature. Assay buffer was removed by vacuum and each standard or positive control was added to the appropriate wells. Assay buffer was used for the 0 pg/mL standard (background). After adding assay buffer and serum matrix to the sample wells, 25  $\mu$ L of each

patient sample was added to the appropriate wells in duplicate. Prior to use in the assay, patient plasma samples were thawed on ice, mixed well by vortexing, and centrifuged at 1100 rpm for 3 minutes. Antibody-immobilized beads for detection of individual cytokines were mixed by sonication and vortexing. For cytokine panel I, 60  $\mu$ L aliquots of antibody-immobilized beads directed against Flt-3 Ligand, G-CSF, GM-CSF, IL-1 $\alpha$ , IL-3, IL-4, or IL-6 were combined and brought to a final volume of 3 mL with bead diluent. For cytokine panel II, 60  $\mu$ L aliquots of antibody-immobilized beads directed against TPO or SCF were combined and brought to a final volume of 3 mL with bead diluent. For cytokine panel III, 60  $\mu$ L of antibody-immobilized beads directed against IL-11 was combined with 2.94 mL of bead diluent. After adding 25  $\mu$ L of mixed beads corresponding to the cytokines included in panels I, II, or III to the wells of the appropriate microtiter plates, plates were incubated with agitation on a plate shaker for 1 hour at room temperature. Fluid was completely removed by vacuum, leaving the bound immunobeads behind to be incubated with detection antibodies followed by streptavidin-phycoerythrin for 30 minutes. Fluid was removed by vacuum, the plates were washed twice, and sheath fluid added to all wells. The plates were run on a Luminex 200™ platform and the Median Fluorescent Intensity (MFI) data were analyzed using a 5-parameter logistic curve-fitting method for calculating cytokine concentrations in patient samples. To determine whether plasma thrombopoietic cytokine levels were associated with platelet count, we calculated Spearman's  $r$  for each pairwise association and tested for a statistically significant difference from 0. We used Wilcoxon rank sum test to test differences in cytokine levels between patients with normal platelet counts and

patients with thrombocytosis. A p-value < 0.05 was considered statistically significant.

Use of human- and murine-specific ELISAs for quantification of plasma IL-6, GCSF, and TPO levels in mouse models of ovarian cancer

Whole blood from healthy control mice and mice with A2780ip2, HeyA8, 2774, and ID8 tumors (n=4 per group) was collected by intracardiac stick with syringes preloaded with 0.1cc of ACD anticoagulant. Plasma was isolated by centrifugation at 1800 rpm for 10 minutes and stored at -80°C until use. Plasma IL-6, GCSF, and TPO levels were measured using human- and murine-specific Quantikine® ELISAs in order to differentiate between orthotopic human ovarian cancers and the murine host as the source of cytokine production (R&D Systems, Minneapolis, MN). The assays were performed as recommended by the kit manufacturer. After development of the colorimetric reaction, the absorbance at 450 nm was quantified by spectrophotometer and the absorbance readings were converted to pg/ml based on standard curves generated with recombinant cytokine in each assay. Absorbance readings never exceeded the linear range of the standard curves. Differences in cytokine expression from baseline levels in healthy controls were tested using Student's t-test with significance set at  $p < 0.05$ .

*In vivo* experiments evaluating the effect of silencing IL-6, G-CSF, and TPO on thrombocytosis

Human- and murine-specific siRNA oligonucleotides targeted against IL-6, G-CSF, and TPO mRNA were purchased from Sigma-Aldrich (The Woodlands, TX). Three oligonucleotides designed against each target except human G-CSF were initially screened for efficacy of gene silencing *in vitro*. Human G-CSF siRNA was

not included because A2780ip2 and 2774 human ovarian cancer cells were not found to express G-CSF. The siRNA oligonucleotide sequences that we screened are listed in Table 4. The sequence that most effectively blocked the expression of each target was selected for gene silencing *in vivo* and is highlighted in red.

**Table 4.** siRNA sequences screened for targeting TPO, IL-6, and G-CSF

siRNA oligo ID	Sense Sequence	Anti-sense Sequence
hTPO sequence 1	5'GACAUUCUGGGAGCAGUGA3'	5'UCACUGCUGCCAGAAUGUC3'
<b>hTPO sequence 2</b>	<b>5'GACAUUCCUCAGGAACAU3'</b>	<b>5'AUGUCCUGAGGAAAUGUC3'</b>
hTPO sequence 3	5'GAGACAACUGGACAAGAUU3'	5'AAUCUUGUCCAGUUGUCUC3'
mTPO sequence 1	5'GAGAUAUACUGCUCUUGAU3'	5'AUCAAGAGCAGUAUAUCUC3'
<b>mTPO sequence 2</b>	<b>5'CACUAAACAAGUCCCAA3'</b>	<b>5'UUUGGGAACUUGUUUAGUG3'</b>
mTPO sequence 3	5'GAAUUAACAGGCUAUCACU3'	5'AGUGAUAGCCUGUUAUUC3'
<b>hIL-6 sequence 1</b>	<b>5'CUUCCAUCUGGAUUCAAU3'</b>	<b>5'AUUGAAUCCAGAUUGGAAG3'</b>
hIL-6 sequence 2	5'CUCACCUCUUCAGAACGAA3'	5'UUCGUUCUGAAGAGGUGAG3'
hIL-6 sequence 3	5'CAUGUAACAAGAGUAACAU3'	5'AUGUUACUCUUGUUACAUG3'
mIL-6 sequence 1	5'CGAUGAUGCACUUGCAGAA3'	5'UUCUGCAAGUGCAUCAUCG3'
<b>mIL-6 sequence 2</b>	<b>5'GCAUAUCAGUUUGUGGACA3'</b>	<b>5'UGUCCACAACUGAUUAGC3'</b>
mIL-6 sequence 3	5'CAGAAACUCUAAUUCAUAU3'	5'AUAUGAAUUAGAGUUUCUG3'
<b>mGCSF sequence 1</b>	<b>5'CCUUCCAGAUAGUUUAUU3'</b>	<b>5'AAUAAACUAUCUGGAAAGG3'</b>
mGCSF sequence 2	5'GGAAGGAGAUGGGUAAUAU3'	5'UAUUUACCCAUCUCCUUC3'
mGCSF sequence 3	5'GCUUAAGUCCUGGAGCAA3'	5'UUGCUCCAGGGACUUAAGC3'

For *in vitro* screening, siRNA (5 µg) was incubated with 30 µL Lipofectamine 2000 reagent (Invitrogen) for 20 minutes at room temperature and added to cells grown to 50% confluence in 10 cm culture plates. The transfection was exchanged with serum containing media after 6 hours, and cells harvested at 24, 36, 48, and 72 hour time points following transfection for assessment of target knockdown by RT-PCR, western blot, or ELISA. A nontargeting siRNA sequence, shown by BLAST search to not share sequence homology with any known human or murine mRNA (target sequence 5'-AAUUCUCCGAACGUGUCACGU-3') was used as control. RT-PCR was used to screen candidate human (hTPO) and murine (mTPO) TPO siRNA sequences for efficacy of TPO gene silencing. MOEC and 2774 cells were

harvested 24 and 48 hours following transfection with murine or human TPO siRNA oligonucleotides, respectively. RNA extraction, cDNA synthesis, and PCR amplification of human TPO, murine TPO, and  $\beta$ -actin were performed as previously described. Amplified PCR products were analyzed by electrophoresis on 1.5% agarose gel with Tris-borate-EDTA buffer and visualized under UV light after staining with ethidium bromide. Near complete silencing of human and murine TPO expression was achieved by 48 hours using siRNA sequence 2 in each case. (Figure 5, green boxes).

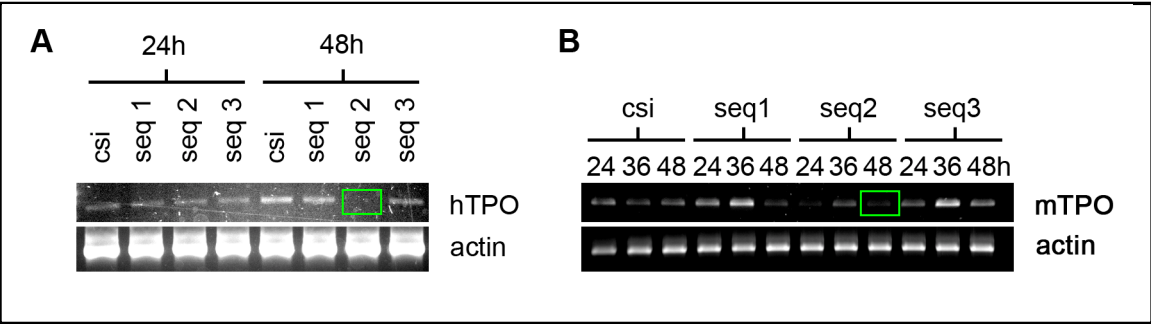


**Figure 5. Selection of effective siRNA sequences for targeting thrombopoietin.** RT-PCR was used to screen three candidate human thrombopoietin (hTPO) (a) and murine thrombopoietin (mTPO) (b) siRNA sequences (seq 1-3). A nontargeting siRNA sequence was used as control (csi).

Human TPO knockdown with siRNA sequence 2 was then validated at the protein level using western blot analysis. Cells were transfected with human TPO siRNA sequence 2, harvested at 24, 48, and 72 hour time points, and lysed with modified radioimmunoprecipitation assay (RIPA) lysis buffer with 1x protease inhibitor (Roche, Mannheim, Germany) and 1 mM sodium orthovanadate for 20

minutes on ice. Cell lysate was centrifuged at 13,000 rpm for 20 min at 4°C. Protein concentration was determined by a bicinchoninic acid protein assay reagent kit. Forty micrograms of protein from whole-cell lysate was fractionated by 12% SDS-PAGE, transferred to nitrocellulose, blocked with 5% nonfat milk for 1 hour at room temperature and probed with rabbit anti-TPO primary antibody (1:500, Abcam, Cambridge, MA) at 4°C overnight. Blots were then incubated with horseradish peroxidase conjugated anti-rabbit secondary antibody (1:3000, The Jackson Laboratory, Bar Harbor, ME). Blots were developed with use of an enhanced chemiluminescence detection kit (ECL, Amersham Pharmacia Biotech, Piscataway, NJ). To ensure equal protein loading, a monoclonal anti- $\beta$ -actin antibody (1:2000, Sigma-Aldrich, St. Louis, MO) was used. At 72 hours following transfection with hTPO siRNA sequence 2, human TPO protein expression was reduced by 75% (Figure 6).

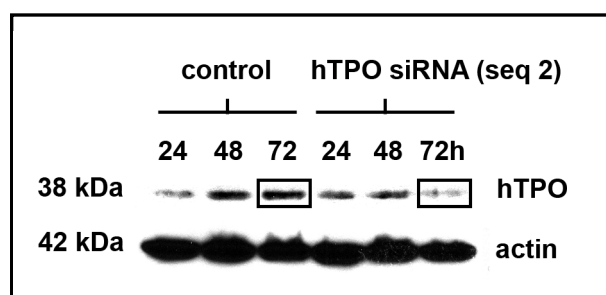


**Figure 6. Validation of human thrombopoietin silencing at the protein level.**

Western blot analysis was used to validate effective human TPO (hTPO) knockdown with hTPO siRNA sequence 2 at the protein level. A nontargeting siRNA sequence was used as control.



Human- and murine-specific ELISAs for IL-6 were used to screen human and murine IL-6 siRNA sequences for efficacy of IL-6 gene silencing. MOEC and 2774 cells were transfected with siRNA directed against murine and human IL-6, respectively. Cells were harvested at 24, 48, and 72 hour time points and lysed with modified radioimmunoprecipitation assay (RIPA) lysis buffer with 1x protease inhibitor (Roche, Mannheim, Germany) and 1 mM sodium orthovanadate for 20 minutes on ice. Cell lysate was centrifuged at 13,000 rpm for 20 min at 4°C. Protein concentration was determined by a bicinchoninic acid protein assay reagent kit. Fifty micrograms of protein from whole-cell lysate was used to perform ELISAs according to the manufacturer's protocol. After development of the colorimetric reaction, the absorbance at 450 nm was quantified by spectrophotometer and the absorbance readings were converted to pg/ml based upon standard curves generated with recombinant human or mouse recombinant cytokine. At 72 hours, transfection with sequence 1 reduced human IL-6 protein expression by 60% and transfection with murine sequence 2 reduced murine IL-6 protein expression by 70% compared to control siRNA (Figure 7a & b).

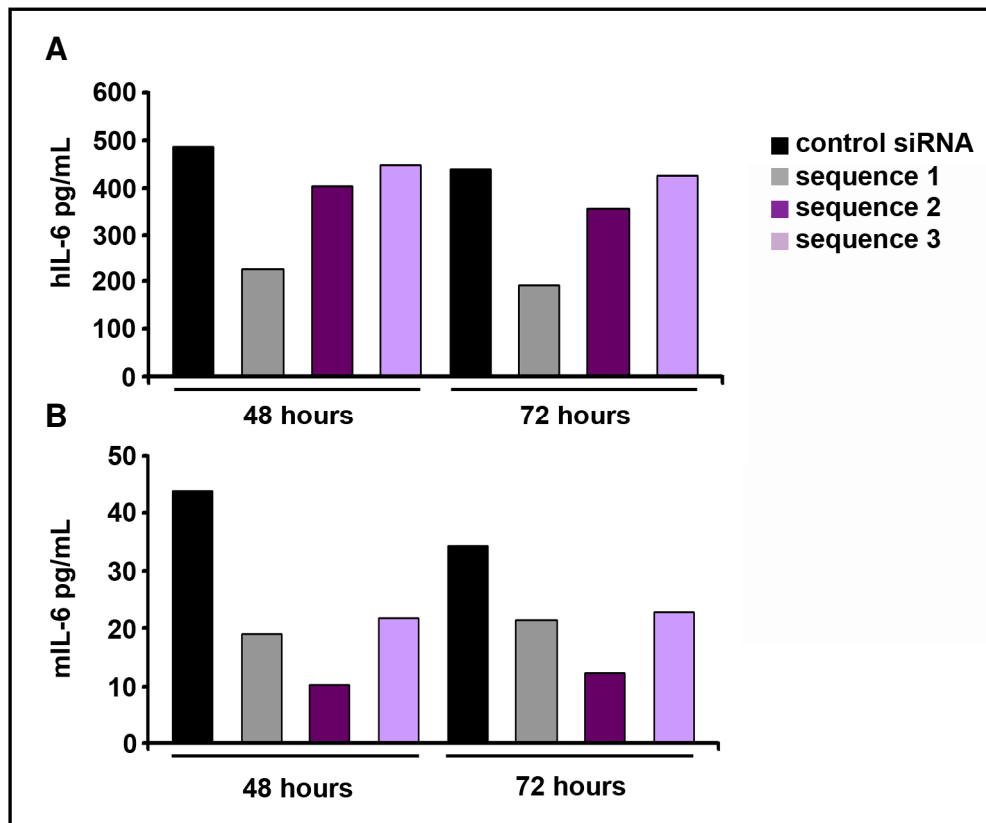


**Figure 7. Selection of effective siRNA sequences for targeting IL-6.** ELISA immunoassays were used to screen three candidate human IL-6 (hIL-6) (a) and murine IL-6 (mIL-6) (b) siRNA sequences. A nontargeting siRNA sequence was used as control.

RT-PCR was used to screen murine G-CSF siRNA sequences for efficacy of G-CSF gene silencing. MOEC cells were harvested 24, 36, and 48 hours following transfection with murine G-CSF siRNA oligonucleotides. RNA extraction and cDNA synthesis were performed as previously described. PCR amplification was performed according to the following conditions: 94°C for 5 minutes for denaturing, followed by 32 cycles of melting at 94°C for 45 seconds and annealing-extending with Taq thermostable polymerase at 66°C for 60 seconds, followed by at final step

at 72°C for 10 minutes. The primers used for PCR amplification were murine G-CSF sense (5'-CTTCCCTGAGTGGCTGCTCT-3') and antisense (5'-AGCCCTGCAGGTACGAAATG-3'). Amplified PCR products were analyzed by electrophoresis on 1.5% agarose gel with Tris-borate-EDTA buffer and visualized under UV light after staining with ethidium bromide. Near complete silencing of murine G-CSF transcript was achieved with sequence 1 (Figure 8).

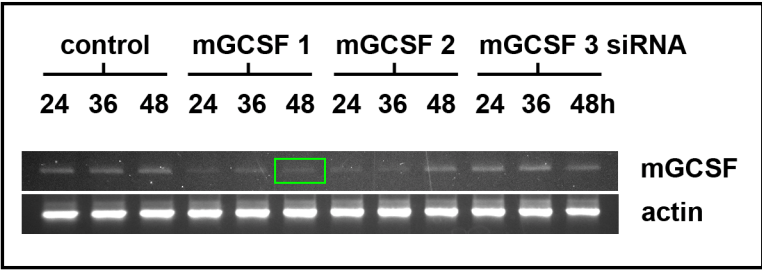


**Figure 8. Selection of effective siRNA sequences for targeting murine G-CSF.** RT-PCR was used to screen three candidate murine G-CSF siRNA sequences (mGCSF 1-3). A nontargeting siRNA sequence was used as control.

After selecting the most effective of three candidate siRNA oligonucleotides for targeting the human and mouse homologs of each cytokine, siRNA oligonucleotides were incorporated into chitosan nanoparticles (spherical, 100-200 nm size) for systemic *in vivo* delivery. Here, we utilized chitosan because of its advantageous biological properties such as biodegradability and biocompatibility with regards to low immunogenicity and lack of toxicity (82). Unpublished data from our laboratory also confirm highly efficient delivery of siRNA incorporated into chitosan nanoparticles into both tumor and tumor-associated endothelial cells (83). Effective delivery of siRNA to endothelial cells was an important consideration for these *in*

*vivo* studies because vascular and liver sinusoidal endothelial cells are rich sources of G-CSF and TPO, respectively (84). Additionally, immunohistochemical staining of patient and *in vivo* ovarian cancer specimens revealed high TPO expression by tumor-associated endothelial cells. Chitosan (CH, molecular weight 50-190 kDa), sodium tripolyphosphate (TPP), and agarose were purchased from Sigma Co. (St. Louis, MO). SiRNA/CH nanoparticles were prepared based on ionic gelation of anionic TPP and siRNA with cationic CH using a 3:1 ratio of CH:TPP. Specifically, CH was dissolved in 0.25% acetic acid and nanoparticles spontaneously generated upon the addition of TPP (0.25% w/v) and siRNA (1  $\mu\text{g}/\mu\text{L}$ ) to CH solution under constant stirring at room temperature. After incubating at 4°C for 40 minutes, siRNA/CH nanoparticles were collected by centrifugation at 12,000 rpm for 40 minutes at 4°C. The pellet was washed 3 times to remove unbound chemicals or siRNA and siRNA/CH nanoparticles were stored at 4°C until used.

The effect of silencing TPO, IL-6, and G-CSF on thrombocytosis was evaluated in two orthotopic mouse models of ovarian cancer previously shown to consistently develop paraneoplastic thrombocytosis. Nude mice were injected with either A2780ip2 ( $1 \times 10^6$  cells/0.2cc HBSS) or 2774 ( $2 \times 10^6$  cells/0.2cc HBSS) human ovarian cancer cells intraperitoneal. After 3-4 weeks, mice had developed palpable tumors in the adnexa and/or omentum and were randomly allocated to one of 5 treatment groups (n = 8 mice/group per cell line): 1) control siRNA/CH, 2) Hs + Mm IL-6 siRNA/CH, 3) Hs + Mm TPO siRNA/CH, 4) Mm G-CSF siRNA + control siRNA/CH, 5) combination IL-6 (Hs + Mm), TPO (Hs + Mm), and Mm G-CSF siRNA/CH. Mice were treated by tail vein injection with 100  $\mu\text{L}$  siRNA/CH nanoparticles which delivered 5 $\mu\text{g}$  siRNA per target every 72 hours for 1 week.

Mice were sacrificed 24 hours after the 3<sup>rd</sup> treatment following intracardiac stick to collect blood for determination of platelet counts by CBCs. Tumor and ascites were carefully measured to ensure uniformity across treatment groups. Since we previously showed that platelet counts correlate with tumor burden, we did not want differences in tumor burden between treatment groups to confound our results.

### Statistical analyses

Details regarding statistical analyses and power considerations used to evaluate individual datasets are embedded in the corresponding methods sections above. Briefly, the Fisher's exact test was used to test the associations between platelet count at the time of initial diagnosis and clinicopathologic variables with SAS. Kaplan-Meier survival curves were generated and compared using a 2-sided log-rank statistic. The Cox proportional hazards model was used for multivariate analysis. Two-tailed Student's t-test was used to test differences in sample means for data resulting from *in vivo* and *in vitro* experiments. Pearson's correlation coefficient was used to test associations between platelet counts, tumor weight, and number of intraperitoneal metastases in tumor- and ascites-bearing mice. A p value < 0.05 was considered statistically significant. To determine whether plasma thrombopoietic cytokine levels were associated with platelet count, we calculated Spearman's r for each pairwise association and tested for a statistically significant difference from 0. With 150 patients we had 82% power to detect a correlation of magnitude 0.28 or higher using a 2-sided z-test with 1% statistical significance. Additionally, we used t-tests to determine whether thrombopoietic cytokines differ between patients with normal platelet counts and thrombocytosis. We had 80%

power to detect a difference of 0.6 standard units between groups using a 2-sided test with 1% statistical significance given a 30% prevalence rate of thrombocytosis.

## Results

### Prevalence and clinical significance of thrombocytosis in epithelial ovarian carcinoma

To ascertain the prevalence and clinical significance of thrombocytosis in epithelial ovarian carcinoma, patient data were collected on 619 women from 4 U.S. centers and used to test associations between platelet count at the time of initial diagnosis, clinicopathologic factors, and outcome. Mean platelet counts in women with and without thrombocytosis were 558,410/ $\mu$ L and 316,570/ $\mu$ L, respectively (Table 5).

<b>Table 5. Platelet counts in patients with invasive ovarian cancer</b>			
	<b>All Patients (N = 619)</b>	<b>No Thrombocytosis (N = 427)</b>	<b>Thrombocytosis (N = 192)</b>
<b>Platelet Count</b>			
N	619	427	192
Mean (SD)	391.46 (135.71)	316.57 (70.14)	558.41 (90.01)
Median	364	318	542
Min – Max	107.00 - 937.00	107.00 - 450.00	451.00 - 937.00

The demographic characteristics of patients are embedded in Table 6. Ninety-two percent and 97% of patients had high stage (III-IV) and high grade (II-III) disease, respectively. Seventy-seven percent had serous histology and 58% underwent optimal surgical cytoreduction. Thirty-one percent of women had thrombocytosis at the time of initial diagnosis, which is considerably higher than the published prevalence of thrombocytosis in other solid malignancies (Table 7).

**Table 6.** Associations between thrombocytosis (platelets > 450,000/ $\mu$ L) and clinicopathological variables

Variable	All Patients (N = 619)	Platelets WNL (N = 427)	Thrombocytosis (N = 192)	p-value
Age				0.15
N	619	427	192	
Mean (SD)	60.68 (11.29)	61.15 (11.66)	59.63 (10.38)	
Median	60	60	60	
Min - Max	13.00 - 92.00	13.00 - 92.00	31.00 - 83.00	
Thromboembolism				0.008
No Thromboembolism	189 (76.83%)	125 (82.78%)	64 (67.37%)	
Thromboembolism	57 (23.17%)	26 (17.22%)	31 (32.63%)	
Stage				<0.001
Low Stage	52 (8.40%)	46 (10.77%)	6 (3.13%)	
High Stage	567 (91.60%)	381 (89.23%)	186 (96.88%)	
Grade				0.15
Low Grade	21 (3.40%)	18 (4.22%)	3 (1.56%)	
High Grade	598 (96.60%)	409 (95.78%)	189 (98.44%)	
Histology				0.099
Other Histology	143 (23.10%)	107 (25.10%)	36 (18.75%)	
Serous	476 (76.90%)	320 (74.94%)	156 (81.25%)	
Cytoreduction				0.51
Suboptimal				
Cytoreduction	236 (42.14%)	162 (41.22%)	74 (44.31%)	
Optimal Cytoreduction	324 (57.86%)	231 (58.78%)	93 (55.69%)	
CA-125				< 0.001
N	335	242	93	
Mean (SD)	2,220.40 (21,158.98)	2,481.41 (24,853.64)	1,541.20 (2,568.12)	
Median	376	324	654	
Min - Max	7 - 385,378	7 - 385,378.00	27 - 16,032	
White Blood Cells				0.002
N	223	163	60	
Mean (SD)	7.97 (2.42)	7.80 (2.59)	8.42 (1.83)	
Median	7.9	7.5	8.6	
Min - Max	2.10 - 17.40	2.10 - 17.40	4.40 - 14.10	
Red Blood Cells				< 0.001
N	220	161	59	
Mean (SD)	4.22 (0.63)	4.31 (0.66)	3.97 (0.46)	
Median	4.2	4.3	3.9	
Min - Max	3.10 - 9.90	3.10 - 9.90	3.12 - 5.14	
Hemoglobin				< 0.001
N	222	162	60	
Mean (SD)	12.23 (1.63)	12.59 (1.58)	11.27 (1.38)	
Median	12.3	12.7	11.3	
Min - Max	7.40 - 17.00	8.90 - 17.00	7.40 - 14.80	
Hematocrit				< 0.001
N	223	163	60	
Mean (SD)	36.56 (4.78)	37.59 (4.53)	33.76 (4.31)	
Median	36.8	38.1	34	
Min - Max	23.10 - 50.30	27.90 - 50.30	23.10 - 43.00	



<b>Table 7. Prevalence of thrombocytosis in solid malignancies</b>			
<b>Malignancy</b>	<b># of patients</b>	<b>Prevalence of Thrombocytosis</b>	<b>Reference</b>
GBM	153	19%	(85)
H&N	270	7.2%	(86)
Breast	4300	3.7%	(87)
NSCLC	240	5.8%	(88)
Gastric	369	11.4%	(32, 89)
HCC	1154	2.7%	(90)
Colon	198	12.1%	(10, 11, 91)
RCC	700	25%	(10, 92)
RCC*	804	7.8%	(93)
Cervix	623	9.5%	(94)
Vulvar	201	15.5%	(95)
Endometrial	135	14%	(96)

\*used  $\geq 450,000/\mu\text{L}$ , others used  $\geq 400,000/\mu\text{L}$

Regarding other blood count parameters, mean leukocyte count was significantly higher in women with thrombocytosis ( $8.42 \pm \text{SD } 1.83 \times 10^3/\mu\text{L}$  *versus*  $7.8 \pm \text{SD } 2.59 \times 10^3/\mu\text{L}$ ,  $p=0.0021$ ) and thrombocytosis was significantly associated with mild anemia (mean Hgb  $11.27 \pm \text{SD } 1.38 \text{ g/dL}$  *versus*  $12.59 \pm \text{SD } 1.58 \text{ g/dL}$ ,  $p<0.001$ ; Figure 9).

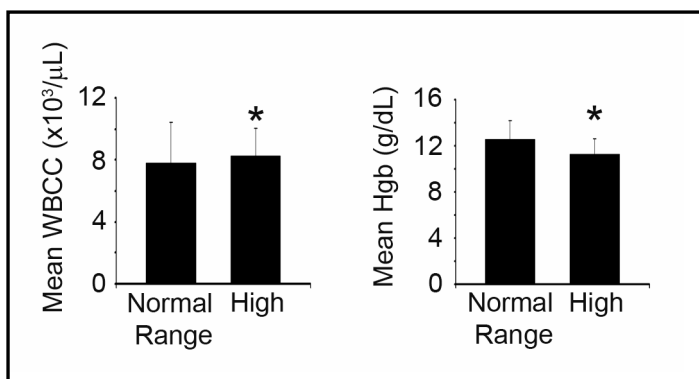


**Figure 9. Changes in other CBC parameters according to platelet count.** Mean white blood cell count (WBCC) and hemoglobin (Hgb)  $\pm$  SD in patients with platelet counts within normal range and in patients with thrombocytosis. \*  $p < 0.01$ .

Univariate analyses testing correlations between platelet count and clinicopathologic variables known to impact disease specific survival revealed that women with thrombocytosis were significantly more likely to have advanced stage disease compared to women with normal platelet counts ( $p<0.001$ ; Table 6). Thrombocytosis was also significantly associated with poor median progression-free and overall survival. Median time to recurrence among women who presented with thrombocytosis was 0.94 years compared to 1.35 years for women with normal platelet counts ( $p<0.001$ , Figure 10a). Median overall survival among patients with thrombocytosis was 2.62 years compared to 4.65 years for patients with normal platelet counts ( $p<0.001$ ; Figure 10b).

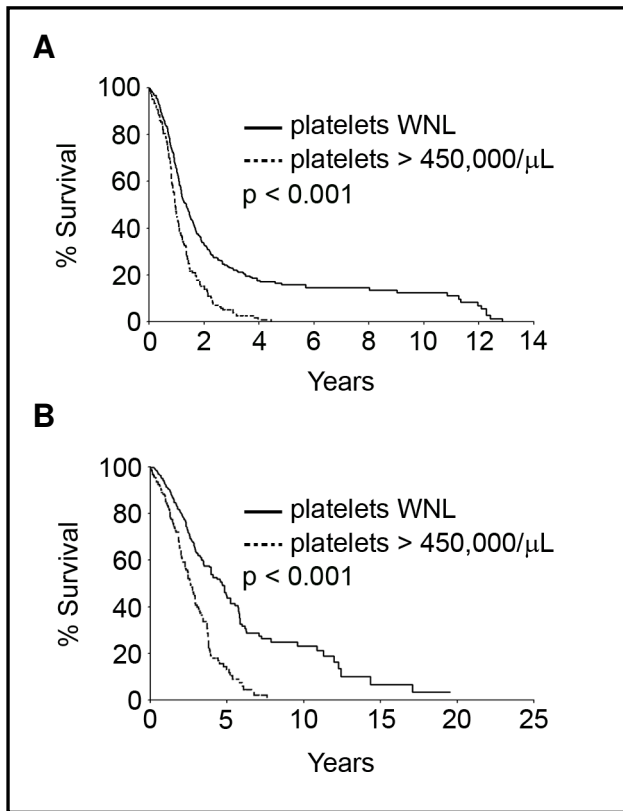


**Figure 10. Thrombocytosis and survival.** Kaplan-Meier analysis evaluating the effect of thrombocytosis on disease-free interval (a) and overall survival (b) in ovarian cancer patients.

On the basis of these findings, we assessed whether there was an independent association between thrombocytosis and prognosis. In a multivariate survival analysis using a Cox proportional hazards model adjusting for age, disease stage, tumor grade, histological type, and extent of surgical cytoreduction, thrombocytosis remained an independent predictor of decreased progression free ( $p < 0.001$ ) and overall survival ( $p < 0.001$ ). In this model, patients who presented with thrombocytosis had a 1.87-fold increased risk of death compared to patients with normal platelet counts (Tables 8a and b).

**Table 8a.** Multivariate Cox proportional hazards analysis of prognostic factors on progression free survival

Variable	HR	p-value	95% CI
Thrombocytosis	1.51	<0.001	1.22 - 1.88
Age	1.01	0.15	1.00 - 1.02
Stage III/IV	4.92	< 0.001	2.93 - 8.25
High Grade	0.89	0.73	0.46 - 1.72
Serous Histology	1.48	0.004	1.13 - 1.94
Suboptimal Cytoreduction	1.13	0.24	0.92-1.40

**Table 8b.** Multivariate Cox proportional hazards analysis of prognostic factors on overall survival

Variable	HR	p-value	95% CI
Thrombocytosis	1.87	< 0.001	1.44 - 2.44
Age	1.00	0.51	0.99 - 1.02
Stage III/IV	4.19	< 0.001	2.05 - 8.55
High Grade	2.80	0.05	1.02 - 7.70
Serous Histology	1.30	0.11	0.94 - 1.80
Suboptimal Cytoreduction	1.39	0.01	1.07-1.80

Given that vascular thromboembolism (VTE) contributes significantly to the morbidity of malignancy and that platelets play a major role in the initiation and growth of thrombi, we determined whether thrombocytosis was associated with increased incidence of VTE in a subset of 246 ovarian cancer patients. We found that patients with thrombocytosis had a 2.3-fold increased risk of VTE compared to individuals with normal platelet counts ( $p < 0.01$ ). Among the 57 (23.2%) women who experienced VTE, 28 cases were simultaneous with a new diagnosis of ovarian carcinoma and 29 cases transpired during the subsequent course of disease. Proportional hazards models that included a term for VTE suggested that thrombocytosis is an independent predictor of decreased time to recurrence and increased mortality in women who do develop a blood clot, but that mortality due to thrombotic complications alone was not significant (Tables 9a and b).

**Table 9a.** Multivariate Cox proportional hazard analysis of prognostic factors including VTE on progression free survival

Variable	HR	p-value	95% CI
Thrombocytosis	1.92	<0.001	1.32 - 2.78
VTE	1.03	0.90	0.68 - 1.56
Age	1.01	0.24	0.99 - 1.03
Stage III/IV	6.16	0.02	1.28 - 29.58
High Grade	0.28	0.19	0.04 - 1.89
Serous Histology	2.41	0.02	1.16 - 5.04
Suboptimal Cytoreduction	0.92	0.66	0.64-1.32

**Table 9b.** Multivariate Cox proportional hazard analysis of prognostic factors including VTE on overall survival

Variable	HR	p-value	95% CI
Thrombocytosis	1.84	0.004	1.21 - 2.80
VTE	0.89	0.68	0.52 - 1.52
Age	1.00	0.93	0.98 - 1.02
Stage III/IV	1.52	0.50	0.45 - 5.18
High Grade	1.42	0.66	0.30 - 6.66
Serous Histology	1.05	0.88	0.56 - 1.97
Suboptimal Cytoreduction	1.14	0.52	0.76-1.73

Paraneoplastic thrombocytosis is recapitulated in mouse models of ovarian carcinoma and other solid malignancies

To assess the relative utility of our existing orthotopic mouse models of ovarian cancer for further investigating clinical observations related to paraneoplastic thrombocytosis, we compared platelet counts between healthy control mice and mice bearing invasive ovarian cancer with and without large volume ascites. We found that compared to controls (mean  $1.05 \pm \text{SEM } 0.05 \times 10^6/\mu\text{L}$ ), tumor-bearing mice had a 31% increase in platelets (mean  $1.37 \pm \text{SEM } 0.07 \times 10^6/\mu\text{L}$ ,  $p=0.003$ ) and that platelet counts more than doubled in tumor-bearing mice with ascites (mean  $2.38 \pm 0.24 \times 10^6/\mu\text{L}$ ,  $p=0.001$ ; Figure 11a). Furthermore, platelet counts strongly correlated with tumor burden ( $r=0.78$ ,  $p<0.01$ ) and number of intraperitoneal metastases ( $r=0.65$ ,  $p<0.01$ ; Figure 11b).

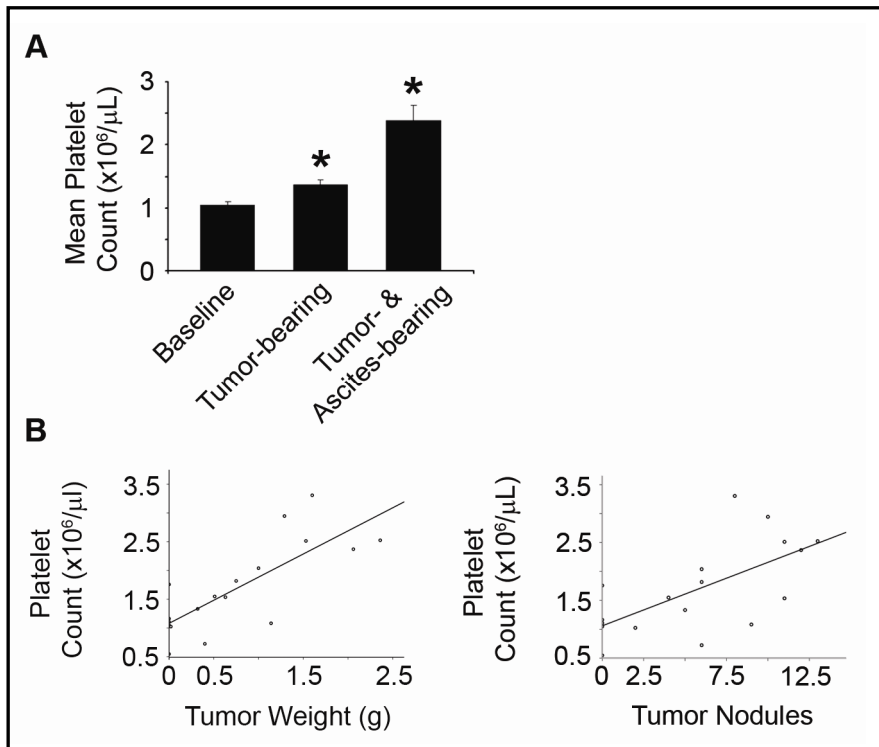


**Figure 11. Platelet counts and correlation with tumor burden in orthotopic mouse models of ovarian cancer.** Platelet counts were measured in whole blood collected from healthy control mice as well as orthotopic mouse models of ovarian cancer bearing invasive tumors with (2774) and without (HeyA8 and A2780ip2) large volume ascites (a). Tumor weight and number of intraperitoneal metastases were correlated with platelet counts in the 2774 model (b).

We observed a non-significant increase in leukocytes and reduction in red blood cell mass in mice with invasive ovarian tumors  $\pm$  ascites compared to healthy controls (Figure 12a & b).

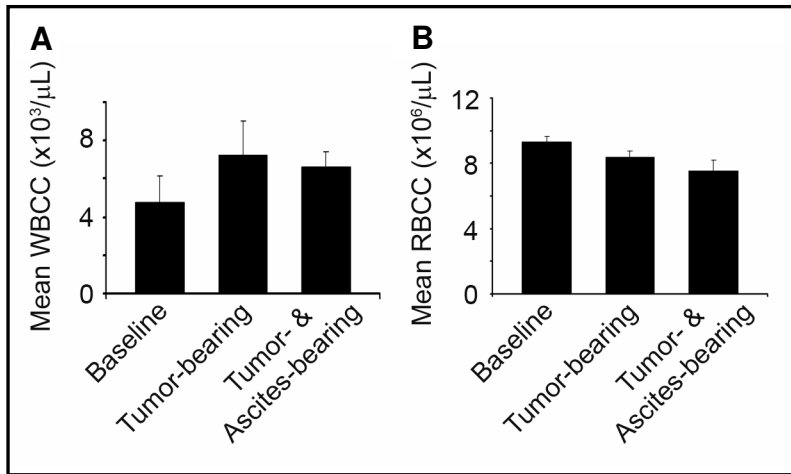


**Figure 12. Changes in other CBC parameters in orthotopic mouse models of ovarian cancer.** Results represent mean white blood cell count (WBCC, a) and mean red blood cell count (RBCC, b)  $\pm$  SEM in orthotopic mouse models of ovarian cancer bearing invasive tumors with (2774) and without (HeyA8 and A2780ip2) large volume ascites.

To determine whether thrombocytosis is idiosyncratic to our orthotopic models of ovarian cancer, we also assessed platelet counts in 2 syngeneic mouse models of ovarian cancer. Both syngeneic models developed significant thrombocytosis. Platelet counts were increased by 64% and 59% ( $p < 0.05$ ) in mice bearing invasive tumors derived from IG10 and ID8<sup>VEGF164</sup> cells, respectively (Figure 13a). To establish the generalizability of our finding of thrombocytosis in mouse models of ovarian cancer to mouse models of other solid malignancies, we quantified platelets in orthotopic mouse models of breast (GILM2 cell line) and uterine cancer (Ishikawa cell line) as well as in a human pancreatic tumor xenograft mouse model. Platelet counts were not elevated over baseline in mice with GILM2 breast tumors, but were significantly increased in Ishikawa uterine (30%,  $p < 0.05$ ) and pancreatic cancer models (39%,  $p < 0.05$ ; Figure 13b).

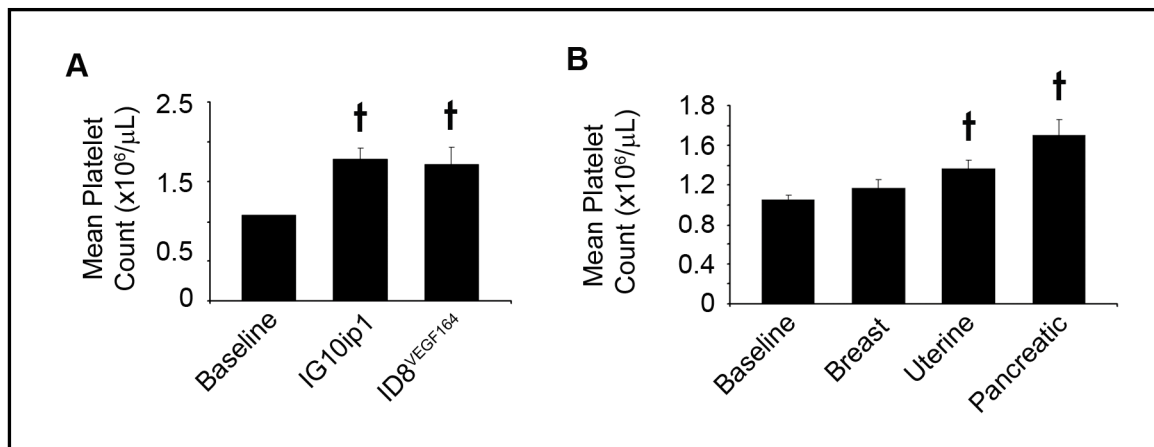


**Figure 13. Platelet counts in syngeneic mouse models of ovarian cancer and mouse models of other solid malignancies.** Platelet counts were evaluated 2 syngeneic mouse models of ovarian cancer (a) and in orthotopic mouse models of metastatic breast and uterine cancer as well as in a heterotopic human pancreatic xenograft model (b). Bars represent mean  $\pm$  SEM. † indicates  $p < 0.05$ .

Given that thrombocytosis was consistently detected in mice with large volume disease, we conducted a time course study to characterize the onset and development of thrombocytosis in an orthotopic mouse model of ovarian cancer by tracking platelet counts with disease progression. Bioluminescence imaging was used to detect disease until it was palpable by physical exam (day 22). We found that platelets began to appreciably rise when mean tumor burden exceeded 0.62 cm, which corresponded to the point at which disease was reliably detectable on exam. Platelet counts continued to increase with disease progression and were highest when mice became moribund (Figure 14).



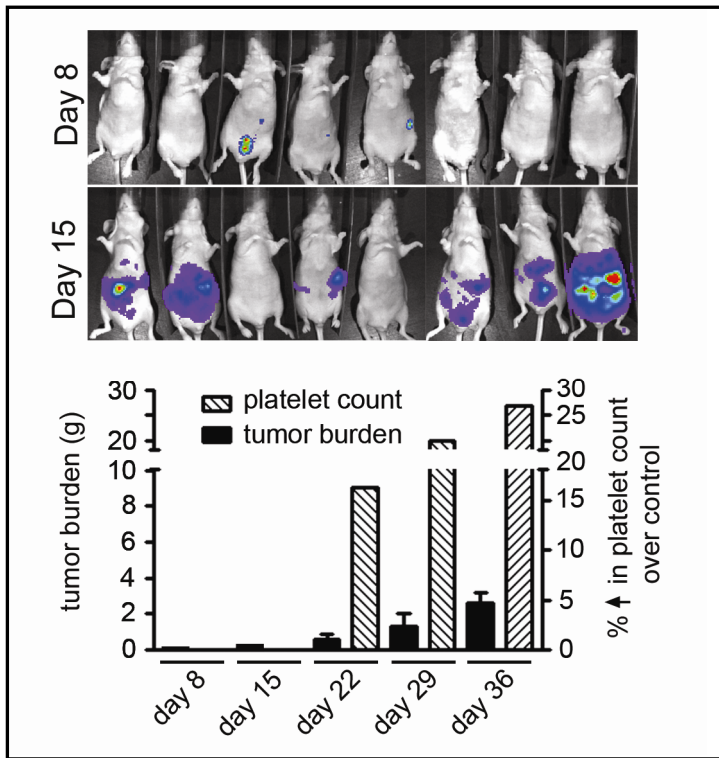
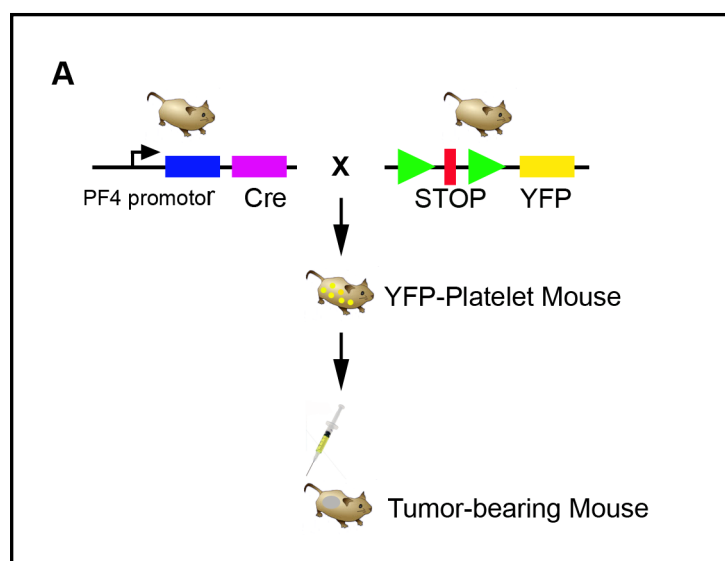


**Figure 14. Time course delineating the onset and progression of thrombocytosis in ovarian cancer-bearing mice.** Bioluminescence imaging was used to detect HeyA8-Luc tumor growth until day 22, when tumors were palpable by physical exam. Tumor burden represents mean tumor weight in grams  $\pm$  SEM (black bars, left-hand y-axis). Platelet count is reported as mean % increase in platelet count compared to control (bars with cross hatching, right-hand x-axis).

#### Platelets extravasate into tumors and ascites

Several mechanisms have been proposed to explain how platelets facilitate the growth and dissemination of malignancy. Platelets may adhere to circulating tumor cells and help them to lodge in the microvasculature where they can form intravascular colonies and/or infiltrate into target organs. Additionally, oncogenic and angiogenic factors released by platelets may support cancer cell survival,

proliferation, and invasion as well as angiogenesis. Given that many solid malignancies, including ovarian cancer, do not have a well defined hematogenous phase, we hypothesized that platelets extravasate into the tumor bed where they can subsequently exert direct effects on cancer cells. To test this hypothesis, we isolated platelets from a transgenic mouse expressing yellow fluorescent protein (YFP) under the control of the platelet specific PF4 promoter and transfused them into ID8<sup>VEGF164</sup> tumor-bearing C57BL/6 mice (Figure 15a). Tumors were resected 1 hour following YFP-platelet transfusion and intravital fixation. To aid in localizing YFP-platelets in tumor sections, immunofluorescent staining with Hoechst and for CD31 antigen was performed to label nuclei and the tumor vasculature, respectively. Within 1 hour of transfusion, YFP-labeled platelets were present in the tumor bed, primarily in a peri-vascular location (Figure 15b). YFP-labeled platelets were also found free-floating and adhered to cells in ascites within 1 hour of transfusion into tumor-bearing recipient mice (Figure 15c).



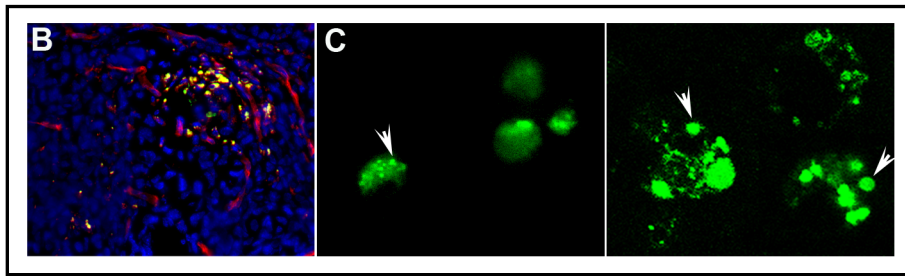
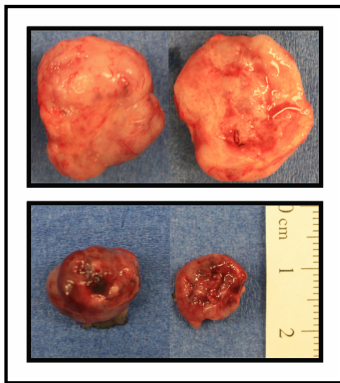


**Figure 15. Platelet extravasation into solid tumor and ascites.** The methodology used to determine if platelets extravasate into solid tumor and ascites is depicted in panel (a). Platelets isolated from transgenic mice expressing yellow fluorescent protein (YFP) under the control of the platelet specific PF4 promoter were transfused into mice with invasive ovarian cancer and ascites. Tumor was resected one hour following intravital fixation. To localize YFP-platelets (yellow) in tumor sections, immunofluorescent staining with Hoechst and for CD31 antigen was performed to label nuclei (blue) and the tumor vasculature (red), respectively (b). Whole mounts of ascites removed by paracentesis prior to intravital fixation were examined with fluorescent (middle panel, 200x) and confocal microscopy (right panel 400x) to visualize YFP-platelets adhered to ascites cells (white arrows, c).

#### Anti-tumor effects of platelet depletion

To evaluate the biological effect of platelet depletion on tumor growth, we used an anti-platelet antibody (APA) directed against platelet glycoprotein  $Ib\alpha$  receptor to decrease platelets in an orthotopic mouse model of ovarian cancer. The rationale for selecting this approach as well as the antibody dose and treatment schedule used for this investigation are addressed in the methods section. After conducting preliminary experiments to characterize the activity and specificity of the antibody, a therapy experiment was initiated. Mice inoculated with A2780ip2 ovarian cancer

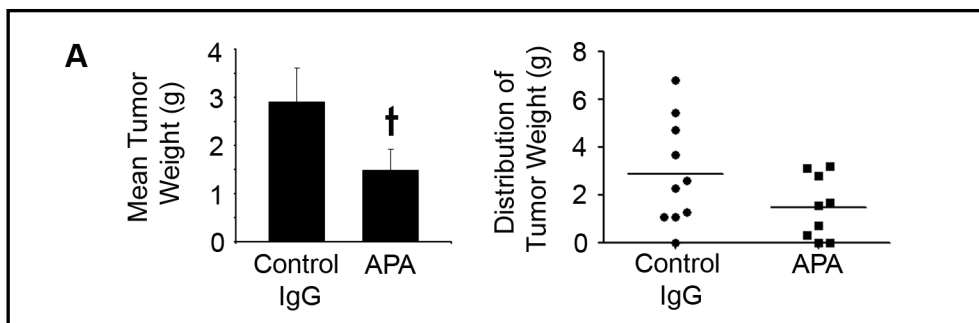
cells were treated with either 0.5  $\mu\text{g/g}$  anti-GP1b $\alpha$  antibody or control IgG by tail vein injection every 4 days until they became moribund. Tumor weight was recorded at the time of necropsy. Overall, ovarian tumors resected from APA treated mice appeared grossly hemorrhagic and smaller than those resected from mice treated with control IgG (Figure 16).



**Figure 16. Macroscopic appearance of A2780ip2 tumors resected from mice treated with control IgG (top panel) and anti-platelet antibody (bottom panel).**

Antibody mediated platelet depletion inhibited tumor growth by 50% compared to control IgG ( $p < 0.05$ ; Figure 17a). To investigate the underlying mechanisms accounting for the anti-tumor effect of platelet depletion in our model, we performed immunohistochemical staining for Ki67 and CD31 antigens to ascertain the proliferative index and microvessel density of tumor specimens, respectively. Compared to control IgG, antibody mediated platelet depletion resulted in a 44% decrease in tumor cell proliferation and a 51% reduction in microvessel density ( $p < 0.001$ ; Figures 17b & c). To further investigate the effects of platelet depletion on the tumor vasculature, we examined microvessel pericyte coverage with dual

immunohistochemical staining for CD31 and desmin. Given that pericytes are PDGF-dependent mesenchymal cells that support and stabilize small blood vessels and that PDGF is one of the principal cytokines released by platelets, we hypothesized that platelet depletion would have a detrimental effect on microvessel pericyte coverage (97, 98). We found that platelet depletion reduced pericyte coverage by 60% ( $p < 0.001$ ). Tumor microvessels were predominantly devoid of pericytes and existing pericytes appeared loosely attached (Figure 17d). Considering that pericytes support endothelial cell survival and that tumor cell survival depends on an intact vascular network, we next determined whether platelet depletion was associated with increased tumor and endothelial cell apoptosis using dual CD31 staining and TUNEL labeling. Compared to control IgG, antibody mediated platelet depletion resulted in a 4- and 8-fold increase in tumor and endothelial cell apoptosis, respectively ( $p < 0.01$ ; Figure 17e). Thus, the anti-tumor effect of platelet depletion was likely multi-factorial and could be attributed to decreased tumor cell proliferation, microvessel density, and pericyte coverage as well as increased tumor and endothelial cell apoptosis.



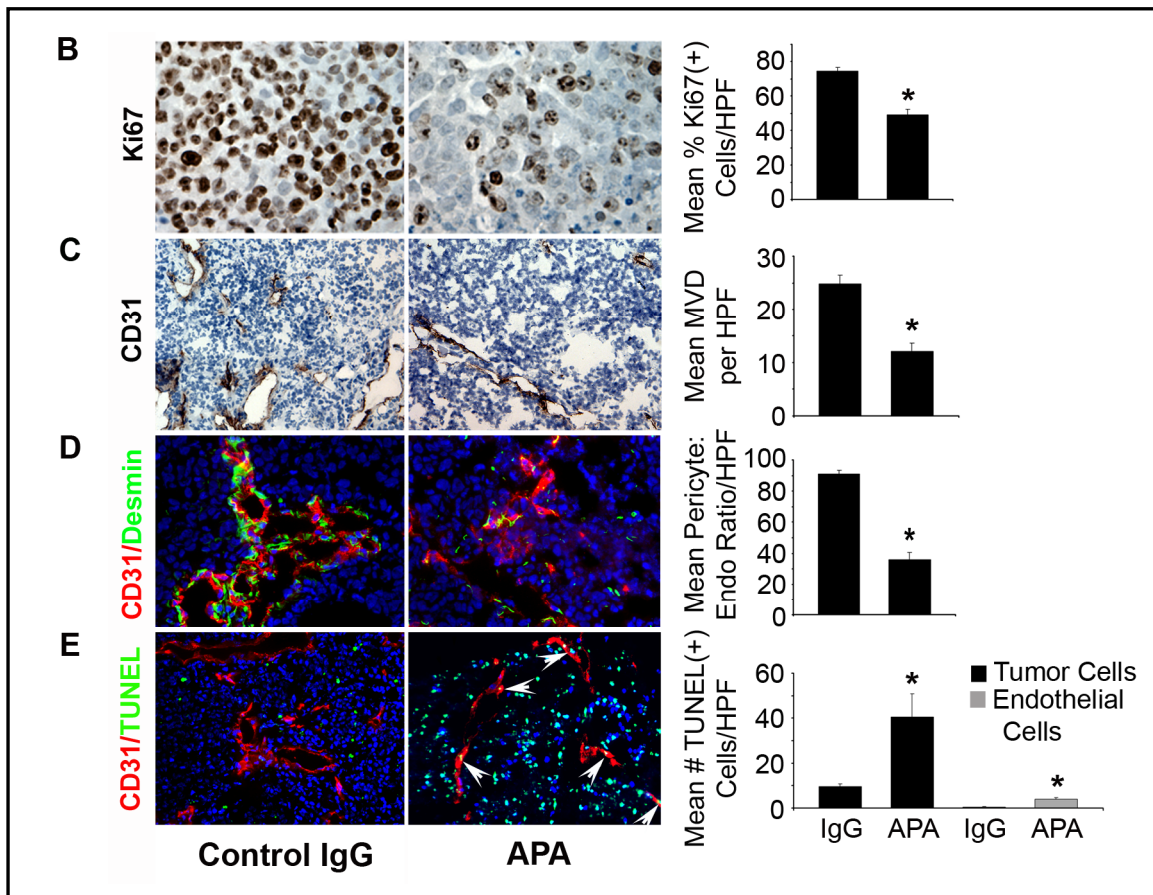


**Figure 17. *In vivo* effects of platelet depletion on tumor growth, cell proliferation, microvessel density, pericyte coverage, and apoptosis.** *In vivo* effects of platelet depletion were examined using an anti-platelet antibody (APA, anti-mouse glycoprotein 1b $\alpha$ ) to reduce platelets by 50%. Nude mice were injected with A2780ip2 ovarian cancer cells i.p. and treated with either 0.5  $\mu$ g/g APA (n=10) or PBS vehicle control (n=10) i.v. every 4 days until they became moribund. Mean tumor weight  $\pm$  SEM (left panel) and corresponding tumor weight distributions are shown (right panel). Proliferation index (b) and tumor vascularity (c) were assessed with immunohistochemical staining for Ki67 and CD31 antigen, respectively. Pericyte coverage was evaluated using dual immunofluorescence staining for CD31 (endothelial cell marker, red) and desmin (pericyte marker, green, d). Tumor and endothelial cell apoptosis was assessed with dual immunofluorescence staining for

CD31 (red) and TUNEL (apoptosis marker, green). Apoptotic tumor cells have green fluorescent nuclei where as colocalization of endothelial cell undergoing apoptosis shows yellow fluorescence (white arrows, e). Representative photomicrographs appear to the left of the graphs. Graphs represent mean  $\pm$  SEM calculated for 5 random x200 HPF. † indicates  $p < 0.05$  and \* indicates  $p < 0.01$ .

#### Functional effects of platelets on ovarian cancer cell proliferation, survival and migration

Given our *in vivo* data suggesting that platelet depletion inhibits tumor growth by several mechanisms including decreased tumor cell proliferation and increased apoptosis, we subsequently explored the stimulatory effects of platelets from tumor-bearing mice on ovarian cancer cells *in vitro*. Specifically, *in vitro* effects of plasma-purified platelets on ovarian cancer cell migration, proliferation, and docetaxel-induced apoptosis were evaluated using two-chamber chemotaxis and BrdU-PI flow cytometric assays. Platelets significantly stimulated A2780ip2, HeyA8, and 2774 ovarian cancer cell migration. The mean number of migrating A2780ip2 ( $141.2 \pm 9.6/\text{HPF}$ ), HeyA8 ( $147.9 \pm 9.8/\text{HPF}$ ), and 2774 ( $113.3 \pm 6.2/\text{HPF}$ ) cells in response to platelets was significantly higher than their chemotactic response to vehicle alone ( $53.2-55 \pm 4.4-5.7/\text{HPF}$ ,  $p < 0.01$ ; Figure 18).

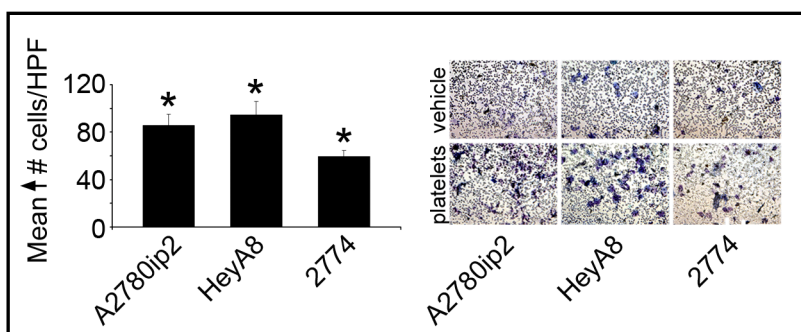


**Figure 18. Effect of platelets on ovarian cancer cell migration *in vitro*.** Results represent mean change in number of cells migrating in response to platelets relative to vehicle control  $\pm$  SEM of triplicate experiments. Representative images of migrated A2780ip2, HeyA8, or 2774 cells in response to platelets or vehicle control are included. \* indicates  $p < 0.01$ .

The impact of platelets on tumor cell proliferation and survival was next evaluated in a panel of 6 ovarian cancer cell lines. For proliferation assays, cells were co-cultured with plasma-purified platelets from tumor-bearing mice ( $10 \times 10^6/\text{mL}$ ) or vehicle alone for 24 hours. To evaluate the effect of platelets on ovarian cancer cell survival, similar co-culture conditions were used except cells were concurrently treated with or without 0.5 nM docetaxel for 72 hours. Cell proliferation and death were measured by flow cytometric analysis of BrdU incorporation and PI staining, respectively. Platelets induced proliferation and protected against cytotoxicity due to docetaxel treatment in every cell line except 2774. Specifically, platelets significantly increased mean percent BrdU positive A2780ip2 cells by  $16.4 \pm 1.2\%$  (4.1-fold increase,  $p=0.006$ ), HeyA8 cells by  $19.7 \pm 3.4\%$  (2.2-fold increase,  $p=0.03$ ), SKOV3ip1 cells by  $23.9 \pm 1.4\%$  (3.4-fold increase,  $p=0.004$ ), OVCA433 cells by  $8.8 \pm 0.2\%$  (1.3-fold increase,  $p=0.02$ ), and ES2 cells



by  $15.6 \pm 1\%$  (3-fold increase,  $p=0.008$ ; Figure 19a). The most robust anti-apoptotic effects of platelets were observed in SKOV3ip1 and ES2 cell lines. Platelets significantly decreased mean percent PI positive SKOV3ip1 cells by  $15.5 \pm 5\%$  (2-fold decrease,  $p=0.03$ ) and ES2 cells by  $19.2 \pm 2.6\%$  (2-fold decrease,  $p<0.001$ ; Figure 19b).

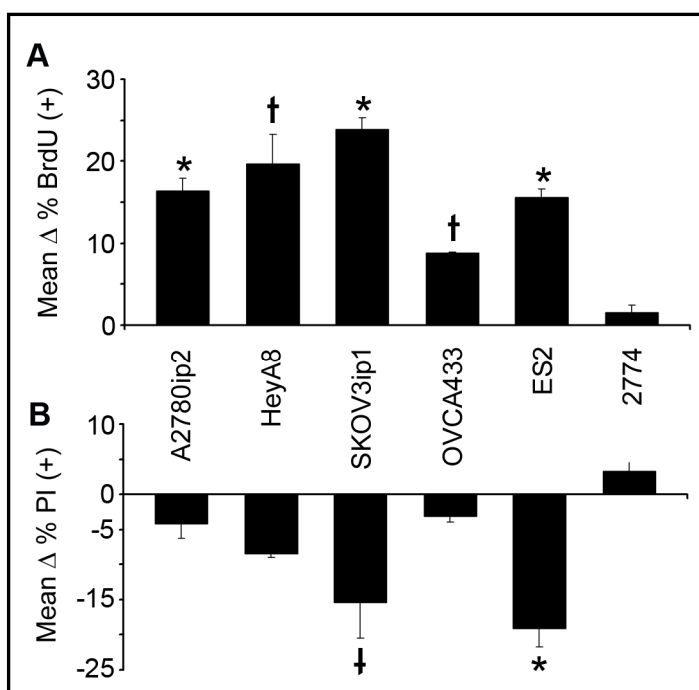


**Figure 19. Effect of platelets on ovarian cancer cell proliferation and apoptosis *in vitro*.** Effect of platelets on ovarian cancer cell proliferation (a) and apoptosis (b) was assayed using flow cytometry for BrdU labeling and PI staining, respectively. Results represent mean change in percent positively staining cells over vehicle control  $\pm$  SEM of triplicate experiments. † represents  $p < 0.05$  and \* represents  $p < 0.01$ .

Given that platelets stimulated proliferation and conferred resistance to docetaxel-induced cytotoxicity in every cell line except 2774 and that these

observed effects could be due at least in part to platelet derived growth factors, we looked for differences in growth factor receptor expression among the ovarian cancer cell lines used in these assays. Relative to the other ovarian cancer cell lines, 2774 has the lowest PDGFR $\alpha$  protein expression (Figure 20a). Knowing that receptor tyrosine kinase receptors contribute to chemoresistance in malignancies and finding that PDGFR $\alpha$  expression is appreciably elevated in the taxane-resistant cell lines HeyA8-MDR and SKOV3-TR relative to their respective parental lines (Figure 20b), raised the question of PDGFR $\alpha$  involvement in platelet-mediated ovarian cancer cell taxane-resistance.

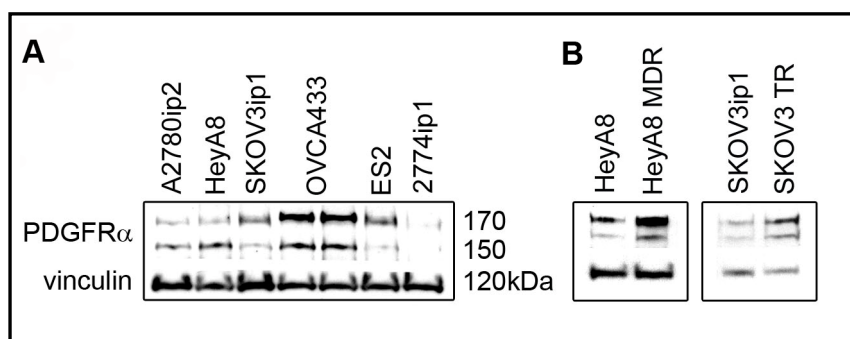


**Figure 20. Platelet derived growth factor alpha (PDGFR $\alpha$ ) expression in ovarian cancer cell lines.** Western blot analysis was used to evaluate PDGFR $\alpha$  expression in a panel of human ovarian cancer cell lines (a) and in the taxane-resistant cell lines HeyA8-MDR and SKOV3-TR compared to their respective parental lines (b). PDGFR $\alpha$  is a dimer formed by 150 and 170 kDa subunits.

To investigate the contribution of PDGFR $\alpha$  to platelet-induced resistance to docetaxel, we pre-treated SKOV3ip1 cells with IMC-3G3, a fully-humanized anti-

PDGFR $\alpha$  antibody, prior to adding platelets +/- docetaxel. Treatment with IMC-3G3 alone was not significantly cytotoxic. The addition of platelets reduced the cytotoxic effect of docetaxel by 17%, which was consistent with our previous findings. However, IMC-3G3 completely abrogated the chemoprotective effect of platelets, suggesting that blocking PDGFR $\alpha$  might be one potential strategy for inhibiting the stimulatory effect of platelets on ovarian cancer cell survival and for combating resultant chemoresistance (Figure 21).

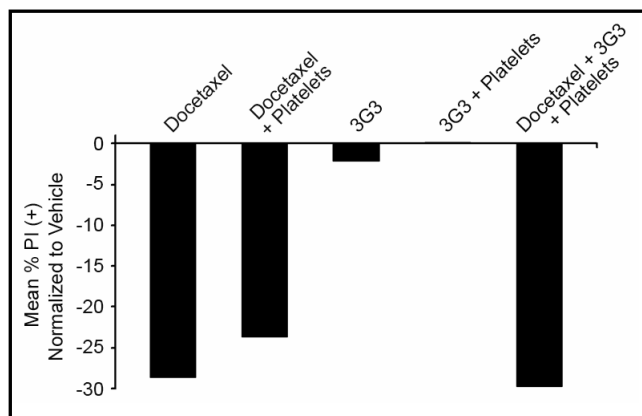


**Figure 21. Effect of fully humanized anti-PDGFR $\alpha$  antibody, IMC-3G3, on platelet induced taxane resistance.** Ovarian cancer cells were pretreated with 100  $\mu$ g/mL IMC-3G3 or PBS vehicle for 2 hours prior to adding platelets  $\pm$  0.5 nM docetaxel. Apoptosis was assessed using flow cytometry to detect PI staining.

Megakaryopoiesis and thrombopoiesis in response to specific cytokines is a potential underlying mechanism of paraneoplastic thrombocytosis

To this point the underlying etiology of paraneoplastic thrombocytosis has remained unknown. Under normal physiological conditions, thrombopoiesis is regulated by several pleiotrophic growth factors and cytokines that influence various

steps in the process, starting with megakaryocyte progenitor proliferation and proceeding through maturation to the eventual release of platelets into circulation (99, 100). While there have been some studies examining the link between perturbations in the humoral regulation of thrombopoiesis and thrombocytopenia, there has not been a concerted effort to explore the role of humoral factors in the development of thrombocytosis associated with malignancy. We hypothesized that factors produced by cancer cells, the tumor vasculature, and/or host tissues stimulate megakaryo- and thrombopoiesis, resulting in paraneoplastic thrombocytosis. To test this hypothesis, we first quantified megakaryocytes in bone marrow and spleens from orthotopic mouse models of ovarian cancer that consistently develop paraneoplastic thrombocytosis. These sites were selected because hematopoiesis is known to occur primarily in the medullary cavity of long bones and spleen in the adult mouse. We found that the mean number of medullary megakaryocytes per HPF was significantly increased in tumor-bearing mice (mean  $4.8 \pm \text{SEM } 0.4$ ) compared to controls (mean  $2.6 \pm \text{SEM } 0.3$ ,  $p < 0.01$ ). Tumor-bearing mice with ascites had a 2.7-fold increase in medullary megakaryocytes (mean  $6.9 \pm \text{SEM } 0.4$ ) compared to controls ( $p < 0.01$ ). Significant megakaryocyte expansion was also observed in the spleen. Compared to controls (mean  $0.84 \pm \text{SEM } 0.3$ ), splenic megakaryocytes were increased 7-fold and 13-fold in tumor-bearing mice (mean  $6.0 \pm \text{SEM } 0.9$ ,  $p < 0.01$ ) and tumor-bearing mice with ascites (mean  $11.2 \pm \text{SEM } 0.8$ ,  $p < 0.01$ ), respectively (Figure 22). Mean platelet counts across control and tumor-bearing mice  $\pm$  ascites strongly correlated with mean megakaryocyte counts in the spleen and bone marrow ( $r = 0.95$ ,  $p < 0.05$ ). Given reports of extramedullary hematopoiesis in the adult mouse liver (101) and of

mature megakaryocytes migrating from the marrow to the pulmonary capillary bed where they release platelets (102, 103), we also examined liver and lung sections from these mice. Megakaryocytes were not present in hepatic and pulmonary tissues (data not shown).

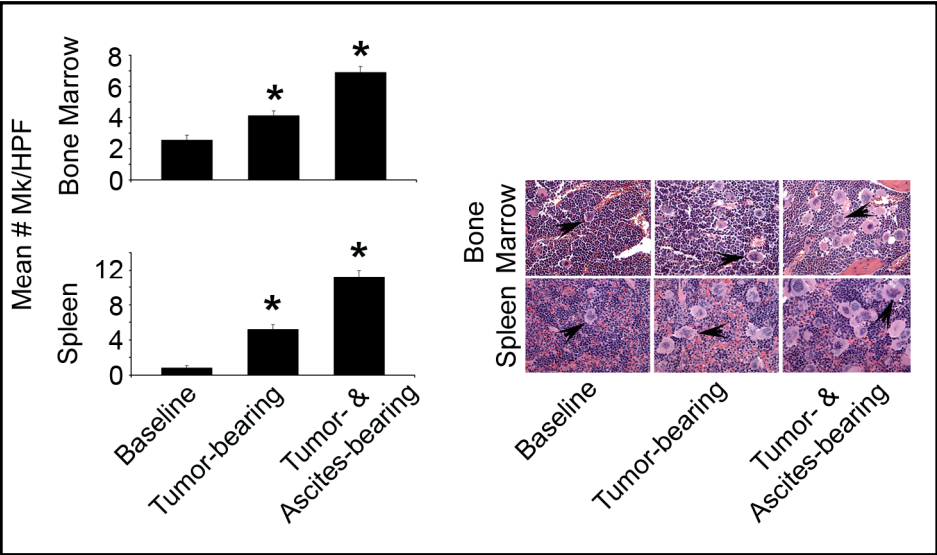


**Figure 22. Medullary and splenic megakaryocyte counts.** Megakaryocytes (Mk) were enumerated in the bone marrow and spleen of healthy control (NCR-*nu*), tumor-bearing (A2780ip2 orthotopic model), and tumor- & ascites-bearing mice (2774 orthotopic model). Graphs represent the mean number of megakaryocytes per 5 randomly selected x200 high power fields (HPF)  $\pm$  SEM. \* indicates  $p < 0.01$ . Representative photomicrographs of megakaryocyte (black arrows) density in bone marrow (top panel) and spleen (bottom panel) from healthy control, tumor-bearing, and tumor- & ascites-bearing mice are included.

Based on finding medullary and splenic megakaryocyte hyperplasia in mice that develop paraneoplastic thrombocytosis in response to orthotopic human ovarian cancers, we next explored the expression of key factors implicated in megakaryo-

and thrombopoiesis. Given that TPO is the primary growth factor responsible for megakaryocyte development and platelet production (43, 104), we first assessed ovarian cancer cell TPO expression *in vitro* and *in vivo*. Thrombopoietin transcript was detected in ovarian cancer cells *in vitro* (Figure 23a) and high cytoplasmic TPO protein expression was observed in A2780ip2, HeyA8, and 2774 *in vivo* tumor specimens (Figure 23b).

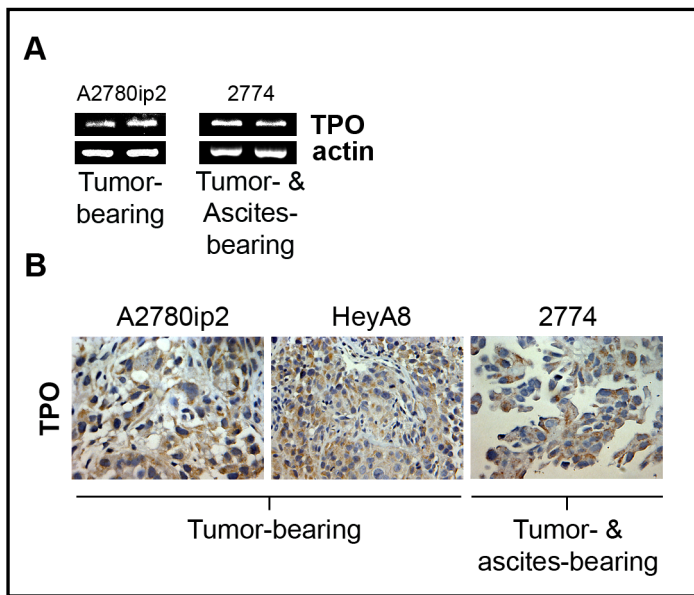


**Figure 23. *In vitro* and *in vivo* ovarian cancer cell thrombopoietin expression.**

Thrombopoietin mRNA expression was assessed in duplicate *in vitro* cultures of A2780ip2 and 2774 human ovarian cancer cells using RT-PCR (a). Thrombopoietin protein expression in *in vivo* specimens of A2780ip2, HeyA8, and 2774 tumors was evaluated using immunochemistry (b).

These findings suggest that ovarian cancer cells can be an ectopic source of TPO. Under physiological conditions, TPO is constitutively produced by hepatic parenchymal and sinusoidal endothelial cells and TPO levels are largely determined

by platelet and megakaryocyte TPO receptor-mediated internalization. This establishes an autoregulatory loop where in blood and marrow levels of TPO are inversely related to platelet and megakaryocyte numbers (105). Although hepatic TPO production is generally considered to be fixed, we speculated that hepatic TPO production might increase in response to other cytokines, such as IL-6, elaborated by ovarian cancer cells. Ovarian cancer cell secretion of IL-6, particularly in response to stress hormones, has been previously characterized by our laboratory (106). IL-6 acts directly as a megakaryocyte maturation factor, but its thrombopoietic effect is thought to be indirect through increasing TPO gene transcription in the liver (44). When we compared TPO mRNA levels in liver harvested from normal mice and from ovarian cancer-bearing mice, we consistently found higher TPO transcript levels in livers from ovarian cancer-bearing mice (Figure 24). Whether increased IL-6 in tumor-bearing mice accounts for this finding remains to be determined.



**Figure 24. Hepatic thrombopoietin transcript levels.** RT-PCR was used to assess hepatic thrombopoietin (TPO) mRNA levels in normal nude mice (n = 3) and ovarian cancer-bearing mice (n = 5).

Regardless, both ectopic tumor and super-physiologic hepatic TPO production might be responsible for high circulating TPO levels when they should otherwise be low in the context of thrombocytosis.

To assess the reproducibility of these findings in ovarian cancer patients with paraneoplastic thrombocytosis, we checked our clinical dataset for women who underwent bone marrow biopsy. Since ovarian cancer patients rarely have indications for bone marrow biopsies, we were only able to identify a handful of patients. Two patients that had thrombocytosis at the time of bone marrow biopsy also had megakaryocyte hyperplasia on pathology report. The remaining patients either had normal platelet and megakaryocyte counts or thrombocytopenia and megakaryocyte hypoplasia. The left panel of figure 25 is a representative image of bone marrow from a patient reported to have increased numbers of mature megakaryocytes, thrombocytosis (platelet count of  $504 \times 10^3/\mu\text{L}$ ), and recent VTE. The right panel of figure 25 is a representative image of bone marrow from a patient about to start her fourth line of chemotherapy with reported megakaryocyte hypoplasia and thrombocytopenia (platelet count of  $127 \times 10^3/\mu\text{L}$ ).

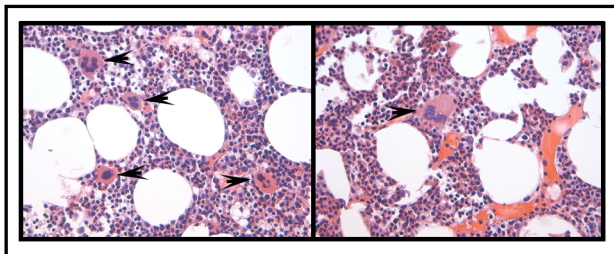


**Figure 25. Bone marrow aspirates from patients with epithelial ovarian cancer.** Representative photomicrographs of bone marrow aspirates from ovarian cancer patients reported to have increased numbers of mature megakaryocytes (left



hand panel) and megakaryocyte hypoplasia (right hand panel). Black arrows point to megakaryocytes.

Although numbers are too small to make any definitive conclusion, this at least provides some anecdotal evidence that platelet counts may be related to the abundance of bone marrow megakaryocytes in ovarian cancer patients as well. Immunohistochemical staining for megakaryocyte markers revealed absence of megakaryocytes in spleens from ovarian cancer patients who had thrombocytosis prior to primary tumor reductive surgery which necessitated splenectomy (Figure 26). This finding was not unexpected given that the spleen is not known to be a hematopoietic organ in adult humans as it is in mice.

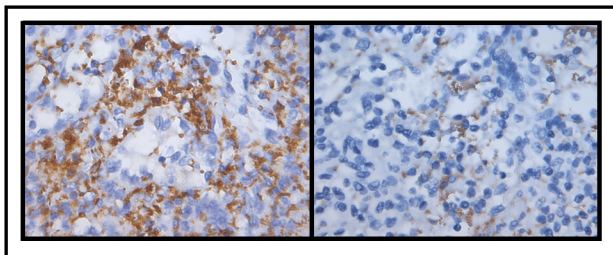


**Figure 26. Examination of ovarian cancer patient spleens for megakaryocytes.** Representative immunohistochemical staining of spleens resected from ovarian cancer patients with thrombocytosis at the time of primary tumor reductive surgery for megakaryocyte and platelet markers CD42b (left hand panel) and CD61 (right hand panel) revealed the presence of platelets and the absence of megakaryocytes.

To date, three tumor types have been reported to produce TPO: hepatoblastoma, hepatocellular carcinoma, and ovarian carcinoma. It is not surprising that hepatoblastoma and hepatocellular carcinoma produce high levels of TPO since the liver is the dominant physiological source of TPO. Furuhashi and colleagues published the only case report of an extrahepatic TPO-producing tumor, an ovarian carcinoma, over a decade ago (107). Since, there have been no follow-up studies examining TPO in ovarian carcinoma despite the high prevalence of thrombocytosis in women with advanced ovarian cancer. Here, we show that ovarian carcinomas from women with thrombocytosis at the time of primary tumor reductive surgery consistently express high cytoplasmic levels of TPO (Figure 27 cases 2-5). Cases 4 and 5 also demonstrate the novel finding of TPO expression in tumor-associated endothelial cells. On the contrary, we found that ovarian carcinomas from patients with normal preoperative platelet counts express relatively low or no TPO (Figure 27, case 1).

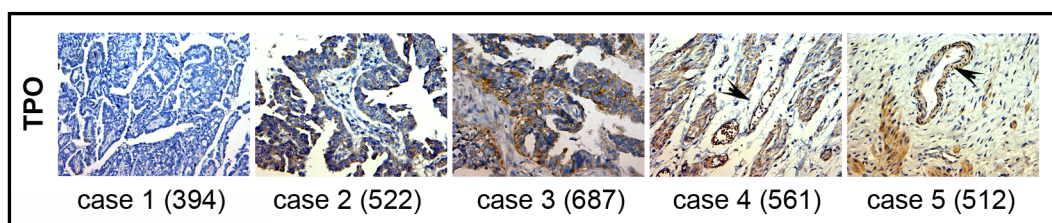


**Figure 27. Thrombopoietin protein expression in patient specimens of serous papillary ovarian carcinoma.** Representative immunohistochemical staining for thrombopoietin in ovarian carcinomas from a patient with a normal platelet count (case 1) and patients with thrombocytosis (cases 2-5) is shown. Tumor and tumor associated endothelial cells (black arrows) in specimens from patients with

thrombocytosis express high levels of thrombopoietin. Preoperative platelet counts appear in parentheses below the photomicrographs.

While TPO is considered the primary physiologic regulator of platelet production, multiple pleiotropic growth factors and cytokines act synergistically on hematopoietic progenitors to promote the growth and maturation of megakaryocytes as well as the enumeration of platelets. In order to identify the relevant humoral factors associated with thrombocytosis in ovarian cancer patients using a high through-put modality, we quantified expression levels of factors known to be implicated in megakaryo- and thrombopoiesis (Table 3) in plasma samples from 150 patients with high grade, advanced stage epithelial ovarian carcinoma using a multiplex bead-based immunoassay. Thirty-one percent of the patients included in this analysis had thrombocytosis, independently validating the prevalence of thrombocytosis we found in our earlier clinical dataset. Platelet counts significantly correlated with plasma levels of IL-6 ( $r_s = 0.4$ ,  $p < 0.0001$ ) and TPO ( $r_s = 0.3$ ,  $p < 0.0001$ , Table 10, Figure 28).

**Table 10.** Spearman's correlation of platelet counts with plasma cytokine levels in 150 ovarian cancer patients

Cytokine	Correlation	p-value
IL-6	0.37	< 0.0001
TPO	0.29	0.0003
G-CSF	0.16	0.0565
IL-3	0.16	0.0570
SCF	0.12	0.1505
IL-1 $\alpha$	0.06	0.4968
IL-11	0.05	0.5299
GM-CSF	0.04	0.5880
FLT3 Ligand	-0.10	0.2335
IL-4	-0.02	0.8361

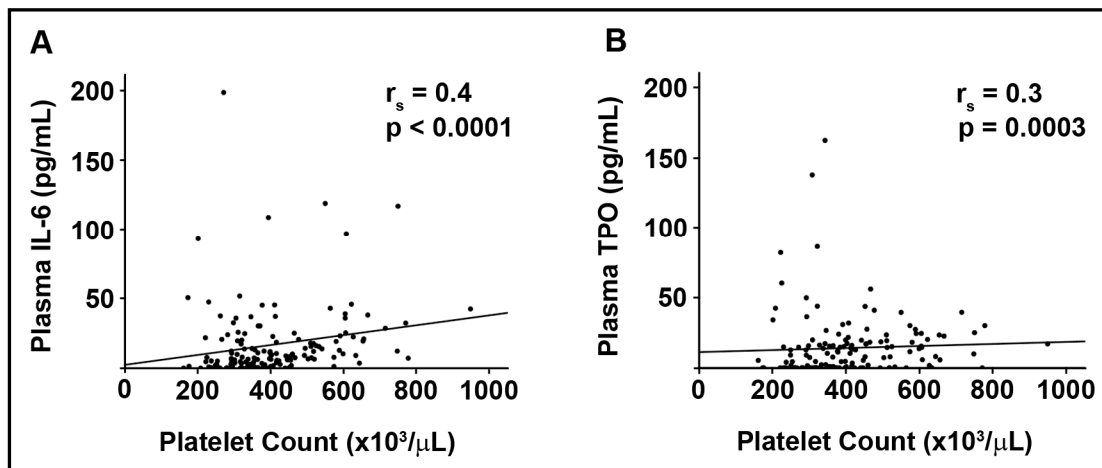


**Figure 28. Spearman's correlation of plasma IL-6 (a) and TPO (b) levels with platelet counts in 150 ovarian cancer patients.**

When we tested differences in plasma cytokine levels between patients with normal platelet counts and thrombocytosis, we found that plasma levels of IL-6, TPO, and granulocyte colony-stimulating factor (G-CSF) were significantly elevated in patients with thrombocytosis. Specifically, patients with thrombocytosis had a mean plasma IL-6 level of 33.42 pg/mL compared to 13.71 pg/mL for patients with normal platelet counts ( $p < 0.0001$ ). Mean plasma TPO levels were 34.43 pg/mL and 16.2 pg/mL for patients with thrombocytosis and normal platelet counts, respectively ( $p = 0.0003$ ). Additionally, mean plasma G-CSF levels were 88.8 pg/mL and 49.02 pg/mL for patients with thrombocytosis and normal platelet counts, respectively ( $p = 0.03$ , Table 11, Figure 29). While plasma levels of IL-4 did not significantly differ between patients with normal platelet counts (mean  $1.32 \pm 12.91$  pg/mL) and thrombocytosis ( $0.13 \pm 0.87$  pg/mL), IL-4 levels were lower in patients with thrombocytosis. This finding is of interest because IL-4 is one of few factors reported to inhibit megakaryopoiesis (46).

**Table 11.** Wilcoxon rank sum test testing differences in plasma cytokine levels (pg/mL) between patients with normal platelet counts and thrombocytosis

Cytokine	Normal platelet counts			Thrombocytosis			P value
	Mean (SD)	Median	Min - Max	Mean (SD)	Median	Min - Max	
IL-6	13.71 (25.61)	5.40	0 - 198.43	33.42 (74.30)	15.50	0.52 - 500.48	< 0.0001
TPO	16.2 (42.61)	3.37	0 - 361.53	34.43 (119.10)	16.96	0 - 819.75	0.0003
G-CSF	49.02 (62.03)	25.97	0 - 403.37	88.8 (127.53)	44.17	3.05 - 709.22	0.0255
IL-3	0.76 (1.27)	0.06	0 - 8.21	1.79 (4.15)	0.45	0 - 21.60	0.1275
SCF	8.9 (13.15)	3.97	0 - 82.13	10.09 (11.21)	7.23	0 - 43.65	0.3070
IL-11	10.34 (29.17)	0	0 - 197.23	15.11 (45.10)	0	0 - 290.13	0.3627
FLT3-Ligand	21.3 (95.35)	0	0 - 917.89	5.12 (15.80)	0	0 - 87.55	0.2481
IL-1 $\alpha$	41.51 (287.84)	0	0 - 2,929.08	11.34 (19.19)	0	0 - 73.51	0.7635
GM-CSF	18.13 (60.06)	0	0 - 366.90	11.5 (40.69)	0	0 - 270.08	0.7963
IL-4	1.32 (12.91)	0	0 - 131.60	0.13 (0.87)	0	0 - 5.94	0.8008

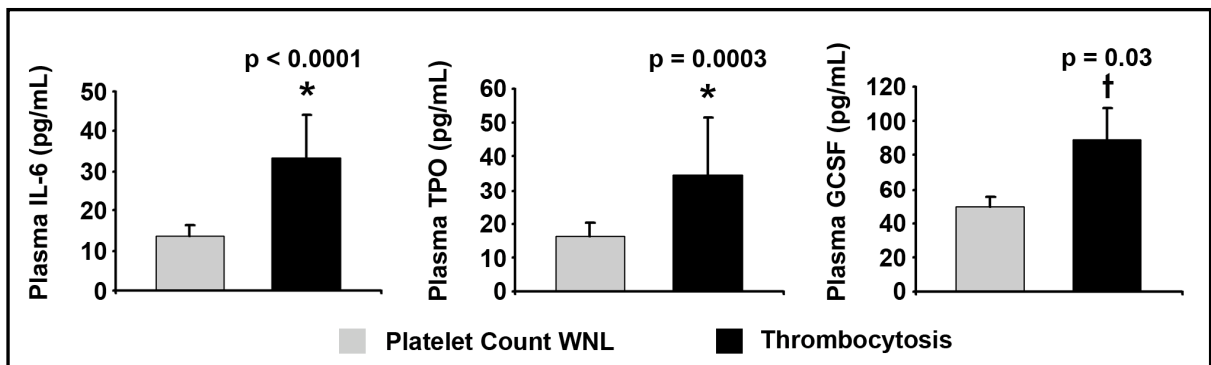


**Figure 29.** IL-6, thrombopoietin, and G-CSF plasma levels in ovarian cancer patients. Graphs show mean differences in plasma IL-6, TPO, and G-CSF levels in patients with normal platelet counts (light bars) and patients with thrombocytosis (dark bars). \* indicates  $p < 0.01$  and † indicates  $p < 0.05$ .

Next, to test whether these same cytokines are also elevated in ovarian cancer-bearing mice known to develop thrombocytosis, we quantified IL-6, TPO, and G-

CSF levels in plasma from healthy control mice and mice bearing A2780ip2, HeyA8, 2774, and ID8 tumors. Plasma cytokine levels were measured using human- and murine-specific ELISAs in order to differentiate orthotopic human ovarian cancers from the murine host as the source of cytokine production. When we tested plasma from our orthotopic mouse models of ovarian cancer for human IL-6, TPO, and G-CSF, human IL-6 was significantly elevated in plasma from mice bearing A2780ip2 (mean  $6.5 \pm \text{SEM } 0.8$  pg/mL,  $p < 0.01$ ), HeyA8 (mean  $61.2 \pm \text{SEM } 20.5$  pg/mL,  $p < 0.05$ ), and 2774 (mean  $392.5 \pm \text{SEM } 86.3$  pg/mL,  $p < 0.01$ ) tumors compared to healthy controls (mean  $1.8 \pm \text{SEM } 0.1$  pg/mL). Plasma levels of human TPO and G-CSF were undetectable, suggesting that the plasma compartment of these factors might predominantly originate from the murine host. To determine if this was the case, we next used murine-specific ELISAs to evaluate plasma levels of TPO and G-CSF. Murine G-CSF was significantly elevated in plasma from mice bearing A2780ip2 (mean  $77.5 \pm \text{SEM } 31.4$  pg/mL,  $p = 0.02$ ), HeyA8 (mean  $352.9 \pm \text{SEM } 25.8$  pg/mL,  $p < 0.01$ ), and 2774 (mean  $71.3 \pm \text{SEM } 13.3$  pg/mL,  $p < 0.01$ ) tumors compared to healthy controls (mean  $22.8 \pm \text{SEM } 4.2$  pg/mL). Plasma levels of murine G-CSF were also significantly increased in the syngeneic ID8 model ( $78.4 \pm \text{SEM } 30.0$  pg/mL,  $p = 0.02$ ) compared to healthy C57/bl6 controls ( $9.5 \pm \text{SEM } 1.0$  pg/mL). Plasma levels of murine TPO were increased by 2-fold and 1.4-fold in mice with 2774 tumors ( $p < 0.05$ ) and ID8 tumors ( $p < 0.01$ ), respectively (Figure 30).

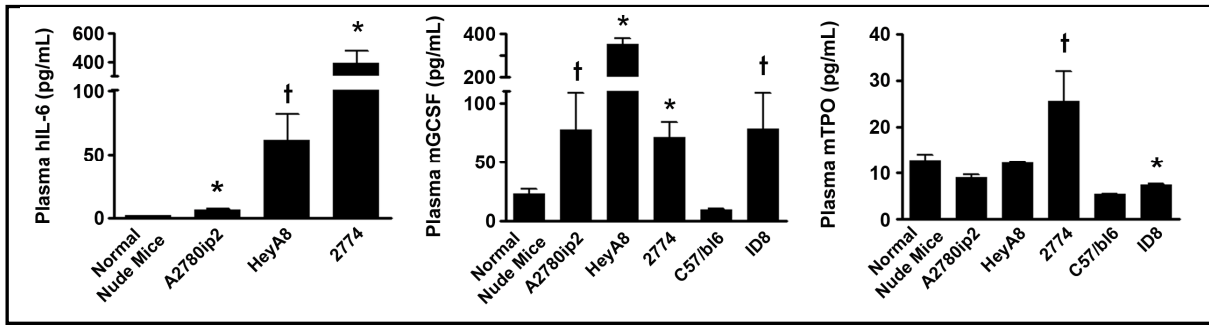


**Figure 30. IL-6, thrombopoietin, and G-CSF plasma levels in non-tumor bearing mice and mouse models of ovarian cancer.** Graphs represent results of ELISA-based quantification of mean IL-6, G-CSF, and TPO plasma levels  $\pm$  SEM in non-tumor bearing mice (normal nude mice and C57/bl6 mice) and mouse models of ovarian cancer (A2780ip2, HeyA8, 2774, and ID8). \* indicates  $p < 0.01$  and † indicates  $p < 0.05$ .

To test whether IL-6, G-CSF, and TPO are not simply associated with, but also play a functional role in paraneoplastic thrombocytosis, we tested the effect of silencing these humoral factors on thrombocytosis in A2780ip2 and 2774 orthotopic mouse models of ovarian cancer. Compared to control siRNA (mean platelet count  $1405 \pm 143 \times 10^3/\mu\text{L}$ ), IL-6 siRNA decreased thrombocytosis by 27% (mean platelet count  $1297 \pm 103 \times 10^3/\mu\text{L}$ ) in mice bearing A2780ip2 tumors. TPO and G-CSF siRNA decreased thrombocytosis by 52% (mean platelet count  $1197 \pm 190 \times 10^3/\mu\text{L}$ ) and 56% (mean platelet count  $1180 \pm 167 \times 10^3/\mu\text{L}$ ), respectively. Combination IL-6, TPO, and G-CSF siRNA was most effective and completely abrogated thrombocytosis in mice bearing A2780ip2 tumors (mean platelet count  $855 \pm 116 \times 10^3/\mu\text{L}$ ,  $p = 0.02$ ). These data are summarized in Table 12.

**Table 12.** Impact of targeting IL-6, TPO, and G-CSF alone and in combination on thrombocytosis in A2780ip2 orthotopic mouse model of ovarian cancer

<b>A2780ip2 Treatment</b>	<b>Mean Platelet Count (<math>\times 10^3/\mu\text{L}</math>) <math>\pm</math> SEM</b>	<b>Percent Abrogation of Thrombocytosis</b>
Control siRNA	1405 $\pm$ 143	
IL-6 siRNA	1297 $\pm$ 103	27%
TPO siRNA	1197 $\pm$ 190	52%
G-CSF siRNA	1180 $\pm$ 167	56%
Combination	855 $\pm$ 116	128%*

\* p < 0.05

In mice bearing 2774 tumors, IL-6 siRNA decreased thrombocytosis by 55% (mean platelet count  $1776 \pm 118 \times 10^3/\mu\text{L}$ , p < 0.01) compared to control siRNA (mean platelet count  $2724 \pm 226 \times 10^3/\mu\text{L}$ ). TPO and G-CSF siRNA decreased thrombocytosis by 44% (mean platelet count  $1959 \pm 184 \times 10^3/\mu\text{L}$ , p = 0.03) and 27% (mean platelet count  $1893 \pm 147 \times 10^3/\mu\text{L}$ ), respectively. Compared to control siRNA, combination IL-6, TPO, and G-CSF siRNA abrogated thrombocytosis by 54% (mean platelet count  $1797 \pm 179 \times 10^3/\mu\text{L}$ , p = 0.01) in mice bearing 2774 tumors. These data are summarized in Table 13.

**Table 13.** Impact of targeting IL-6, TPO, and G-CSF alone and in combination on thrombocytosis in 2774 orthotopic mouse model of ovarian cancer

<b>2774 Treatment</b>	<b>Mean Platelet Count (<math>\times 10^3/\mu\text{L}</math>) <math>\pm</math> SEM</b>	<b>Percent Abrogation of Thrombocytosis</b>
Control siRNA	2724 $\pm$ 226	
IL-6 siRNA	1776 $\pm$ 118	55%*
TPO siRNA	1959 $\pm$ 184	44%*
G-CSF siRNA	2240 $\pm$ 187	27%
Combination	1797 $\pm$ 179	54%*

\* p < 0.05



Given that IL-6 siRNA, TPO siRNA, and combination treatment abrogated thrombocytosis to similar extent, it is possible that TPO is the operative factor driving thrombocytosis at least in this model and that targeting TPO directly or indirectly via inhibition of IL-6 has the same net effect on reducing thrombocytosis. Platelet counts and plasma levels of IL-6 and TPO are also disproportionately elevated in mice with 2774 tumors compared to A2780ip2 tumor-bearing mice. This might explain why we were able to completely abrogate thrombocytosis in the A2780ip2 model, while achieving a 50% reduction in the 2774 model. Complete abrogation of thrombocytosis in the 2774 model might not have been possible with the dose and/or number of siRNA treatments administered in these experiments. Alternatively, other cytokines might contribute to thrombocytosis in the 2774 model.

## Summary

The present investigation makes several important contributions to our current understanding of the clinical implications, biological significance, and underlying etiology of paraneoplastic thrombocytosis.

1) One in three women diagnosed with epithelial ovarian cancer has thrombocytosis and development of this paraneoplastic syndrome is associated with increased risk of VTE and compromised disease specific survival.

2) Platelets are host components that can be co-opted into facilitating the growth and dissemination of ovarian cancer. Functioning in this capacity, platelets increase tumor cell proliferation and migration, support microvessel pericytes, and promote tumor and endothelial cell survival. The pro-survival effect of platelets on tumor cells may be a novel mechanism of chemoresistance mediated by platelet derived growth factor activation of tumor cell tyrosine kinase receptors such as PDGFR $\alpha$ .

3) Megakaryo- and thrombopoietic factors IL-6, TPO, and G-CSF produced by both the tumor and reciprocally by the host play a major role in the development of paraneoplastic thrombocytosis in ovarian carcinoma. Targeting tumor and host derived TPO, IL-6, and G-CSF significantly abrogates paraneoplastic thrombocytosis *in vivo*.

## Discussion

### Clinical implications of paraneoplastic thrombocytosis

Emerging clinical evidence suggests that thrombocytosis, high platelet turnover, and the presence of activated platelets in circulation portend poor prognosis in many cancers (34). These data introduce the possibility of exploiting platelets as therapeutic targets for anticancer therapies. However, the fundamental involvement of platelets in important physiological processes such as hemostasis complicates the development and implementation of anti-platelet strategies. Moreover, our limited understanding of the precise mechanisms by which platelets facilitate growth and dissemination of malignancy has been a major hurdle in selectively blocking their tumor promoting activities. A necessary first step is to identify the cancer types in which platelets play significant biological roles. The current investigation provides both clinical and experimental evidence implicating platelets in the growth and progression of epithelial ovarian carcinoma. Analysis of clinical data from over 600 ovarian cancer patients treated at 4 centers makes this one of the largest studies of the prevalence and prognostic significance of thrombocytosis in oncology patients to date. Our findings indicate that up to 1 in 3 women with newly diagnosed ovarian cancer will have platelet counts exceeding 450,000/ $\mu$ L. To the best of our knowledge, this is the highest reported rate of paraneoplastic thrombocytosis in any solid malignancy, emphasizing that ovarian cancer is an exceptionally relevant context in which to study this process. Rates of thrombocytosis in association with other solid malignancies typically range from 3-25% and this likely represents an overestimation, as the majority of investigators have defined thrombocytosis as a platelet count >400,000/uL, instead of >450,000/uL according to NHLBI criteria

(Table 7). In addition to arising in a substantial proportion of ovarian cancer patients, thrombocytosis is associated with several aggressive clinical features including advanced stage disease, higher median preoperative serum CA-125 levels, and significantly worse progression free and overall survival. These findings are supported by those of Li and colleagues who identified statistically significant associations between thrombocytosis and advanced stage disease, high grade tumors, and elevated CA-125 levels in 183 patients with invasive epithelial ovarian and primary peritoneal carcinomas (108). This study and a smaller investigation by Menczer and co-investigators also demonstrated that thrombocytosis may signify increased risk of suboptimal surgical cytoreduction and is an independent poor prognostic factor (109). While Li and colleagues also considered the relationship between thrombocytosis and postoperative DVT/PE in their analysis, there was no discernable link, possibly due to the limited number of cases of DVT/PE in their cohort of patients. To date, no other studies have examined the predictive value of thrombocytosis for risk of VTE in ovarian cancer. However, the association between thrombosis and cancer in general is well recognized. Existing data indicate that thromboembolism occurs in 4-20% of patients with malignancies and is the initial clinical manifestation in ~10% of patients with an occult malignancy (110-112). Recently, Vemulapalli et al. published their analysis of the clinical outcomes and factors predicting development of venous thromboembolic complications in Phase I patients at MDACC. Factors predicting the development of new thromboembolic episodes included diagnosis of pancreatic cancer, history of previous venous thromboembolism, and platelet count  $>440,000/\mu\text{L}$  (113). Platelet microthrombi formation associated with Trousseau's syndrome is often found in

mucin-producing carcinomas, classically pancreatic and not uncommonly ovarian cancer (114). On this basis, we performed a predefined subset analysis to clarify the relationship between thrombocytosis and VTE in ovarian cancer patients. Our analysis revealed that thrombocytosis significantly increases the risk of VTE in ovarian cancer patients and that thrombocytosis is an independent predictor of increased mortality in women who do develop a blood clot. Currently, the American Society of Clinical Oncology guidelines recommend that all hospitalized cancer patients and patients undergoing major surgery for malignant disease be considered for pharmacologic thromboprophylaxis. At present, routine prophylaxis with anticoagulation for ambulatory cancer patients is only recommended for those receiving thalidomide or its derivative, lenalidomide (110). However, our findings, taken together with those of Vemulapalli and colleagues, suggest that instituting thromboprophylaxis in cancer patients with thrombocytosis might be prudent. Prophylaxis options could include low-dose unfractionated heparin, low-molecular-weight heparin (LMWH), warfarin, and aspirin. In addition to lowering the risk of VTE, there is growing evidence that heparins and aspirin may confer added benefit of anti-tumor activity, primarily by interfering with aggregation dependent platelet-tumor cell cross-talk. Several prospective clinical trials indicate that LMWH improves survival in cancer patients, and that this effect cannot be ascribed to prevention of VTE alone (115). Additionally, a recent epidemiological study by Chan and colleagues provides compelling data that regular use of aspirin after the diagnosis of colorectal cancer is associated with lower risk of cancer-specific and overall mortality (116). Heparins and aspirin likely have anti-neoplastic activities independent of their anticoagulation properties. For example, heparin may

sequester growth factors released from tumor and endothelial cells away from their receptors and have an inhibitory effect on angiogenesis. Additionally, heparin may prevent metastasis by blocking selectin- and integrin-mediated adhesion of tumor cells and leukocytes to endothelial cells. Heparins also potently inhibit heparanase, an endo-glycosidase that facilitates tumor cell invasion through degradation and remodeling of the extracellular matrix (117). The chemopreventive and tumor growth inhibitory effects of aspirin have largely been ascribed to inhibition of prostaglandin synthesis by cyclooxygenase COX-1 and COX-2 enzymes (118).

#### Biological significance of paraneoplastic thrombocytosis

Platelets likely induce growth and progression of malignancy by diverse mechanisms. Platelet adherence may shield tumor cells from immune surveillance, particularly from the cytotoxic activity of natural killer cells. Direct interactions between platelets and tumors cells may also aid tumor cells in lodging in the microvasculature where they form intravascular colonies or extravasate into target organs. In the tumor microenvironment, platelets release a plethora of bioactive factors, such as chemokines, cytokines, growth factors, and metalloproteinases, which are capable of promoting angiogenesis and stimulating tumor cell survival, proliferation, and invasion (34). While the observational data we and others have generated establish strong associations between thrombocytosis and aggressive clinicopathologic features, they do not confirm a causal relationship between thrombocytosis and tumor progression. Thus, the present investigation extends the current body of knowledge by providing experimental evidence for the functional role of platelets in driving ovarian cancer progression. The finding that mouse models of ovarian cancer and other solid malignancies consistently recapitulate

paraneoplastic thrombocytosis served as the foundation for this work. To illustrate that this is a dynamic process, we showed that platelet counts rise with increasing tumor burden and that platelets traffic into the tumor bed and ascites where they rapidly adhere to free-floating cells. To further build a case for the supportive role of platelets in the development of invasive tumors, we demonstrated that halving the circulating platelet mass significantly inhibits tumor growth *in vivo*. Histopathological analysis of tumors from platelet depleted mice revealed that the anti-tumor effect of platelet depletion was likely multi-factorial and could be attributed to decreased tumor cell proliferation, microvessel density, and pericyte coverage as well as increased tumor and endothelial cell apoptosis. These results suggest that platelets can exert direct stimulatory effects on tumor cells and support angiogenesis. To corroborate this, we performed *in vitro* studies to evaluate the impact of plasma-purified platelets on ovarian cancer cells more definitively. Our results reveal that platelets potently induce tumor cell migration, proliferation, and survival. The finding that platelets can protect tumor cells from the cytotoxic insult of taxanes is particularly intriguing because, to the best of our knowledge, this has not been previously reported. Among the potential mechanisms by which platelets may confer chemoresistance, one particularly logical possibility is that factors released by platelets, such as PDGF, activate survival signaling pathways in tumor cells. In fact, PDGFR $\alpha$  blockade with the fully humanized antibody IMC-3G3 restored the cytotoxic effect of docetaxel in spite of platelets. There is also recent evidence to suggest that the secretory activities of platelets stabilize the tumor vasculature and prevent tumor hemorrhage. The platelet-derived factors involved in the maintenance of angiogenic microvessel integrity have yet to be identified.

Additionally, the cell type that platelets influence most is not yet known (39). Our histopathological analysis of tumors resected from platelet depleted mice revealed lack of pericytes and disruption of endothelial-pericyte association. Given that pericytes are PDGF-dependent mesenchymal cells that support and stabilize small blood vessels, it is possible that platelets regulate tumor vasculature homeostasis, in part, by nurturing pericytes.

#### Mechanisms of paraneoplastic thrombocytosis

These data in combination with contributions from other investigations provide strong biological plausibility for the role of platelets in the growth and dissemination of cancer in general and ovarian cancer specifically. Based on these findings, inhibition of paraneoplastic thrombocytosis may be an innovative approach to breaking the circuit between cancer cells and platelets. Such an approach could be an attractive alternative to directly targeting platelets, particularly in a patient population heavily treated with myelosuppressive chemotherapeutic agents. However, to this point there have been surprisingly few studies addressing the mechanism of paraneoplastic thrombocytosis and thus, the underlying etiology has remained unknown. An expanding body of knowledge indicates that multiple cytokines regulate the complex physiological process of megakaryo- and thrombopoiesis. Aberrations in humoral stimuli have been the focus of intense investigation in patients with thrombocytopenia, but there has been less interest in examining such perturbations in the converse scenario of thrombocytosis. To our knowledge this is the largest study examining the relationship between circulating levels of megakaryo- and thrombopoietic cytokines and paraneoplastic thrombocytosis. Of the 10 key cytokines assayed in 150 advanced stage ovarian



cancer patients, IL-6, TPO, and G-CSF were significantly associated with thrombocytosis. This finding is supported by several smaller reports published over the past 20 years. In one study of colorectal cancer patients, significantly higher platelet counts and plasma TPO levels were identified in patients with stage III (n = 10) compared to patients with stage I (n = 11) disease (119). Elevated plasma granulocyte colony-stimulating factor (G-CSF) and granulocyte macrophage colony-stimulating factor (GM-CSF) were also found to be associated with thrombocytosis in a case study of patients (n = 14) with a variety of solid malignancies (120). Blay and colleagues demonstrated that serum IL-6 levels significantly correlate with platelet count in renal cell carcinoma patients (n = 100). A small subset of patients with metastatic disease who participated in a phase II trial of anti-IL6 antibody (n = 12) all experienced a reduction in platelet counts by at least 20% during treatment. Moreover, platelet counts normalized during anti-IL6 treatment in all patients with thrombocytosis upon entry into the trial (n = 5) (121). Clinical studies examining the effectiveness of recombinant human IL-6 in stimulating platelet production in patients with advanced solid malignancies including ovarian cancer have demonstrated that IL-6 potently increases thrombopoiesis prior to and accelerates platelet recovery after chemotherapy (122, 123). These patients also developed mild anemia and leukopoiesis (specifically increased neutrophils, monocytes, and lymphocytes). This is of interest because the same shift in these blood count parameters was observed in patients with thrombocytosis in the current study. While we did not specifically track changes in hemoglobin and white blood cell counts with IL-6 levels, the strong association we uncovered between thrombocytosis and high IL-6 levels raises the question of whether high circulating

levels of IL-6 also account for mild anemia and leukocytosis in patients with thrombocytosis. Taken together, these findings suggest that IL-6, TPO, and G-CSF may be operative humoral factors implicated in paraneoplastic thrombocytosis. However, these observational data are limited by their correlative nature. Therefore, to test whether these cytokines are not simply associated with, but also significantly contribute to paraneoplastic thrombocytosis, we evaluated the effect of siRNA-induced silencing of these cytokines alone and in combination in two orthotopic mouse models of ovarian cancer that characteristically develop paraneoplastic thrombocytosis. The results of these *in vivo* experiments provide the first evidence of a causative role for IL-6, TPO, and G-CSF in paraneoplastic thrombocytosis.

From an experimental point of view, several issues should be addressed regarding the experimental protocol chosen. Given that we targeted both human (tumor) and murine (host) homologs of IL-6 and TPO, we cannot determine the relative contribution of tumor verses host tissues to the production of these cytokines. Since G-CSF was only expressed and thus silenced in the murine host and since targeting murine G-CSF abrogated thrombocytosis by 27-56% depending on the model, we can at least conclude that host tissues are a predominant and important source of increased circulating G-CSF. Inflammatory stimuli such as IL-1, LPS, and TNF- $\alpha$  induce G-CSF production by macrophages, endothelial cells, fibroblasts and related mesenchymal cells. At the cellular level, G-CSF induces proliferation of all mitogenic cells in the granulocyte lineage starting with uncommitted hematopoietic stem cells. In the first phase I studies of G-CSF, G-CSF administration resulted in mobilization of large numbers of progenitor and stem

cells (myeloid, erythroid, megakaryocytic) from the marrow into the peripheral blood. In particular, platelet recovery was markedly accelerated. This became the basis for using G-CSF mobilized blood stem cells in lieu of bone marrow as the standard source of hematopoietic stem cells for allogenic bone marrow transplantation (124, 125). In keeping with these functional data, it is possible that host macrophages, endothelial cells, and fibroblasts increase their production of G-CSF in response to inflammatory stimuli part of the cancer milieu and that G-CSF in turn stimulates increased megakaryopoiesis from progenitors in the bone marrow.

Interleukin 6 is also upregulated in response to inflammatory cytokines including IL-1, LPS, TNF- $\alpha$ , and PDGF, while the IL-6 promoter is inhibited by p53. Thus, overexpression of IL-6 in many malignancies could occur in response to inflammatory cytokines and/or as a result of p53 loss. Given the high incidence of p53 mutations in epithelial ovarian cancer (23-79% of cases), the later is a distinct possibility (126). An elevated serum IL-6 level has been correlated with an adverse prognosis in patients with several different types of malignancy, including ovarian cancer (127). *In vitro* studies also demonstrate that ovarian cancer cell lines and primary ovarian tumor cultures constitutively produce IL-6 (128). There is growing evidence that IL-6 can enhance hepatic TPO production, which is otherwise thought to occur at a constant rate. IL-6 may also act in an autocrine fashion to increase TPO expression by cancer cells themselves. IL-6 stimulation of TPO transcription has been reported in hepatocellular carcinoma cells (129). The 5'-untranslated region of the TPO gene contains 13 segments that match the type II IL-6 response element consensus sequence (CTGGGA) (130). Further, the binding of Ets family transcription factors to the sequence 5'-ACTTCCG-3' in the human TPO promoter

has been implicated in the expression of the TPO gene in the liver. IL-6 has been shown to rapidly induce DNA-binding activity to the Ets motif of the JunB promoter, which suggests that an Ets family transcription factor might be involved in the enhancement of TPO gene expression by IL-6 (129). Here, we demonstrate increased TPO protein and mRNA expression in orthotopic ovarian cancers and livers resected from tumor-bearing mice which also have high plasma TPO levels and thrombocytosis. Our *in vivo* data suggest that silencing TPO more effectively decreased thrombocytosis than silencing IL-6 in the A2780ip2 model. In the 2774 model, IL-6 siRNA, TPO siRNA, and combination treatment abrogated thrombocytosis to similar extent. This might suggest that targeting TPO directly or indirectly via inhibition of IL-6 has the same net effect on reducing thrombocytosis. Thus, based on these observations and existing knowledge about the source and biological function of these cytokines, we can propose a revised hypothesis. Tumor derived IL-6 stimulates host production of G-CSF and TPO which induce megakaryopoiesis and thrombopoiesis, respectively. Megakaryopoiesis is attributed to G-CSF because of the known stimulatory effect of G-CSF on megakaryocyte progenitor cells and thrombopoiesis is attributed to increased TPO because TPO predominantly drives this process. Tumor TPO production may also occur to some degree (Figure 31).

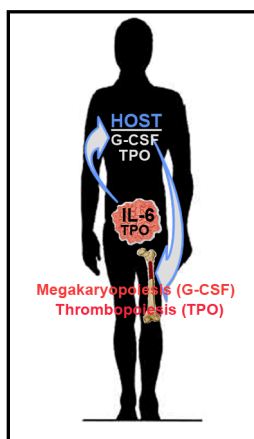


**Figure 31. Revised hypothesis.** Tumor derived IL-6 stimulates host production of G-CSF and TPO which induce megakaryopoiesis and thrombopoiesis, respectively. Tumor TPO production may also occur to some degree. Megakaryopoiesis is attributed to G-CSF because of the known stimulatory effect of G-CSF on megakaryocyte progenitor cells and thrombopoiesis is attributed to increased TPO because TPO predominantly drives this process.

Follow-up *in vivo* experiments using IL-6 deficient mice would be useful for testing this hypothesis and for further dissecting out the relative contributions of the host verses tumor. Additionally, enumeration of splenic and bone marrow megakaryocytes following G-CSF, IL-6, and/or TPO silencing would provide insight into the involvement of these targets in megakaryopoiesis verses thrombopoiesis. Lastly, platelet-megakaryocyte TPO receptor-mediated uptake of TPO is the canonical mechanism for regulating circulating TPO levels. However, our finding that platelets, megakaryocytes, and plasma thrombopoietin increase concomitantly in patients with paraneoplastic thrombocytosis indicates that the number of megakaryocytes or platelets by themselves might not be the sole determinant of circulating TPO levels and thus thrombopoiesis. Further, there are data to suggest

that mutations in the TPO receptor itself can result in decreased membrane expression of TPO receptor by platelets and megakaryocytes. Thus, it is also possible that TPO receptor mutations or other factors leading to a decrease in cell surface receptor expression leads to decreased TPO clearance.

#### Limitations and conclusion

While the current study provides new understanding of the clinical implications, biological significance, and underlying etiology of paraneoplastic thrombocytosis, it has several potential limitations. Our clinical observations are based on a retrospective analysis, which has the possible associated issues of selection bias and incomplete data collection. Additionally, the present analysis only takes into account platelet counts at the time of initial presentation. Understanding how closely platelet counts track with disease status after completion of primary therapy could strengthen the predictive value of thrombocytosis in this and other patient populations. Further, while the present study focuses on quantitative differences in platelet counts, other differences in platelets in the context of cancer may be equally important. In particular, alterations in platelet signaling proteins and granule content related to active malignancy could represent a rich source of novel biomarkers and therapeutic targets. These are areas that deserve much consideration particularly given that paraneoplastic thrombocytosis is not simply an epiphenomenon of cancer progression, but rather plays a central role in the complex process of malignancy. Blocking the development of paraneoplastic thrombocytosis and interfering with platelet-cancer cell interactions could represent new strategical approaches for improving anti-cancer therapies and patient outcomes.

## Bibliography

1. Jemal, A., Siegel, R., Ward, E., Hao, Y., Xu, J., and Thun, M. J. Cancer statistics, 2009. *CA Cancer J Clin*, 59: 225-249, 2009.
2. Huang, L., Cronin, K. A., Johnson, K. A., Mariotto, A. B., and Feuer, E. J. Improved survival time: what can survival cure models tell us about population-based survival improvements in late-stage colorectal, ovarian, and testicular cancer? *Cancer*, 112: 2289-2300, 2008.
3. Modesitt, S. C. and Jazaeri, A. A. Recurrent epithelial ovarian cancer: pharmacotherapy and novel therapeutics. *Expert Opin Pharmacother*, 8: 2293-2305, 2007.
4. Ozols, R. F., Bundy, B. N., Greer, B. E., Fowler, J. M., Clarke-Pearson, D., Burger, R. A., Mannel, R. S., DeGeest, K., Hartenbach, E. M., and Baergen, R. Phase III trial of carboplatin and paclitaxel compared with cisplatin and paclitaxel in patients with optimally resected stage III ovarian cancer: a Gynecologic Oncology Group study. *J Clin Oncol*, 21: 3194-3200, 2003.
5. Markman, M. The promise and perils of 'targeted therapy' of advanced ovarian cancer. *Oncology*, 74: 1-6, 2008.
6. Mutch, D. G., Orlando, M., Goss, T., Teneriello, M. G., Gordon, A. N., McMeekin, S. D., Wang, Y., Scribner, D. R., Jr., Marciniack, M., Naumann, R. W., and Secord, A. A. Randomized phase III trial of gemcitabine compared with pegylated liposomal doxorubicin in patients with platinum-resistant ovarian cancer. *J Clin Oncol*, 25: 2811-2818, 2007.
7. Ferrandina, G., Ludovisi, M., Lorusso, D., Pignata, S., Breda, E., Savarese, A., Del Medico, P., Scaltriti, L., Katsaros, D., Priolo, D., and Scambia, G.

- Phase III trial of gemcitabine compared with pegylated liposomal doxorubicin in progressive or recurrent ovarian cancer. *J Clin Oncol*, 26: 890-896, 2008.
8. Gordon, A. N., Fleagle, J. T., Guthrie, D., Parkin, D. E., Gore, M. E., and Lacave, A. J. Recurrent epithelial ovarian carcinoma: a randomized phase III study of pegylated liposomal doxorubicin versus topotecan. *J Clin Oncol*, 19: 3312-3322, 2001.
  9. du Bois, A., Luck, H. J., Meier, W., Adams, H. P., Mobus, V., Costa, S., Bauknecht, T., Richter, B., Warm, M., Schroder, W., Olbricht, S., Nitz, U., Jackisch, C., Emons, G., Wagner, U., Kuhn, W., and Pfisterer, J. A randomized clinical trial of cisplatin/paclitaxel versus carboplatin/paclitaxel as first-line treatment of ovarian cancer. *J Natl Cancer Inst*, 95: 1320-1329, 2003.
  10. Muggia, F. M., Braly, P. S., Brady, M. F., Sutton, G., Niemann, T. H., Lentz, S. L., Alvarez, R. D., Kucera, P. R., and Small, J. M. Phase III randomized study of cisplatin versus paclitaxel versus cisplatin and paclitaxel in patients with suboptimal stage III or IV ovarian cancer: a gynecologic oncology group study. *J Clin Oncol*, 18: 106-115, 2000.
  11. Ozols, R. F., Markman, M., and Thigpen, J. T. ICON3 and chemotherapy for ovarian cancer. *Lancet*, 360: 2086-2087; author reply 2088, 2002.
  12. Bookman, M. A., Brady, M. F., McGuire, W. P., Harper, P. G., Alberts, D. S., Friedlander, M., Colombo, N., Fowler, J. M., Argenta, P. A., De Geest, K., Mutch, D. G., Burger, R. A., Swart, A. M., Trimble, E. L., Accario-Winslow, C., and Roth, L. M. Evaluation of new platinum-based treatment regimens in



- advanced-stage ovarian cancer: a Phase III Trial of the Gynecologic Cancer Intergroup. *J Clin Oncol*, 27: 1419-1425, 2009.
13. Burger, R. A., Sill, M. W., Monk, B. J., Greer, B. E., and Sorosky, J. I. Phase II trial of bevacizumab in persistent or recurrent epithelial ovarian cancer or primary peritoneal cancer: a Gynecologic Oncology Group Study. *J Clin Oncol*, 25: 5165-5171, 2007.
  14. Cannistra, S. A., Matulonis, U. A., Penson, R. T., Hambleton, J., Dupont, J., Mackey, H., Douglas, J., Burger, R. A., Armstrong, D., Wenham, R., and McGuire, W. Phase II study of bevacizumab in patients with platinum-resistant ovarian cancer or peritoneal serous cancer. *J Clin Oncol*, 25: 5180-5186, 2007.
  15. Markman, M. and Bookman, M. A. Second-line treatment of ovarian cancer. *Oncologist*, 5: 26-35, 2000.
  16. White, R. H., Chew, H. K., Zhou, H., Parikh-Patel, A., Harris, D., Harvey, D., and Wun, T. Incidence of venous thromboembolism in the year before the diagnosis of cancer in 528,693 adults. *Arch Intern Med*, 165: 1782-1787, 2005.
  17. Clarke-Pearson, D. L., Coleman, R. E., Synan, I. S., Hinshaw, W., and Creasman, W. T. Venous thromboembolism prophylaxis in gynecologic oncology: a prospective, controlled trial of low-dose heparin. *Am J Obstet Gynecol*, 145: 606-613, 1983.
  18. von Tempelhoff, G. F., Heilmann, L., Hommel, G., Schneider, D., Niemann, F., and Zoller, H. Hyperviscosity syndrome in patients with ovarian carcinoma. *Cancer*, 82: 1104-1111, 1998.

19. Satoh, T., Oki, A., Uno, K., Sakurai, M., Ochi, H., Okada, S., Minami, R., Matsumoto, K., Tanaka, Y. O., Tsunoda, H., Homma, S., and Yoshikawa, H. High incidence of silent venous thromboembolism before treatment in ovarian cancer. *Br J Cancer*, 97: 1053-1057, 2007.
20. Duska, L. R., Garrett, L., Henretta, M., Ferriss, J. S., Lee, L., and Horowitz, N. When 'never-events' occur despite adherence to clinical guidelines: the case of venous thromboembolism in clear cell cancer of the ovary compared with other epithelial histologic subtypes. *Gynecol Oncol*, 116: 374-377.
21. Tateo, S., Mereu, L., Salamano, S., Klersy, C., Barone, M., Spyropoulos, A. C., and Piovella, F. Ovarian cancer and venous thromboembolic risk. *Gynecol Oncol*, 99: 119-125, 2005.
22. Black, D., Iasonos, A., Ahmed, H., Chi, D. S., Barakat, R. R., and Abu-Rustum, N. R. Effect of perioperative venous thromboembolism on survival in ovarian, primary peritoneal, and fallopian tube cancer. *Gynecol Oncol*, 107: 66-70, 2007.
23. Rodriguez, A. O., Wun, T., Chew, H., Zhou, H., Harvey, D., and White, R. H. Venous thromboembolism in ovarian cancer. *Gynecol Oncol*, 105: 784-790, 2007.
24. Fotopoulou, C., duBois, A., Karavas, A. N., Trappe, R., Aminossadati, B., Schmalfeldt, B., Pfisterer, J., and Sehouli, J. Incidence of venous thromboembolism in patients with ovarian cancer undergoing platinum/paclitaxel-containing first-line chemotherapy: an exploratory analysis by the Arbeitsgemeinschaft Gynaekologische Onkologie Ovarian Cancer Study Group. *J Clin Oncol*, 26: 2683-2689, 2008.

25. Tetsche, M. S., Norgaard, M., Pedersen, L., Lash, T. L., and Sorensen, H. T. Prognosis of ovarian cancer subsequent to venous thromboembolism: a nationwide Danish cohort study. *BMC Cancer*, 6: 189, 2006.
26. Levitan, N., Dowlati, A., Remick, S. C., Tahsildar, H. I., Sivinski, L. D., Beyth, R., and Rimm, A. A. Rates of initial and recurrent thromboembolic disease among patients with malignancy versus those without malignancy. Risk analysis using Medicare claims data. *Medicine (Baltimore)*, 78: 285-291, 1999.
27. Trousseau, A., Bazire, V., and Cormack, J. Lectures on clinical medicine, delivered at the Hotel-Dieu, Paris London: R. Hardwicke. 1867.
28. Levine, M. N. Prevention of thrombotic disorders in cancer patients undergoing chemotherapy. *Thromb Haemost*, 78: 133-136, 1997.
29. Wang, X., Wang, E., Kavanagh, J. J., and Freedman, R. S. Ovarian cancer, the coagulation pathway, and inflammation. *J Transl Med*, 3: 25, 2005.
30. Levin, J. and Conley, C. L. Thrombocytosis Associated with Malignant Disease. *Arch Intern Med*, 114: 497-500, 1964.
31. Shivdasani, R. A., Rosenblatt, M. F., Zucker-Franklin, D., Jackson, C. W., Hunt, P., Saris, C. J., and Orkin, S. H. Transcription factor NF-E2 is required for platelet formation independent of the actions of thrombopoietin/MGDF in megakaryocyte development. *Cell*, 81: 695-704, 1995.
32. Camerer, E., Qazi, A. A., Duong, D. N., Cornelissen, I., Advincula, R., and Coughlin, S. R. Platelets, protease-activated receptors, and fibrinogen in hematogenous metastasis. *Blood*, 104: 397-401, 2004.

33. Karpatkin, S., Pearlstein, E., Ambrogio, C., and Collier, B. S. Role of adhesive proteins in platelet tumor interaction in vitro and metastasis formation in vivo. *J Clin Invest*, *81*: 1012-1019, 1988.
34. Borsig, L. The role of platelet activation in tumor metastasis. *Expert Rev Anticancer Ther*, *8*: 1247-1255, 2008.
35. Nieswandt, B., Hafner, M., Echtenacher, B., and Mannel, D. N. Lysis of tumor cells by natural killer cells in mice is impeded by platelets. *Cancer Res*, *59*: 1295-1300, 1999.
36. Italiano, J. E., Jr., Richardson, J. L., Patel-Hett, S., Battinelli, E., Zaslavsky, A., Short, S., Ryeom, S., Folkman, J., and Klement, G. L. Angiogenesis is regulated by a novel mechanism: pro- and antiangiogenic proteins are organized into separate platelet alpha granules and differentially released. *Blood*, *111*: 1227-1233, 2008.
37. Rhee, J. S., Black, M., Schubert, U., Fischer, S., Morgenstern, E., Hammes, H. P., and Preissner, K. T. The functional role of blood platelet components in angiogenesis. *Thromb Haemost*, *92*: 394-402, 2004.
38. Nachman, R. L. and Rafii, S. Platelets, petechiae, and preservation of the vascular wall. *N Engl J Med*, *359*: 1261-1270, 2008.
39. Ho-Tin-Noe, B., Goerge, T., and Wagner, D. D. Platelets: guardians of tumor vasculature. *Cancer Res*, *69*: 5623-5626, 2009.
40. Fukumura, D. and Jain, R. K. Tumor microvasculature and microenvironment: targets for anti-angiogenesis and normalization. *Microvasc Res*, *74*: 72-84, 2007.

41. Kaushansky, K. Determinants of platelet number and regulation of thrombopoiesis. *Hematology Am Soc Hematol Educ Program*: 147-152, 2009.
42. Branehog, I., Ridell, B., Swolin, B., and Weinfeld, A. Megakaryocyte quantifications in relation to thrombokinetis in primary thrombocythaemia and allied diseases. *Scand J Haematol*, *15*: 321-332, 1975.
43. Deutsch, V. R. and Tomer, A. Megakaryocyte development and platelet production. *Br J Haematol*, *134*: 453-466, 2006.
44. Ciurea, S. O. and Hoffman, R. Cytokines for the treatment of thrombocytopenia. *Semin Hematol*, *44*: 166-182, 2007.
45. Bluteau, D., Lordier, L., Di Stefano, A., Chang, Y., Raslova, H., Debili, N., and Vainchenker, W. Regulation of megakaryocyte maturation and platelet formation. *J Thromb Haemost*, *7 Suppl 1*: 227-234, 2009.
46. Battinelli, E. M., Hartwig, J. H., and Italiano, J. E., Jr. Delivering new insight into the biology of megakaryopoiesis and thrombopoiesis. *Curr Opin Hematol*, *14*: 419-426, 2007.
47. Italiano, J. E., Jr. and Shivdasani, R. A. Megakaryocytes and beyond: the birth of platelets. *J Thromb Haemost*, *1*: 1174-1182, 2003.
48. Radley, J. M. and Haller, C. J. The demarcation membrane system of the megakaryocyte: a misnomer? *Blood*, *60*: 213-219, 1982.
49. Schulze, H. and Shivdasani, R. A. Mechanisms of thrombopoiesis. *J Thromb Haemost*, *3*: 1717-1724, 2005.
50. Broudy, V. C., Lin, N. L., and Kaushansky, K. Thrombopoietin (c-mpl ligand) acts synergistically with erythropoietin, stem cell factor, and interleukin-11 to

- enhance murine megakaryocyte colony growth and increases megakaryocyte ploidy in vitro. *Blood*, *85*: 1719-1726, 1995.
51. Gurney, A. L., Carver-Moore, K., de Sauvage, F. J., and Moore, M. W. Thrombocytopenia in c-mpl-deficient mice. *Science*, *265*: 1445-1447, 1994.
  52. Qian, S., Fu, F., Li, W., Chen, Q., and de Sauvage, F. J. Primary role of the liver in thrombopoietin production shown by tissue-specific knockout. *Blood*, *92*: 2189-2191, 1998.
  53. Kaushansky, K. Lineage-specific hematopoietic growth factors. *N Engl J Med*, *354*: 2034-2045, 2006.
  54. Tiedt, R., Coers, J., Ziegler, S., Wiestner, A., Hao-Shen, H., Bornmann, C., Schenkel, J., Karakhanova, S., de Sauvage, F. J., Jackson, C. W., and Skoda, R. C. Pronounced thrombocytosis in transgenic mice expressing reduced levels of Mpl in platelets and terminally differentiated megakaryocytes. *Blood*, *113*: 1768-1777, 2009.
  55. Moliterno, A. R., Hankins, W. D., and Spivak, J. L. Impaired expression of the thrombopoietin receptor by platelets from patients with polycythemia vera. *N Engl J Med*, *338*: 572-580, 1998.
  56. Cazzola, M. and Skoda, R. C. Translational pathophysiology: a novel molecular mechanism of human disease. *Blood*, *95*: 3280-3288, 2000.
  57. Avecilla, S. T., Hattori, K., Heissig, B., Tejada, R., Liao, F., Shido, K., Jin, D. K., Dias, S., Zhang, F., Hartman, T. E., Hackett, N. R., Crystal, R. G., Witte, L., Hicklin, D. J., Bohlen, P., Eaton, D., Lyden, D., de Sauvage, F., and Rafii, S. Chemokine-mediated interaction of hematopoietic progenitors with the

- bone marrow vascular niche is required for thrombopoiesis. *Nat Med*, 10: 64-71, 2004.
58. McCormack, M. P., Hall, M. A., Schoenwaelder, S. M., Zhao, Q., Ellis, S., Prentice, J. A., Clarke, A. J., Slater, N. J., Salmon, J. M., Jackson, S. P., Jane, S. M., and Curtis, D. J. A critical role for the transcription factor Scl in platelet production during stress thrombopoiesis. *Blood*, 108: 2248-2256, 2006.
  59. National Heart, Lung, and Blood Institute. What are thrombocythemia and thrombocytosis? (2008, February) Retrieved from: <http://www.nhlbi.nih.gov/health/dci/Diseases/thrm/thrm>.
  60. Landen, C. N., Kim, T. J., Lin, Y. G., Merritt, W. M., Kamat, A. A., Han, L. Y., Spannuth, W. A., Nick, A. M., Jennings, N. B., Kinch, M. S., Tice, D., and Sood, A. K. Tumor-selective response to antibody-mediated targeting of alphavbeta3 integrin in ovarian cancer. *Neoplasia*, 10: 1259-1267, 2008.
  61. Buick, R. N., Pullano, R., and Trent, J. M. Comparative properties of five human ovarian adenocarcinoma cell lines. *Cancer Res*, 45: 3668-3676, 1985.
  62. Yoneda, J., Kuniyasu, H., Crispens, M. A., Price, J. E., Bucana, C. D., and Fidler, I. J. Expression of angiogenesis-related genes and progression of human ovarian carcinomas in nude mice. *J Natl Cancer Inst*, 90: 447-454, 1998.
  63. Bast, R. C., Jr., Feeney, M., Lazarus, H., Nadler, L. M., Colvin, R. B., and Knapp, R. C. Reactivity of a monoclonal antibody with human ovarian carcinoma. *J Clin Invest*, 68: 1331-1337, 1981.

64. Lau, D. H., Lewis, A. D., Ehsan, M. N., and Sikic, B. I. Multifactorial mechanisms associated with broad cross-resistance of ovarian carcinoma cells selected by cyanomorpholino doxorubicin. *Cancer Res*, *51*: 5181-5187, 1991.
65. Janat-Amsbury, M. M., Yockman, J. W., Anderson, M. L., Kieback, D. G., and Kim, S. W. Comparison of ID8 MOSE and VEGF-modified ID8 cell lines in an immunocompetent animal model for human ovarian cancer. *Anticancer Res*, *26*: 2785-2789, 2006.
66. Roby, K. F., Taylor, C. C., Sweetwood, J. P., Cheng, Y., Pace, J. L., Tawfik, O., Persons, D. L., Smith, P. G., and Terranova, P. F. Development of a syngeneic mouse model for events related to ovarian cancer. *Carcinogenesis*, *21*: 585-591, 2000.
67. Shima, D. T., Kuroki, M., Deutsch, U., Ng, Y. S., Adamis, A. P., and D'Amore, P. A. The mouse gene for vascular endothelial growth factor. Genomic structure, definition of the transcriptional unit, and characterization of transcriptional and post-transcriptional regulatory sequences. *J Biol Chem*, *271*: 3877-3883, 1996.
68. Lev, D. C., Kiriakova, G., and Price, J. E. Selection of more aggressive variants of the gl101A human breast cancer cell line: a model for analyzing the metastatic phenotype of breast cancer. *Clin Exp Metastasis*, *20*: 515-523, 2003.
69. Kuramoto, H., Tamura, S., and Notake, Y. Establishment of a cell line of human endometrial adenocarcinoma in vitro. *Am J Obstet Gynecol*, *114*: 1012-1019, 1972.



70. Langley, R. R., Ramirez, K. M., Tsan, R. Z., Van Arsdall, M., Nilsson, M. B., and Fidler, I. J. Tissue-specific microvascular endothelial cell lines from H-2K(b)-tsA58 mice for studies of angiogenesis and metastasis. *Cancer Res*, 63: 2971-2976, 2003.
71. Reznikoff, C. A., Brankow, D. W., and Heidelberger, C. Establishment and characterization of a cloned line of C3H mouse embryo cells sensitive to postconfluence inhibition of division. *Cancer Res*, 33: 3231-3238, 1973.
72. Landen, C. N., Jr., Lu, C., Han, L. Y., Coffman, K. T., Bruckheimer, E., Halder, J., Mangala, L. S., Merritt, W. M., Lin, Y. G., Gao, C., Schmandt, R., Kamat, A. A., Li, Y., Thaker, P., Gershenson, D. M., Parikh, N. U., Gallick, G. E., Kinch, M. S., and Sood, A. K. Efficacy and antivasular effects of EphA2 reduction with an agonistic antibody in ovarian cancer. *J Natl Cancer Inst*, 98: 1558-1570, 2006.
73. Thaker, P. H., Han, L. Y., Kamat, A. A., Arevalo, J. M., Takahashi, R., Lu, C., Jennings, N. B., Armaiz-Pena, G., Bankson, J. A., Ravoory, M., Merritt, W. M., Lin, Y. G., Mangala, L. S., Kim, T. J., Coleman, R. L., Landen, C. N., Li, Y., Felix, E., Sanguino, A. M., Newman, R. A., Lloyd, M., Gershenson, D. M., Kundra, V., Lopez-Berestein, G., Lutgendorf, S. K., Cole, S. W., and Sood, A. K. Chronic stress promotes tumor growth and angiogenesis in a mouse model of ovarian carcinoma. *Nat Med*, 12: 939-944, 2006.
74. Merritt, W. M., Lin, Y. G., Spannuth, W. A., Fletcher, M. S., Kamat, A. A., Han, L. Y., Landen, C. N., Jennings, N., De Geest, K., Langley, R. R., Villares, G., Sanguino, A., Lutgendorf, S. K., Lopez-Berestein, G., Bar-Eli, M. M., and Sood, A. K. Effect of interleukin-8 gene silencing with liposome-

- encapsulated small interfering RNA on ovarian cancer cell growth. *J Natl Cancer Inst*, *100*: 359-372, 2008.
75. Kamat, A. A., Merritt, W. M., Coffey, D., Lin, Y. G., Patel, P. R., Broaddus, R., Nugent, E., Han, L. Y., Landen, C. N., Jr., Spannuth, W. A., Lu, C., Coleman, R. L., Gershenson, D. M., and Sood, A. K. Clinical and biological significance of vascular endothelial growth factor in endometrial cancer. *Clin Cancer Res*, *13*: 7487-7495, 2007.
76. Kim, M. P., Evans, D. B., Wang, H., Abbruzzese, J. L., Fleming, J. B., and Gallick, G. E. Generation of orthotopic and heterotopic human pancreatic cancer xenografts in immunodeficient mice. *Nat Protoc*, *4*: 1670-1680, 2009.
77. Lu, C., Kamat, A. A., Lin, Y. G., Merritt, W. M., Landen, C. N., Kim, T. J., Spannuth, W., Arumugam, T., Han, L. Y., Jennings, N. B., Logsdon, C., Jaffe, R. B., Coleman, R. L., and Sood, A. K. Dual targeting of endothelial cells and pericytes in antivasular therapy for ovarian carcinoma. *Clin Cancer Res*, *13*: 4209-4217, 2007.
78. Watson, S. P. and Authi, K. S. *Platelets: A Practical Approach*, p. 370. Oxford: Oxford University Press, 1996.
79. Lin, Y. G., Han, L. Y., Kamat, A. A., Merritt, W. M., Landen, C. N., Deavers, M. T., Fletcher, M. S., Urbauer, D. L., Kinch, M. S., and Sood, A. K. EphA2 overexpression is associated with angiogenesis in ovarian cancer. *Cancer*, *109*: 332-340, 2007.
80. Lin, Y. G., Kunnumakkara, A. B., Nair, A., Merritt, W. M., Han, L. Y., Armaiz-Pena, G. N., Kamat, A. A., Spannuth, W. A., Gershenson, D. M., Lutgendorf, S. K., Aggarwal, B. B., and Sood, A. K. Curcumin inhibits tumor growth and

- angiogenesis in ovarian carcinoma by targeting the nuclear factor-kappaB pathway. *Clin Cancer Res*, 13: 3423-3430, 2007.
81. Levine, R. F. Isolation and characterization of normal human megakaryocytes. *Br J Haematol*, 45: 487-497, 1980.
  82. Kumar, M. N. V. R. A review of chitin and chitosan applications. *Reactive and Functional Polymers.*, 46: 1-27, 2000.
  83. Mangala, L. S., Han, H. D., Lu, C., Ali-Fehmi, R., Newton, C., Ozbun, L., Armaiz-Pena, G., Hu, W., Stone, R., Munkarah, A., Ravoori, M. K., Mian Shahzad, Lee, J.-W., Mora, E., Langley, R. R., Carroll, A. R., Matsuo, K., Spannuth, W. A., Schmandt, R., Jennings, N. B., Goodman, B. W., Jaffe, R. B., Nick, A. M., Kim, H. S., Guven, E. O., Ya-Huey Chen, Li, L.-Y., Hsu, M.-C., Coleman, R. L., Calin, G. A., Denkbass, E. B., Lim, J. Y., Lee, J.-S., Kundra, V., Birrer, M. J., Hung, M.-C., Lopez-Berestein, G., and Sood, A. K. Regulation of Tumor Angiogenesis by EZH2. 2010.
  84. Zsebo, K. M., Yuschenkoff, V. N., Schiffer, S., Chang, D., McCall, E., Dinarello, C. A., Brown, M. A., Altrock, B., and Bagby, G. C., Jr. Vascular endothelial cells and granulopoiesis: interleukin-1 stimulates release of G-CSF and GM-CSF. *Blood*, 71: 99-103, 1988.
  85. Brockmann, M. A., Giese, A., Mueller, K., Kaba, F. J., Lohr, F., Weiss, C., Gottschalk, S., Nolte, I., Leppert, J., Tuettenberg, J., and Groden, C. Preoperative thrombocytosis predicts poor survival in patients with glioblastoma. *Neuro Oncol*, 9: 335-342, 2007.
  86. Chen, M. H., Chang, P. M., Chen, P. M., Tzeng, C. H., Chu, P. Y., Chang, S. Y., and Yang, M. H. Prognostic significance of a pretreatment hematologic

- profile in patients with head and neck cancer. *J Cancer Res Clin Oncol*, 135: 1783-1790, 2009.
87. Taucher, S., Salat, A., Gnant, M., Kwasny, W., Mlineritsch, B., Menzel, R. C., Schmid, M., Smola, M. G., Stierer, M., Tausch, C., Galid, A., Steger, G., and Jakesz, R. Impact of pretreatment thrombocytosis on survival in primary breast cancer. *Thromb Haemost*, 89: 1098-1106, 2003.
  88. Tomita, M., Shimizu, T., Hara, M., Ayabe, T., and Onitsuka, T. Preoperative leukocytosis, anemia and thrombocytosis are associated with poor survival in non-small cell lung cancer. *Anticancer Res*, 29: 2687-2690, 2009.
  89. Ikeda, M., Furukawa, H., Imamura, H., Shimizu, J., Ishida, H., Masutani, S., Tatsuta, M., and Satomi, T. Poor prognosis associated with thrombocytosis in patients with gastric cancer. *Ann Surg Oncol*, 9: 287-291, 2002.
  90. Hwang, S. J., Luo, J. C., Li, C. P., Chu, C. W., Wu, J. C., Lai, C. R., Chiang, J. H., Chau, G. Y., Lui, W. Y., Lee, C. C., Chang, F. Y., and Lee, S. D. Thrombocytosis: a paraneoplastic syndrome in patients with hepatocellular carcinoma. *World J Gastroenterol*, 10: 2472-2477, 2004.
  91. Kandemir, E. G., Mayadagli, A., Karagoz, B., Bilgi, O., Turken, O., and Yaylaci, M. Prognostic significance of thrombocytosis in node-negative colon cancer. *J Int Med Res*, 33: 228-235, 2005.
  92. Suppiah, R., Shaheen, P. E., Elson, P., Misbah, S. A., Wood, L., Motzer, R. J., Negrier, S., Andresen, S. W., and Bukowski, R. M. Thrombocytosis as a prognostic factor for survival in patients with metastatic renal cell carcinoma. *Cancer*, 107: 1793-1800, 2006.

93. Bensalah, K., Leray, E., Fergelot, P., Rioux-Leclercq, N., Tostain, J., Guille, F., and Patard, J. J. Prognostic value of thrombocytosis in renal cell carcinoma. *J Urol*, 175: 859-863, 2006.
94. Hernandez, E., Heller, P. B., Whitney, C., Diana, K., and Delgado, G. Thrombocytosis in surgically treated stage IB squamous cell cervical carcinoma (A Gynecologic Oncology Group study). *Gynecol Oncol*, 55: 328-332, 1994.
95. Lavie, O., Comerci, G., Daras, V., Bolger, B. S., Lopes, A., and Monaghan, J. M. Thrombocytosis in women with vulvar carcinoma. *Gynecol Oncol*, 72: 82-86, 1999.
96. Gucer, F., Moser, F., Tamussino, K., Reich, O., Haas, J., Arikan, G., Petru, E., and Winter, R. Thrombocytosis as a prognostic factor in endometrial carcinoma. *Gynecol Oncol*, 70: 210-214, 1998.
97. Lu, C., Thaker, P. H., Lin, Y. G., Spannuth, W., Landen, C. N., Merritt, W. M., Jennings, N. B., Langle, R. R., Gershenson, D. M., Yancopoulos, G. D., Ellis, L. M., Jaffe, R. B., Coleman, R. L., and Sood, A. K. Impact of vessel maturation on antiangiogenic therapy in ovarian cancer. *Am J Obstet Gynecol*, 198: 477 e471-479; discussion 477 e479-410, 2008.
98. Blair, P. and Flaumenhaft, R. Platelet alpha-granules: basic biology and clinical correlates. *Blood Rev*, 23: 177-189, 2009.
99. Bruno, E., Miller, M. E., and Hoffman, R. Interacting cytokines regulate in vitro human megakaryocytopoiesis. *Blood*, 73: 671-677, 1989.

100. Estrov, Z., Talpaz, M., Mavligit, G., Pazdur, R., Harris, D., Greenberg, S. M., and Kurzrock, R. Elevated plasma thrombopoietic activity in patients with metastatic cancer-related thrombocytosis. *Am J Med*, 98: 551-558, 1995.
101. Cardier, J. E. and Barbera-Guillem, E. Extramedullary hematopoiesis in the adult mouse liver is associated with specific hepatic sinusoidal endothelial cells. *Hepatology*, 26: 165-175, 1997.
102. Levine, R. F., Eldor, A., Shoff, P. K., Kirwin, S., Tenza, D., and Cramer, E. M. Circulating megakaryocytes: delivery of large numbers of intact, mature megakaryocytes to the lungs. *Eur J Haematol*, 51: 233-246, 1993.
103. Zucker-Franklin, D. and Philipp, C. S. Platelet production in the pulmonary capillary bed: new ultrastructural evidence for an old concept. *Am J Pathol*, 157: 69-74, 2000.
104. Kaushansky, K. Thrombopoietin. *N Engl J Med*, 339: 746-754, 1998.
105. Kaushansky, K. The molecular mechanisms that control thrombopoiesis. *J Clin Invest*, 115: 3339-3347, 2005.
106. Nilsson, M. B., Armaiz-Pena, G., Takahashi, R., Lin, Y. G., Trevino, J., Li, Y., Jennings, N., Arevalo, J., Lutgendorf, S. K., Gallick, G. E., Sanguino, A. M., Lopez-Berestein, G., Cole, S. W., and Sood, A. K. Stress hormones regulate interleukin-6 expression by human ovarian carcinoma cells through a Src-dependent mechanism. *J Biol Chem*, 282: 29919-29926, 2007.
107. Furuhashi, M., Miyabe, Y., and Oda, H. A case of thrombopoietin-producing ovarian carcinoma confirmed by immunohistochemistry. *Gynecol Oncol*, 74: 278-281, 1999.

108. Li, A. J., Madden, A. C., Cass, I., Leuchter, R. S., Lagasse, L. D., and Karlan, B. Y. The prognostic significance of thrombocytosis in epithelial ovarian carcinoma. *Gynecol Oncol*, 92: 211-214, 2004.
109. Menczer, J., Schejter, E., Geva, D., Ginath, S., and Zakut, H. Ovarian carcinoma associated thrombocytosis. Correlation with prognostic factors and with survival. *Eur J Gynaecol Oncol*, 19: 82-84, 1998.
110. Lyman, G. H., Khorana, A. A., Falanga, A., Clarke-Pearson, D., Flowers, C., Jahanzeb, M., Kakkar, A., Kuderer, N. M., Levine, M. N., Liebman, H., Mendelson, D., Raskob, G., Somerfield, M. R., Thodiyil, P., Trent, D., and Francis, C. W. American Society of Clinical Oncology guideline: recommendations for venous thromboembolism prophylaxis and treatment in patients with cancer. *J Clin Oncol*, 25: 5490-5505, 2007.
111. Baron, J. A., Gridley, G., Weiderpass, E., Nyren, O., and Linet, M. Venous thromboembolism and cancer. *Lancet*, 351: 1077-1080, 1998.
112. Prandoni, P., Lensing, A. W., Buller, H. R., Cogo, A., Prins, M. H., Cattelan, A. M., Cuppini, S., Noventa, F., and ten Cate, J. W. Deep-vein thrombosis and the incidence of subsequent symptomatic cancer. *N Engl J Med*, 327: 1128-1133, 1992.
113. Vemulapalli, S., Chintala, L., Tsimberidou, A. M., Dhillon, N., Lei, X., Hong, D., and Kurzrock, R. Clinical outcomes and factors predicting development of venous thromboembolic complications in patients with advanced refractory cancer in a Phase I Clinic: the M. D. Anderson Cancer Center experience. *Am J Hematol*, 84: 408-413, 2009.

114. Varki, A. Trousseau's syndrome: multiple definitions and multiple mechanisms. *Blood*, 110: 1723-1729, 2007.
115. Akl, E. A., van Doormaal, F. F., Barba, M., Kamath, G., Kim, S. Y., Kuipers, S., Middeldorp, S., Yosuico, V., Dickinson, H. O., and Schunemann, H. J. Parenteral anticoagulation for prolonging survival in patients with cancer who have no other indication for anticoagulation. *Cochrane Database Syst Rev*: CD006652, 2007.
116. Chan, A. T., Ogino, S., and Fuchs, C. S. Aspirin use and survival after diagnosis of colorectal cancer. *Jama*, 302: 649-658, 2009.
117. Mousa, S. A. and Petersen, L. J. Anti-cancer properties of low-molecular-weight heparin: preclinical evidence. *Thromb Haemost*, 102: 258-267, 2009.
118. Jacobs, E. J., Thun, M. J., Bain, E. B., Rodriguez, C., Henley, S. J., and Calle, E. E. A large cohort study of long-term daily use of adult-strength aspirin and cancer incidence. *J Natl Cancer Inst*, 99: 608-615, 2007.
119. Dymicka-Piekarska, V. and Kemon, H. Thrombopoietin and reticulated platelets as thrombopoietic markers in colorectal cancer. *Thromb Res*, 122: 141-143, 2008.
120. Suzuki, A., Takahashi, T., Nakamura, K., Tsuyuoka, R., Okuno, Y., Enomoto, T., Fukumoto, M., and Imura, H. Thrombocytosis in patients with tumors producing colony-stimulating factor. *Blood*, 80: 2052-2059, 1992.
121. Blay, J. Y., Favrot, M., Rossi, J. F., and Wijdenes, J. Role of interleukin-6 in paraneoplastic thrombocytosis. *Blood*, 82: 2261-2262, 1993.
122. D'Hondt, V., Humblet, Y., Guillaume, T., Baatout, S., Chatelain, C., Berliere, M., Longueville, J., Feyens, A. M., de Greve, J., Van Oosterom, A., and et al.



- Thrombopoietic effects and toxicity of interleukin-6 in patients with ovarian cancer before and after chemotherapy: a multicentric placebo-controlled, randomized phase Ib study. *Blood*, 85: 2347-2353, 1995.
123. van Gameren, M. M., Willemse, P. H., Mulder, N. H., Limburg, P. C., Groen, H. J., Vellenga, E., and de Vries, E. G. Effects of recombinant human interleukin-6 in cancer patients: a phase I-II study. *Blood*, 84: 1434-1441, 1994.
  124. Roberts, A. W. G-CSF: a key regulator of neutrophil production, but that's not all! *Growth Factors*, 23: 33-41, 2005.
  125. Duhrsen, U., Villeval, J. L., Boyd, J., Kannourakis, G., Morstyn, G., and Metcalf, D. Effects of recombinant human granulocyte colony-stimulating factor on hematopoietic progenitor cells in cancer patients. *Blood*, 72: 2074-2081, 1988.
  126. Meinhold-Heerlein, I., Ninci, E., Ikenberg, H., Brandstetter, T., Ihling, C., Schwenk, I., Straub, A., Schmitt, B., Bettendorf, H., Iggo, R., and Bauknecht, T. Evaluation of methods to detect p53 mutations in ovarian cancer. *Oncology*, 60: 176-188, 2001.
  127. Plante, M., Rubin, S. C., Wong, G. Y., Federici, M. G., Finstad, C. L., and Gastl, G. A. Interleukin-6 level in serum and ascites as a prognostic factor in patients with epithelial ovarian cancer. *Cancer*, 73: 1882-1888, 1994.
  128. Watson, J. M., Sensintaffar, J. L., Berek, J. S., and Martinez-Maza, O. Constitutive production of interleukin 6 by ovarian cancer cell lines and by primary ovarian tumor cultures. *Cancer Res*, 50: 6959-6965, 1990.

129. Kaser, A., Brandacher, G., Steurer, W., Kaser, S., Offner, F. A., Zoller, H., Theurl, I., Widder, W., Molnar, C., Ludwiczek, O., Atkins, M. B., Mier, J. W., and Tilg, H. Interleukin-6 stimulates thrombopoiesis through thrombopoietin: role in inflammatory thrombocytosis. *Blood*, 98: 2720-2725, 2001.
130. Wolber, E. M. and Jelkmann, W. Thrombopoietin: the novel hepatic hormone. *News Physiol Sci*, 17: 6-10, 2002.

## **Vita**

Rebecca was born in El Paso, TX, on May 31, 1976, the daughter of vascular surgeon Jerry R. Youkey and of Sharon A. Youkey, RN. After graduating from Lewisburg Area High School, Lewisburg, PA, in 1994, she enrolled in the University of Virginia, Charlottesville, VA. She received her Bachelors degree in Biology in 1998. She was then accepted into the University of Virginia School of Medicine, and graduated with a Doctor of Medicine in 2004. She entered the Obstetrics and Gynecology residency program at the University of Virginia, graduating in 2008. In July 2008, she began a fellowship in Gynecologic Oncology at M.D. Anderson Cancer Center. Her two-year Master's program during this fellowship was mentored by Dr. Anil Sood and focused on the role of platelets in ovarian carcinoma. During her research years, she also investigated focal adhesion kinase as a novel target for anti-angiogenic therapy in ovarian cancer.